OFFICIAL JOURNAL OF THE SCIENTIFIC SOCIETY OF ANATOMISTS, HISTOLOGISTS, EMBRYOLOGISTS AND TOPOGRAPHIC ANATOMISTS OF UKRAINE

DOI: 10.31393
ISSN 1818-1295
eISSN 2616-6194

# ВІСНИК МОРФОЛОГІЇ
# REPORTS OF MORPHOLOGY

Vol. 27, №2, 2021

Scientific peer-reviewed journal in the fields of normal and pathological anatomy, histology, cytology and embryology, topographical anatomy and operative surgery, biomedical anthropology, ecology, molecular biology, biology of development

Published since 1993
Periodicity: 4 times a year

Vinnytsya · 2021

# ВІСНИК МОРФОЛОГІЇ - REPORTS OF MORPHOLOGY

Founded by the "Scientific Society of Anatomists, Histologists, Embryologists, and Topographic Anatomists of Ukraine" and National Pyrogov Memorial Medical University, Vinnytsya in 1993

Certificate of state registration КВ №9310 from 02.11.2004

*Professional scientific publication of Ukraine in the field of medical sciences in specialties 221, 222, 228, 229*
According to the list of professional scientific publications of Ukraine, approved by the order of the Ministry of Education and Science of Ukraine No. 1188 of 24.09.2020
*Professional scientific publication of Ukraine in the field of biological sciences in specialty 091*
According to the list of professional scientific publications of Ukraine, approved by the order of the Ministry of Education and Science of Ukraine No. 1471 of 26.11.2020



Approved by the Academic Council of National Pyrogov Memorial Medical University, Vinnytsya, protocol №12 from 22.06.2021.

***Indexation:*** CrossRef, Index Copernicus, Google Schoolar Metrics, National Library of Ukraine Vernadsky

**Address editors and publisher:**
Pyrogov Str. 56,
Vinnytsya, Ukraine - 21018
*Tel.:* +38 (0432) 553959
*E-mail:* nila@vnmu.edu.ua

**Computer page-proofs** - Klopotovska L.O.
**Translator** - Gunas V.I.
**Technical support** - Levenchuk S.S., Parashuk O.I.
**Scientific editing** - editorship

**The site of the magazine** - https://morphology-journal.com

# CONTENT

DOI: 10.31393/morphology-journal-2021-27(2)-01 Reports of Morphology, Vol. 27, №2, Pages 5-10

ISSN 1818-1295 eISSN 2616-6194

**REPORTS OF MORPHOLOGY**

***Official Journal of the Scientific Society of Anatomists, Histologists, Embryologists and Topographic Anatomists of Ukraine***

journal homepage: https://morphology-journal.com

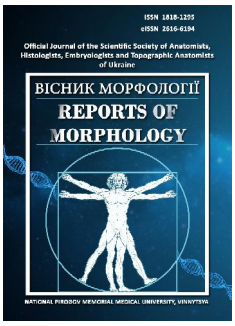


# Dynamics of anthropometric indicators in girls within the pubertal period of ontogenesis

***Sarafyniuk P.V.[1], Sarafyniuk L.A.[2], Khapitska O.P.[2], Kovalchuk O.V.[2], Muzyka N.O.[2]***

[1]Vinnytsya State Pedagogical University named after Mykhailo Kotsyubynsky, Vinnytsya, Ukraine
[2]National Pirogov Memorial Medical University, Vinnytsya, Ukraine

**ARTICLE INFO**
Received: 7 April 2021
Accepted: 12 May 2021

**UDC:** 572.51-612.014.5

**CORRESPONDING AUTHOR**
e-mail: lsarafinyuk@gmail.com
Sarafyniuk L.A.

*The harmony of the organism development in different periods of ontogenesis, and especially puberty, determines the future fate of women in both medical and social aspects. The aim of the research was to study the total and partial body sizes in girls of pubertal period of ontogenesis. We surveyed 128 schoolgirls of 5-8 grades. We evaluated the stages of development of secondary sexual characteristics by hair growth in the axilla and pubis, the development of the mammary glands and age of onset of the first menstruation. According to G.G. Avtandilov's classification, all girls were divided into three groups - prepubertal (preceding the appearance of pubic hair), pubertal (puberty before menarche) and postpubertal period (fixed and completed pubertal maturation). The group of pubertal girls consisted of 106 schoolgirls, who were divided into groups according to calendar age: 13-year-old (n=29), 12-year-old (n=30), 11-year-old (n=24) and 10-year-old (n=23). Anthropometric survey was conducted according to the scheme of V.V. Bunak and contained the definition of total (length and body weight) and partial (longitudinal, transverse and anterior-posterior) dimensions. The analysis of the obtained results was performed in the license package Statistica 5.5 using non-parametric methods of evaluation of indicators. In our study, it was found that anthropometric indicators characterize the physical development, the level of its harmony and morphofunctional maturity of girls within the pubertal period of ontogenesis. We found a progressive age dynamics of total and partial body size in girls of this age period. The periods of the most intensive growth within the pubertal period of ontogenesis of total and partial sizes of a body are established. At the end of puberty there is the most intense age increase in body length: a rapid increase in body weight begins at the age of 12, the most intense processes of longitudinal growth of the torso and lower extremities in girls are observed from 11 years. Most of the transverse dimensions within the pubertal period of ontogenesis have a pronounced progressive age dynamic. Lower thoracic size, interspinous distance, and external conjugate did not differ statistically significantly between girls of different ages during puberty.*

**Keywords:** *girls, biological age, puberty, physical development, anthropometric dimensions.*

## Introduction

Health care for girls - as expectant mothers - is one of the primary tasks of integrative anthropology, given the deteriorating demographics against the background of declining birth rates and socio-economic level of the population, and, moreover, against the background of increasing overall morbidity [9, 13, 21]. The state of health characterizes the gene pool of the nation, especially when it comes to maintaining the reproductive health of the younger generation [7, 11]. Statistics in recent years remain disappointing and show a negative natural increase and decrease in the share of children, which leads to the so-called "aging of the nation". Today, Ukraine ranks 186th out of 226 countries in terms of birth rate and 4th in the world (3rd in Europe) in terms of infant mortality. This raises the issue of early diagnosis and timely treatment of girls with puberty and menstrual disorders to one of the highest priorities, because their health is crucial for the formation of the next generation [12]. It is noted that on average 19% of adolescent girls in Ukraine have menstrual disorders [26].

Morphofunctional reorganization of a woman's body determines many life processes [18, 19]. Indicators of biological age - a reliable criterion by which you can "catch" the inadequacy of the restructuring of certain parts of the human body. The harmony of the development of the organism in different periods of ontogenesis largely determines the further life and destiny of a woman in both medical and social aspects [15, 17]. From this point of view, it is especially important to study these processes during puberty, because it is accompanied by physical and psycho-emotional changes, which are aimed at maintaining and developing one of the main physiological functions of the female body - fertility [19]. The age at which girls reach puberty is of considerable interest in various fields of medicine and science in general, affects the problems of prevention and early diagnosis in medical practice and is the subject of many scientific studies on the preservation and development of reproductive potential [11]. Puberty should be considered as a complex sequence of anatomical and physiological changes, and anthropometric parameters of physical development, along with secondary sexual characteristics, are the basis for assessing the child's development, which helps the doctor during the examination of the child to identify atypical signs of puberty [10, 14, 20].

*The aim* of the research was to study the total and partial body sizes in girls of pubertal period of ontogenesis.

## Materials and methods

The study was conducted in September - November 2019 on the basis of Chernivtsi Secondary School I-III degrees №1. We surveyed 128 schoolgirls of 5-8 grades: 32 girls of 5th grade, 33 girls of 6th grade, 31 girls of 7th grade, 32 girls of 8th grade.

We evaluated the stages of development of secondary sexual characteristics according to the scheme of V.B. Schwartz and S.V. Khrushchev [25], determined the hair in the axilla (Ax) and pubis (P), the development of the mammary glands (Ma) and the age of start of period (Me).

According to the classification of G.G. Avtandilov [6], all girls were divided into three groups - prepubertal (preceding the appearance of pubic hair), pubertal (puberty before menarche) and postpubertal period (fixed and completed puberty).

Thus, the group of adolescent girls consisted of 106 schoolgirls, including 23 girls of 5th grade, 33 girls of 6th grade, 32 girls of 7th grade, 15 girls of 8th grade. All schoolgirls of pubertal ontogenesis were divided into groups according to calendar age (full years): 13-year-old - 29 people, 12-year-old - 30 people, 11-year-old - 24 people, 10-year-old - 23 people.

In addition, it was found that the average age of onset of menarche in girls of Chernivtsi Secondary School I-III grades №1 was 13 years 2 months.

The anthropometric survey was performed according to the scheme of V.V. Bunak [8] and included the determination of total (length and body weight) and partial (longitudinal, transverse and anterior-posterior) dimensions.

The analysis of the obtained results was performed in the license package Statistica 5.5 using non-parametric methods of evaluation of indicators.

## Results

As a result of our study, we established the average parameters of weight, length, longitudinal, transverse, anterior-posterior body size in girls of different calendar ages, but which according to the development of secondary sexual characteristics belonged to the pubertal period of ontogenesis. The data obtained by us show a general tendency to increase with age all the average anthropometric indicators of physical development of girls. We compared the corresponding indicators in girls in pairs between comparison groups. The calendar age of the subjects differed by 1 year.

Thus, body length in girls of different ages is statistically significantly different. Significant differences were observed between girls aged 10 and 11 years ($p<0.01$) and 12 and 13 years ($p<0.001$) (Table 1).

Significant differences in body weight were found between 11 and 12 and 12 and 13-year-old girls, in all cases $p<0.01$ (see Table 1).

The height of the thoracic point differs statistically significantly between girls aged 11 and 12 years ($p<0.05$) and 12 and 13 years ($p<0.001$), the height of the shoulder - between 11 and 12-year-old girls ($p<0$, 01) and 12- and 13-year-olds ($p<0.001$) (see Table 1).

We found that the height of the pubic point is significantly higher in 11-year-old girls compared to 10-year-olds and in 13-year-old girls compared to 12-year-olds (in both cases $p<0.05$). This indicator has a pronounced age dynamics of increase, but between the groups of 12 and 13 years the difference in the value of this indicator is not significant. A similar pattern can be traced for the height of the trochanteric point: a statistically significant difference in the value of this indicator of physical development when comparing groups 10 and 11 years ($p<0.05$) and 12 and 13 years ($p<0.01$) (see Table. 1). The height of these anthropometric points reflects the processes of longitudinal growth of the lower extremities.

Analyzing the height of the finger point in girls of all ages, we found a significant difference in the value of this indicator between all groups of comparisons, but the most intense processes of longitudinal growth in girls are observed in the period from 12 to 13 years ($p<0,001$) (see Table 1).

In the study of transverse and anterior-posterior body size in girls of pubertal period of ontogenesis, we found certain features.

Let's focus on the transverse dimensions of the chest (Table 2). Thus, the middle thoracic diameter in 11-year-old girls was significantly larger ($p<0.01$) compared to 10-

**Table 1.** Changes in total and longitudinal body size in girls of pubertal ontogenesis, (M±m).

| Indicators | Age (years) | | | | $p_1$ | $p_2$ | $p_3$ |
|---|---|---|---|---|---|---|---|
| | 10 | 11 | 12 | 13 | | | |
| Body length (cm) | 146.1±3.2 | 151.3±2.4 | 153.1±6.5 | 160.5±6.4 | <0.01 | >0.05 | <0.001 |
| Body weight (kg) | 36.12±5.14 | 36.55±4.66 | 41.25±4.08 | 47.51±3.07 | >0.05 | <0.01 | <0.01 |
| Height of the suprathoracic point (cm) | 117.2±3.3 | 119.8±4.6 | 124.0±5.9 | 130.2±6.3 | >0.05 | <0.05 | <0.001 |
| Pubic point height (cm) | 68.34±3.15 | 72.15±2.63 | 75.45±3.93 | 80.91±3.99 | <0.05 | >0.05 | <0.05 |
| Shoulder point height (cm) | 118.5±4.2 | 120.7±2.9 | 124.5±3.8 | 131.3±4.7 | >0.05 | <0.01 | <0.001 |
| Finger point height (cm) | 50.22±4.02 | 54.04±2.55 | 57.99±3.32 | 61.45±1.85 | <0.05 | <0.05 | <0.001 |
| Height of the trochanteric point (cm) | 72.62±3.02 | 76.05±2.44 | 77.95±3.88 | 80.82±3.78 | <0.05 | >0.05 | <0.01 |

**Notes** (here and in the future): $p_1$ - the reliability of the difference between 10-11-year-old girls; $p_2$ - the reliability of the difference between 11-12-year-old girls; $p_3$ - the reliability of the difference between 12-13-year-old girls.

**Table 2.** Changes in transverse and anterior-posterior body size in girls of pubertal ontogenesis, (M±m, cm).

| Indicators | Age (years) | | | | $p_1$ | $p_2$ | $p_3$ |
|---|---|---|---|---|---|---|---|
| | 10 | 11 | 12 | 13 | | | |
| Middle thoracic size | 17.83±1.07 | 20.01±2.12 | 21.83±1.67 | 23.95±1.99 | <0.01 | >0.05 | <0.01 |
| Lower thoracic size | 17.34±1.83 | 18.50±1.05 | 19.80±1.23 | 19.42±1.69 | >0.05 | >0.05 | >0.05 |
| Anterior-posterior chest size | 13.82±1.12 | 14.19±0.58 | 15.05±1.06 | 16.77±1.20 | >0.05 | >0.05 | <0.01 |
| Shoulder width | 27.06±2.05 | 27.22±0.93 | 30.36±1.89 | 33.98±1.01 | >0.05 | <0.01 | <0.01 |
| Interspinous distance | 21.11±1.56 | 21.34±1.59 | 21.48±1.32 | 21.65±2.10 | >0.05 | >0.05 | >0.05 |
| Intercristal distance | 22.15±1.22 | 23.88±1.52 | 24.25±1.42 | 24.88±1.71 | <0.05 | >0.05 | >0.05 |
| Intertrochanteric distance | 23.86±1.68 | 24.22±1.33 | 26.26±1.03 | 28.76±1.67 | >0.05 | <0.05 | <0.01 |
| External conjugate | 15.26±1.22 | 15.92±1.53 | 16.16±1.34 | 16.83±1.27 | >0.05 | >0.05 | >0.05 |

year-old schoolgirls, between 11 and 12-year-old girls there was no significant difference in the value of this indicator, between 12 and 13-year-old girls there was a significant difference ($p<0.01$). Lower thoracic size does not differ significantly between girls of different calendar ages within the pubertal period of ontogenesis.

It was found that the width of the shoulders has no significant differences when comparing groups of girls 10 and 11 years. We found a significant difference in the magnitude of this transverse torso size between girls 11 and 12 years and 12 and 13 years (in both cases $p<0.05$). Anterior-posterior chest size has a statistically significant difference only between girls aged 12 and 13 ($p<0.01$). When comparing the value of this indicator between other observation groups, no significant difference was found (see Table 2).

It was found that interspinous distance has no statistically significant differences between any comparison group, in addition, it should be noted that the absolute values of this pelvic size are in girls of different calendar ages during puberty at almost the same level. Analyzing the age-related changes in intercristal distance, we found that this figure in 11-year-old girls is significantly higher than in 10-year-old ($p<0.01$), and then the growth rate of this pelvic size is slowed down, differences in the comparison of groups of girls 11 and 12 years, 12 and 13 years (see Table 2).

In contrast to previous indicators, the pelvic intertrochanteric distance has a pronounced age-related dynamics of changes within the pubertal period of ontogenesis, despite the fact that we did not find a significant difference between the comparison groups at the beginning of pubertal development. It should be noted that, starting at age 11, intertrochanteric distance increases rapidly. We recorded a statistically significant difference in the size of this transverse pelvic size between groups of girls 11 and 12 years ($p<0.05$) and 12 and 13 years ($p<0.01$). We found that the anteroposterior size of the pelvis, which is indicated by the size of the external conjugate in girls of different calendar ages of puberty ontogenesis, has no significant differences (see Table 2).

## Discussion

Scientists point out that the study of morphofunctional features of the organism should be based on the ontogenetic approach, because within certain annual age-sex groups individuals have different anatomical and physiological level of development [2, 4, 23]. Among the many methods of assessing biological age is particularly popular, quite reliable and affordable is to determine the stages of development of secondary sexual characteristics [1, 3, 5]. The results of our study are a confirmation of this opinion, especially clearly reflect the uneven physical development in certain groups, divided by calendar age, survey data of 10-year-old and 13-year-old schoolgirls. Thus, among 10-year-old girls, 20.69% have zero stages

of development of secondary sexual characteristics and belonged to the prepubertal period of ontogenesis, and 9.37% of 13-year-old schoolgirls belonged to the postpubertal period of ontogenesis. We found that the mean age of onset of menarche in the girls we examined was 13 years and 2 months. These results are comparable to the parameters of girls living in developed countries, where the age of onset of menarche is from 12 to 13 years [22].

The age of onset of menarche is directly proportional to height and inversely proportional to body mass index [28]. The relation between the onset of menarche and body weight was established in 1974 by American scientist Rosa Frisch, who studied the issue of infertility. Over time, the minimum body weight at which the onset of menarche is possible is called "critical body weight". Its value at a height of not less than 155 cm ranges from 44 to 47 kg [11, 22]. When conducting surveys of schoolgirls in Ukraine, the average body weight, height and body mass index at the time of the onset of menarche were: city residents body weight - 47.20±1.40 kg, height - 158.0±0.01 cm, body mass index - 18.80±0.53 kg/m2, the villagers had a body weight of 45.90±2.40 kg, height - 157.0±0.03 cm, body mass index - 18.40±0.57 kg/m2. The study for girls (regardless of their place of residence) found an inverse association between age of onset of menarche and body mass index, as well as a direct relationship between age of onset of menarche and height [11]. In our study, it was determined that at the end of the pubertal period of ontogenesis in girls living in an urban-type settlement of Vinnytsia region, body length was 160.5±6.4 cm, and body weight - 47.51±3.07 kg. It should be noted that at the end of puberty ontogenesis in girls there are the most intense age increases in body length, and between 11 and 12 years - the rate of increase of this total body size is slowed, as evidenced by the lack of significant difference between the respective age groups. It should be noted that at the beginning of puberty, a significant increase in body weight in girls is not observed, despite significant increases in body length. And starting from the age of 12, a rapid increase in this total body size begins. According to the research of some scientists, it is known that body weight in girls is undeniable for puberty [11, 28]. In our opinion, the amount of body fat is especially important for the onset of menarche, because in girls the subcutaneous fat acts as a depot for the accumulation of female sex hormones, including estrogen, which affect puberty and puberty.

Analyzing the age dynamics of longitudinal body size, it is necessary to note the non-synchronicity of the detected changes in adolescent girls. Thus, the height of the sternum and shoulder points have similar age-related changes, as evidenced by our established significant differences in the value of these two indicators. Thus, we can conclude that the most intense processes of longitudinal growth of the torso and lower extremities, as evidenced by the magnitude of these two anthropometric parameters, in girls is observed from 11 years.

Chest sizes are one of the most important anthropometric indicators of physical development. These parameters determine not only the somatotypological affiliation of the person, but also play an important role in the prognostic and ascertaining sports selection [24]. Analyzing the age dynamics within the pubertal period of ontogenesis of middle-thoracic diameter, it should be noted that this figure increases sharply in girls 11 years compared with 10 years, during the next calendar age the growth rate of this transverse size of the chest slows down, and at the end of puberty ontogenesis, the size of the middle-thoracic diameter increases sharply, as evidenced by a significant difference found between groups of girls 12 and 13 years. We found that the value of the lower thoracic size does not have a significant difference when comparing girls of different calendar ages, but it should be noted that this anthropometric indicator in girls within the pubertal period of ontogenesis has a positive age dynamic. In the analysis of shoulder width, it was found that this figure in girls 10 and 11 years is almost at the same level. And from the age of 12 it begins to increase rapidly. The anteroposterior size of the thorax (or its thickness) begins to increase significantly only after 12 years. We found a statistically significant difference only between groups of girls 12 and 13 years.

Transverse dimensions of the pelvis during puberty in girls are marked by some asynchrony of changes. Thus, interspinous distance and external conjugate in girls within the pubertal period of ontogenesis did not differ significantly between any comparison group. It was found that only in 11-year-old girls the value of intercristal distance is significantly greater than in 10-year-olds, and then the growth rate of this pelvic size slows down. Intertrochanteric distance has a pronounced age dynamics of changes within the pubertal period of ontogenesis, despite the fact that we did not find a significant difference between comparison groups at the beginning of pubertal development, but from 11 years, intertrochanteric distance increases rapidly.

The analysis of anthropometric indicators of physical development in girls of pubertal period of ontogenesis indicates a pronounced age dynamic. The most significant changes during puberty are the longitudinal dimensions of the body, length and weight of the body, as well as the transverse dimensions of the pelvis and chest. Thus, the pubertal period of ontogenesis can be defined as a set of successive biological stages [11, 15, 16, 27], which are reflected in the features of anthropometric body size, which leads to the further formation of a woman's full reproductive function.

## Conclusions

1. We found that body length in girls of different calendar ages within the pubertal period of ontogenesis is statistically significantly different, at the end of the pubertal period of ontogenesis in girls there are the most intense

age gains of this total body size, and in 11 to 12 years - slow longitudinal growth.

Significant differences ($p<0.01$) in body weight were found between 11 and 12, as well as between 12 and 13-year-old girls. Rapid weight gain begins at the age of 12.

2. Significant differences in the magnitude of anthropometric longitudinal body size in girls of pubertal ontogenesis were found: the height of the suprathoracic and shoulder points differed statistically significantly between groups of girls aged 11 and 12 years, as well as 12 and 13 years; pubic and acetabular points are significantly higher in 11-year-old girls compared to 10-year-old and in 13-year-old girls compared to 12-year-old. The identified patterns are evidence that the most intense processes of longitudinal growth of the torso and lower extremities in girls are observed from 11 years.

A significant difference in the height of the finger point was found between girls of all ages, but the most intense processes of longitudinal growth in girls are observed in the period from 12 to 13 years.

3. It was found that most of the transverse dimensions of the torso, with the exception of the lower thoracic size, within the pubertal period of ontogenesis has a pronounced progressive age dynamic, which is confirmed by significant differences between the comparison groups. The anteroposterior size of the chest increases significantly only after 12 years. We found a difference ($p<0.01$) only between groups of girls 12 and 13 years.

4. A significant increase in the individual transverse dimensions of the pelvis in girls during puberty ontogenesis was found. It was found that in the group of 11-year-old girls the value of intercristal distance was significantly higher than in the group of 10-year-olds. Intertrochanteric distance has a pronounced age dynamics of changes within the pubertal period of ontogenesis, a statistically significant difference was found between groups of girls 11 and 12 years, as well as 12 and 13 years. Interspinous distance and external pelvic conjugate have no statistically significant differences between any comparison group.

## References


[1] Eyer, M., Dainat, B., Neumann, P., & Dietemann, V. (2017). Social regulation of ageing by young workers in the honey bee, Apis mellifera. *Experimental Gerontology,* 87, 84-91, doi: 10.1016/j.exger.2016.11.006

[2] Freitas, A.S., Figueiredo, A.J., deFreitas, A.L., Rodrigues, V.D., daCunha, A.A., Deusdara, F.F. … Silva, M.J. (2014). Biological Maturation, Body Morphology and Physical Performance in 8-16 year-old obese girls from Montes Claros - MG. *J. Hum. Kinet.,* 43, 169-176, doi: 10.2478/hukin-2014-0102

[3] Linpei, J., Weiguang, Z., & Xiangmei, C. (2017). Common methods of biological age estimation. *Clin. Interv. Aging,* 12, 759-772, doi: 10.2147/CIA.S134921

[4] Cairney, J., Veldhuizen, S., Kwan, M., Hay, J., & Faught, B.E. (2014). Biological age and sex-related declines in physical activity during adolescence. *Med. Sci. Sports Exerc.,* 46(4), 730-735, doi: 10.1249/MSS.0000000000000168

[5] Alaux, C., Soubeyrand, S., Prado, A., Peruzzi, M., Maisonnasse, A., Vallon, J. ... Conte, Y. (2018). Measuring biological age to assess colony demographics in honeybees. *PLoS ONE.,* 13(12): e0209192. doi: 10.1371/journal.pone.0209192

[6] Avtandilov, G.G. (1990). *Medical Morphometry*. Moscow: Medicine.

[7] Biro, F.M., Greenspan, L.C., Galvez, M.P., Pinney, S.M., Teitelbaum, S., Windham, G.C. … Wolff, M.S. (2013). Onset of breast development in a longitudinal cohort. *Pediatrics*, 132(6), 1019-1027, doi: 10.1542/peds.2012-3773

[8] Bunak, V.V. (1941). *Anthropometry: a practical course*. M.: Uchpedgiz.

[9] Byrskog, U., Olsson, P., Essen, B., & Allvin, M. K. (2014). Violence and reproductive health preceding flight from war: accounts from Somali born womenin Sweden. *BMC Public Health,* 14, 892, doi: 10.1186/1471-2458-14-892

[10] Cairney, J., Veldhuizen, S., Kwan, M., & Hay, J. (2014). Biological Age and Sex-Related Declines in Physical Activity during Adolescence. *Med. Sci. Sports Exerc.*, 46(4), 730-735, doi: 10.1249/MSS.0000000000000168

[11] Dinnik, V.A. (2017). The current trend to the hour of the start of the state development of the girls (look around the literature and the authorities). *Journal of the National Academy of Medical Sciences of Ukraine*, 23(1-2), 122-128.

[12] Dynnik, V.A. (2015). Pathomorphosis of physical, sexual development and concomitant extragenital pathology in patients with abnormal uterine bleeding during puberty over the past 30 years. *Modern Pediatrics,* 67(3), 120-124, doi: 10.15574/SP.2015.67.120

[13] Dynnik, V.A. (2017). Problems associated with the reproductive potential of girls from the zone of military conflict. *Modern Pediatrics,* 81(1), 34-38, doi: 10.15574/SP.2017.81.34

[14] Elchuri, S.V., & Momen, J.J. (2020). Disorders of Pubertal Onset. *Prim. Care*, 47(2), 189-216, doi: 10.1016/j.pop.2020.02.001

[15] Freitas, A.S., Figueiredo, A.J., de Freitas, A.L., Rodrigues, V.D., da Cunha, A.A. … Silva, M.J. (2014). Biological Maturation, Body Morphology and Physical Performance in 8-16 year-old obese girls from Montes Claros - MG. *Journal of Human Kinetics,* 43, 169-176, doi: 10.2478/hukin-2014-0102

[16] Freitas, A.S., Silveira, M.F., Francisco de Santana, J.J., D'Ângelo, M.F., Haikal, D.S., & Monteiro-Junior, R.S. (2021). New reference parameters for body mass index in children aged six to ten years. *Rev. Paul. Pediatr.,* 39. doi: 10.1590/1984-0462/2021/39/2019129

[17] Herbison, A.E. (2016). Control of puberty onset and fertility by gonadotropin-releasing hormone neurons. *Nat. Rev. Endocrinol.,* 12(8), 452-466, doi: 10.1038/nrendo.2016.70

[18] Kaplowitz, P. (2011). Update on precocious puberty: Girls are showing signs of puberty earlier, but most do not require treatment. *Adv. Pediatrics,* 58(1), 243-58, doi: 10.1016/j.yapd.2011.03.004

[19] Kaplowitz, P., & Bloch, C. (2016). Evaluation and Referral of Children With Signs of Early Puberty. *Pediatrics,* 137(1), doi: 10.1542/peds.2015-3732

[20] Klein, D.A., Emerick, J.E., Sylvester, J.E., & Vogt, K.S. (2017). Disorders of Puberty: An Approach to Diagnosis and Management. *Am. Fam. Physician*, 96(9), 590-599.

[21] Masterson, A.R., J. Usta, J. & Gupta, A.S. (2014). Ettinger Assessment of reproductive health and violence against women among displaced Syrians in Lebanon. *BMC Womens Health*, 14(1), 25. doi: 10.1186/1472-6874-14-25

[22] Morris, D.H., Jones, M.E., Schoemaker, M.J., Ashworth, A., & Swerdlow, A.J. (2011). Secular trends in age at menarche in women in the UK born 1908-93: results from the Breakthrough Generations Study. *Pediatr. Perinat. Epidemiol.,* 25(4), 394-400, doi: 10.1111/j.1365-3016.2011.01202.x

[23] Sarafyniuk, L.A., Khapitska, O.P., Yakusheva, Yu.I., Ivanytsia, A.O., & Sarafyniuk, P.V. (2018). Somatotypological features of acrobat girl in different periods of ontogenesis. *Biomedical and Biosocial Anthropology,* 32, 43-47, doi: 10.31393/bba32-2018-06

[24] Sarafyniuk, L.A., Pivtorak, V.I., Khavtur, V.O., Fedoniuk, L.Ia., & Khapitska, O.P. (2018). Peculiarities of the chest's size in volleyball players of different constitutional types. *Biomedical and Biosocial Anthropology,* 33, 47-52, doi: 10.31393/bba33-2018-08

[25] Schwartz, V.B., & Khrushchev, S.V. (1984). *Biomedical aspects of sports orientation and selection.* Moscow: Physical education and sports.

[26] Sirotchenko, T.A., & Belykh, N.A. (2011). Adolescence in the Mirror of Medical and Social Problems. *Modern Pediatrics,* 38(4), 188-190.

[27] Weiss, K.M., Leal D.B., Assis, M.A., & Pelegrini, A. (2016). Diagnostic accuracy of anthropometric indicators to predict excess body fat in adolescents aged 11-14 years. *Rev. Bras. Cineantropom. Desempenho Hum.,* 18, 548-556, doi: 10.5007/1980-0037.2016v18n5p548/

[28] Zhu, H., Sun, H. P., Pan, C. W., & Xu, Y. (2016). Secular trends of age at menarche from 1985 to 2010 among Chinese urban and rural girls. *Universal J. Publ. Health,* 4(1), 1-7, doi: 10.13189/ujph.2016.040101

**ДИНАМІКА АНТРОПОМЕТРИЧНИХ ПОКАЗНИКІВ У ДІВЧАТОК В МЕЖАХ ПУБЕРТАТНОГО ПЕРІОДУ ОНТОГЕНЕЗУ**

***Сарафинюк П.В., Сарафинюк Л.А., Хапіцька О.П., Ковальчук О.В., Музика Н.О.***

*Гармонійність розвитку організму в різні періоди онтогенезу, а особливо пубертатного, визначає подальшу долю жінки як в медичному, так і в соціальному аспектах. Метою дослідження було вивчення тотальних і парціальних розмірів тіла у дівчаток пубертатного періоду онтогенезу. Нами було обстежено 128 школярки 5-8 класів. Проводили оцінку стадій розвитку вторинних статевих ознак за обволосінням у пахвовій западині і на лобку, розвитком молочних залоз і віком настання першої менструації. Згідно класифікації Г.Г. Автандилова всі дівчатка були розділені на три групи - препубертатного (передування появі лобкового обволосіння), пубертатного (статеве дозрівання до появи менархе) і постпубертатного періоду (закріплюється і завершується пубертатне дозрівання). Групу дівчаток пубертатного віку склали 106 школярок, які були розділені на групи за календарним віком: 13-річні (n=29), 12-річні (n=30), 11-річні (n=24) і 10-річні (n=23). Антропометричне обстеження було проведено згідно схеми В.В. Бунака і містило у собі визначення тотальних (довжини і маси тіла) і парціальних (поздовжніх, поперечних і передньо-задніх) розмірів. Аналіз отриманих результатів проведений в ліцензійному пакеті Statistica 5.5 з використанням непараметричних методів оцінки показників. У нашому дослідженні встановлено, що антропометричні показники характеризують фізичний розвиток, рівень його гармонійності та морфофункціональну зрілість дівчаток у межах пубертатного періоду онтогенезу. Нами виявлена прогресивна вікова динаміка тотальних та парціальних розмірів тіла у дівчаток даного вікового періоду. Встановлені періоди найінтенсивнішого зростання в межах пубертатного періоду онтогенезу тотальних і парціальних розмірів тіла. Наприкінці пубертатного періоду відбувається найінтенсивніший віковий приріст довжин тіла: стрімке збільшення маси тіла починається з 12 років, найінтенсивніші процеси поздовжнього росту тулуба та нижніх кінцівок у дівчаток спостерігаються з 11 років. Більшість поперечних розмірів у межах пубертатного періоду онтогенезу має виражену прогресивну вікову динаміку. Нижньогрудний розмір, міжостьова відстань і зовнішня кон'югата статистично значуще не відрізняються між дівчатками різного віку пубертатного періоду.*

**Ключові слова:** *дівчатка, біологічний вік, пубертатний період, фізичний розвиток, антропометричні розміри.*

DOI: 10.31393/morphology-journal-2021-27(2)-02 Reports of Morphology, Vol. 27, №2, Pages 11-15

ISSN 1818-1295 eISSN 2616-6194

REPORTS OF MORPHOLOGY

*Official Journal of the Scientific Society of Anatomists, Histologists, Embryologists and Topographic Anatomists of Ukraine*

journal homepage: https://morphology-journal.com

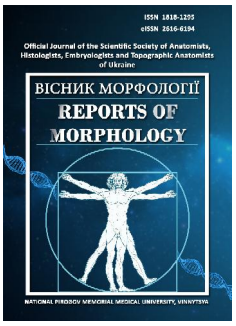


# Morphological changes in the ventilated lung after thoracic surgery

***Sydiuk A.V., Sydiuk O.Ye., Kropelnytskyi V.O., Klimas A.S.***

SI "National Institute of Surgery and Transplantology named after O.O. Shalimov" NAMS of Ukraine

**ARTICLE INFO**

Received: 11 February 2021

Accepted: 2 April 2021

**UDC:** 617.54-089.5:616.24-06-089.163

**CORRESPONDING AUTHOR**

e-mail: siduk1978@gmail.com

Sydiuk A.V.

*There are many studies of single lung ventilation (SLV), which are mostly limited to reducing lung damage by changing ventilation strategies or comparing differences in lung damage caused by different lung isolation devices. There is no study comparing the morphological changes of ventilated lungs using different strategies of artificial lung ventilation. The aim of the study was to examine pathomorphological changes in the ventilated lung during thoracic surgery using SLV. A randomized study was performed on 40 patients who underwent thoracic surgery using SLV. After signing the informed consent, the patients were divided into two groups. In the control group (40 patients) with ventilation "by volume" (VCV), in the study group - ventilation "by pressure" (PCV) with the addition of PEEP 5 mm. During surgery in the thoracic cavity with the help of SLV performed transbronchial biopsy of the parenchyma of the ventilated lung to study the pathomorphological changes after ventilation with different modes. The biopsy was performed using a bronchoscope, which was inserted through the endotracheal tube into the lung, opposite the side of the operation (after the end of SLV and "inclusion" of the collapsed lung). The morphological changes caused by the ventilator were investigated. Pathomorphological examination of the non-collapsed lung (which participated in gas exchange during SLV) was as follows: the control group found significant changes in the alveolar wall with its edema, thickening of the interstitial lung, vascular occlusion, severe inflammatory cell infiltration and damage to alveolar structures. The alveoli collapsed and disappeared. The alveolar structures of the study group were better than the control group: pulmonary interstitial and alveolar exudates, as well as inflammatory cell infiltration were significantly reduced compared to those in the control group. The results of the study suggest that the use of PCV with "moderate" PEEP can significantly improve oxygenation and reduce acute ventilatory injury of the lungs compared to VCV during SLV.*

**Keywords:** *lung morphology, single lung ventilation.*

## Introduction

Single lung ventilation (SLV) is a common method of artificial lung ventilation used in thoracic surgery [4]. It is also well known that SLV is one of the most complex intraoperative methods of respiratory support for anesthesiologists [24]. It should provide the most comfortable surgical field, maintaining proper gas exchange and minimizing damage to the two lungs [17]. Achieving this largely depends on how well the unventilated lung is isolated from the other lung. To ensure sufficient space during surgery, it is recommended to use a complete collapse of the lung. Therefore, an endotracheal tube with a double lumen is usually used. However, this traditional method of ventilation can cause an imbalance of ventilation flow, thereby increasing the number of pulmonary bypass surgery and leading to hypoxemia (occurs in 9-27% of patients) [23]; and can also lead to secondary lung injury. Lung damage caused by ventilator induced lung injury (VILI) [1] has a negative effect [13, 27] and a significant impact on the prognosis of recovery of the patient after surgery [3, 9].

The occurrence of hypoxemia in SLV mainly depends on the correct location of the double lumen tube, the underlying disease and comorbidities, the establishment of the necessary mode of artificial ventilation and the experience of the anesthesiologist in thoracic anesthesiology [12, 15]. Significant hypoxemia [21] is observed in 5-20% of patients who underwent SLV due to increased mismatch of ventilation-perfusion ratio and intrapulmonary shunting [6].

There are many studies of SLV that are mostly limited to reducing lung injury by changing ventilation strategies or comparing differences in lung injuries caused by different

lung isolation devices [6, 8, 18], but there is no study comparing morphological changes in ventilated lungs using different modes of artificial lung ventilation.

Therefore, *the aim* of the study was to study pathomorphological changes in the ventilated lung during thoracic surgery using SLV.

## Materials and methods

A randomized study was performed on 40 patients operated on the thoracic cavity using SLV. After signing the informed consent, the patients were divided into groups. In the study group (40 patients) performed artificial lung ventilation "by volume", in the study group - artificial lung ventilation "by pressure" with the addition of PEEP 5 mm wg. During surgery in the thoracic cavity using SLV performed transbronchial biopsy of the parenchyma of the ventilated lung to study pathomorphological changes after ventilation with different modes. The study was approved at a meeting of the Bioethics Committee.

The biopsy was performed using a bronchoscope, which was inserted through the endotracheal tube into the lung, opposite the side of the operation (after the end of SLV and "inclusion" of the collapsed lung). The morphological changes caused by the ventilator were investigated.

Pathological examination of lung tissue: lung biopsy was fixed in 10% neutral formaldehyde for 24 hours, followed by dehydration and fixation in paraffin. The tissue was cut into sections 5 ?m thick, which were stained with hematoxylin and eosin. Histopathological changes in lung tissue were studied under a light microscope (Olympus, Tokyo, Japan) and evaluated in four categories: 1) alveolar hyperemia, 2) hemorrhage, 3) neutrophilic infiltration or aggregation of the alveolar or vascular wall, or 4) thickening and thickening hyaline membrane. The calculation was performed on a scale of 0-4 points according to the severity of the lesion; 0 points: no or very light lesions; 1 point: light lesions; 2 points: moderate lesions; 3 points: severe lesions; 4 points: very severe lesions. The sum of all scores was taken as a general assessment of acute lung injury (ALI) [26].

The author's package MedStat (Lyakh Yu.E., Guryanov V.G., 2004-2012) was used for statistical calculations, and the Mann-Whitney test was used to compare the obtained results.

## Results

Pathomorphological examination of the non-collapsed lung (which took part in gas exchange during SLV) showed that the control group revealed significant changes in the alveolar wall with its edema, thickening of the interstitial lungs, vascular occlusion, severe inflammatory infiltration of cells and damage to the alveolar structure (Fig. 1) as a result of which some alveoli collapsed and disappeared (Fig. 2). Atelectasis of a part of alveolus with existence in their gleam of single alveolar macrophages is also noted (Fig. 3). Edema and intraalveolar hemorrhages were found

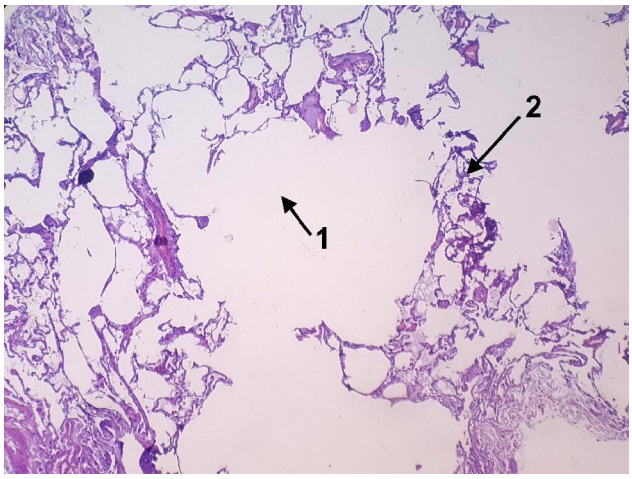


**Fig. 1.** A fragment of the lung parenchyma with a site of pronounced emphysematous transformation of the alveoli. 1 - emphysematous changes, 2 - destroyed alveolar wall. Control group. Hematoxylin-eosin. x40.

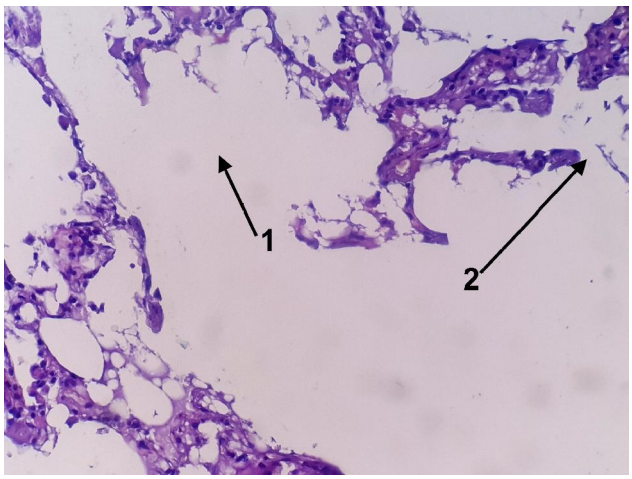


**Fig. 2.** Emphysematous changes in the lung parenchyma: a significant expansion of the lumen of the alveoli with the destruction of part of adjacent alveoli walls. 1 - the lumen of the alveoli, 2 - the destroyed wall of the alveoli. Control group. Hematoxylin-eosin. x200.

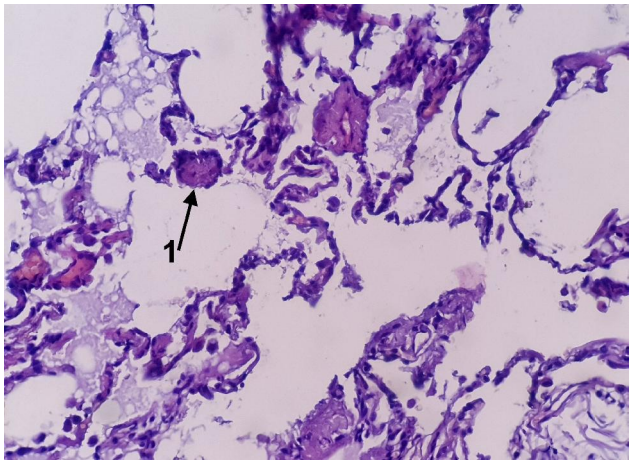


**Fig. 3.** A fragment of the lung parenchyma with atelectasis of the alveoli. In the lumen of the alveoli single alveolar macrophages. 1 - alveolar macrophage. Control group. Hematoxylin-eosin. x200.

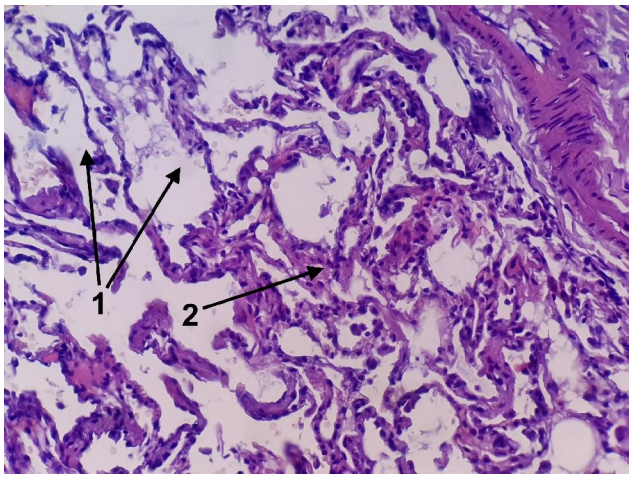


**Fig. 4.** Fragment of the lung parenchyma with the phenomena of alveolar atelectasis, intraalveolar hemorrhage, edema. 1 - atelectasis of the alveoli, 2 - hemorrhage, edema of the alveolar wall. Control group. Hematoxylin-eosin. x200.

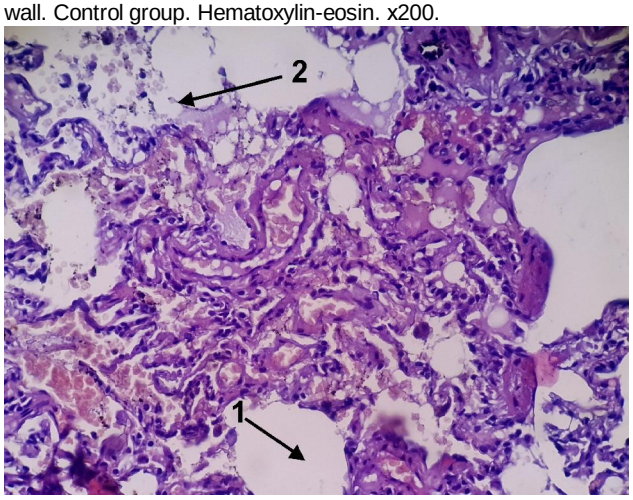


**Fig. 5.** A fragment of the lung parenchyma with normal histological structure. 1 - the lumen of the alveoli, 2 - the wall of the alveoli. The study group. Hematoxylin-eosin. x200.

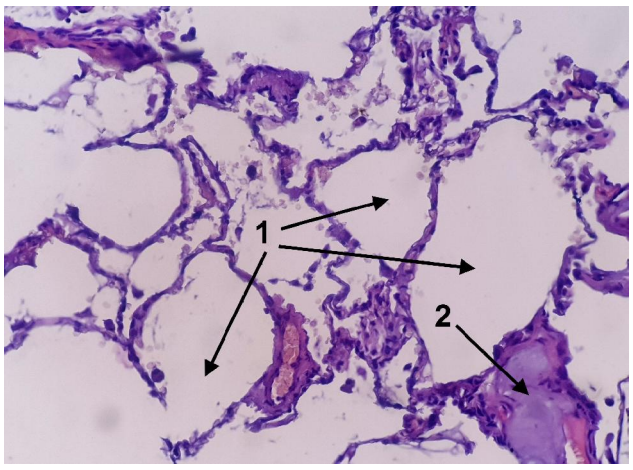


**Fig. 6.** A fragment of lung tissue with a relatively preserved configuration of the alveoli. In the lumen of the alveoli weakly basophilic exudate. 1 - lumen of the alveoli, 2 - exudate. The study group. Hematoxylin-eosin. x200.

in atelectasis alveoli (Fig. 4).

Thus, hyperemia and marked hemorrhages were observed in the lung tissue. In alveolar cavities the big infiltration by erythrocytes and inflammatory cells was found. The alveolar wall was hyperemic, thickened, with serous exudation and the formation of a transparent membrane.

Alveolar structures in the study group were more preserved than in the control group; most often the lung parenchyma was of normal histological structure (Fig. 5), exudates of the pulmonary interstitial and alveolar cavities, as well as inflammatory cell infiltration were significantly reduced compared with those of the control group, in the lumen of the alveoli observed weak basophilic exudate (Fig. 6).

Score ALI in each group: control group: 11.13±0.78 points; study group: 6.942±0.523 points ($p<0.05$).

## Discussion

Excessive dilation of the alveoli during mechanical ventilation, which occurs when overstretched during SLV, can cause inflammatory reactions in the ventilated lung and initiate a cascade of inflammation [10, 14]. Pulmonary shunting, high airway pressure, ischemic-reperfusion injury and ventilatory imbalance can damage the alveolar capillary endothelium and stimulate alveolar macrophages to release large amounts of proinflammatory mediators [7].

Due to the imbalance of the ventilation/perfusion ratio during SLV, hypoxemia can occur, causing the release of a large number of inflammatory mediators, increasing the permeability of the pulmonary capillaries [11] and increasing the water content in the lungs on the destroyed side, eventually to acute lung injury (ALI). The main pathological changes are severe pneumonia, neutrophil aggregation, edema of the interstitial space of the lung, damage to the endothelial cells of the pulmonary capillary, the integrity of the cells of the alveolar epithelium and the penetration of protein-rich fluids into the alveolar cavities.

Due to pathomorphological observation this study revealed edema of the alveolar wall, thickening of the interstitial space of the lungs, significant inflammatory infiltration of cells in the alveolar cavities and damaged alveolar structure.

G.F. Nieman and co-authors [19] also suggested that mechanical ventilation can lead to lung damage due to collapse and re-expansion of the operated lung during SLV. High oxygen pressure in hypoxic-ischemic lung tissue can lead to the production of reactive oxygen species, cell damage and local leukocyte infiltration. The number of oxygen free radicals is proportional to the duration of SLV [5, 20]. It has been reported [22, 25] that re-expansion of the operated lung may lead to increased expression of inflammatory mediators [2].

In our study, significant hemorrhages with hyperemia of lung tissue, as well as infiltration of alveoli by leukocytes and erythrocytes were also found after SLV. However, when using the developed ventilation methods, these changes

were minimal and morphological examination of lung tissue revealed that its appearance was as close as possible to physiological.

Our study has successfully shown that the use of SLV "with controlled pressure" and "moderate" PEEP can significantly improve oxygenation and reduce acute ventilatory damage.

## Conclusions

The results of the study indicate that the use of SLV "with controlled pressure" and "moderate" PEEP can significantly improve oxygenation and reduce acute ventilatory damage to the lungs compared to SLV "by volume".

## References


[1] Ahmed, L.A., El-Maraghy, S.A., & Rizk, S.M. (2015). Role of the KATP channel in the protective effect of nicorandil on cyclophosphamide-induced lung and testicular toxicity in rats. *Sci. Rep.,* 5, 14-43. https://doi.org/10.1038/srep14043

[2] Arnal, J.M., Paquet, J., Wysocki, M., Demory, D., Donati, S., Granier, I. … Durand-Gasselin, J. (2011). Optimal duration of a sustained inflation recruitment maneuver in ARDS patients. *Intensive Care Med.,* 37, 1588-1594. doi: 10.1007/s00134-011-2323-0

[3] Ary Serpa Neto, Cardoso, S.O., Manetta, J.A., Pereira, V.G.M., Esposito D.C., Pasqualucci, de O. Prado M. … Schultz, M.J. (2012). Association between use of lung-protective ventilation with lower tidal volumes and clinical outcomes among patients without acute respiratory distress syndrome: A meta-analysis. *JAMA,* 308(16), 1651-1659. doi: 10.1001/jama.2012.13730

[4] Bernasconi, F., & Piccioni, F. (2017). One-lung ventilation for thoracic surgery: Current perspectives. *Tumori,* 103(6), 495-503. doi: 10.5301/tj.5000638

[5] Cheng, Y.J., Chan, K.C., Chien, C.T., Sun, W.Z., & Lin, C.J. (2006). Oxidative stress during 1-lung ventilation. *J. Thorac. Cardiovasc. Surg.,* 132, 513-518. doi: 10.1016/j.jtcvs.2006.03.060

[6] Clayton-Smith, A., Bennett, K., Alston, R.P., Adams, G., Brown, G., Hawthorne, T. … Tan, J. (2015). A comparison of the efficacy and adverse effects of double-lumen endobronchial tubes and bronchial blockers in thoracic surgery: A systematic review and meta-analysis of randomized controlled trials. *J. Cardiothorac. Vasc. Anesth.*, 29, 955-966. doi: 10.1053/j.jvca.2014.11.017

[7] Ding, N., Wang, F., Xiao, H., Xu, L., & She, S. (2013). Mechanical ventilation enhances HMGB1 expression in an LPS-induced lung injury model. *PLoS One*, 8(9), e74633. https://doi.org/10.1371/journal.pone.0074633

[8] Falzon, D., Alston, R.P., Coley, E., & Montgomery, K. (2017). Lung isolation for thoracic surgery: From inception to evidence-based. *J. Cardiothorac. Vasc. Anesth.*, 31, 678-693. doi: 10.1053/j.jvca.2016.05.032

[9] Gajic, O., Dara, S.I., Mendez, J.L., Adesanya, A.O., Festic, E., Caples, S.M. … Hubmayr, R.D. (2004). Ventilator-associated lung injury in patients without acute lung injury at the onset of mechanical ventilation. *Crit. Care Med.*, 32, 1817-1824. doi: 10.1097/01.ccm.0000133019.52531.30

[10] Garcia-de-la-Asuncion, J., Garcia-del-Olmo, E., Perez-Griera, J., Marti, F., Galan, G., Morcillo, A. … Belda, J. (2015). Oxidative lung injury correlates with one-lung ventilation time during pulmonary lobectomy: A study of exhaled breath condensate and blood. *Eur. J. Cardiothorac. Surg.,* 48, e37-e44, doi: 10.1093/ejcts/ezv207

[11] Helenius, I.T., Dada, L.A., & Sznajder, J.I. (2010). Role of ubiquitination in Na,K-ATPase regulation during lung injury. *Proc. Am. Thorac. Soc.*, 7, 65-70. doi: 10.1513/pats.200907-082JS

[12] Ishikawa, S., & Lohser, J. (2011). One-lung ventilation and arterial oxygenation. *Curr. Opin. Anaesthesiol.,* 24, 24-31, 2011. doi: 10.1097/ACO.0b013e3283415659

[13] Jeon, K., Yoon, J.W., Suh, G.Y., Kim, J., Kim, K., Yang, M. … Shim, Y.M. (2009). Risk factors for post-pneumonectomy acute lung injury/acute respiratory distress syndrome in primary lung cancer patients. *Anaesth. Intensive Care,* 37, 14-19. doi: 10.1177/0310057X0903700110

[14] Jin, Y., Zhao, X., Li, H., Wang, Z., & Wang, D. (2013). Effects of Sevoflurane and Propofol on the inflammatory response and pulmonary function of perioperative patients with one-lung ventilation. *Exp. Ther. Med.,* 6, 781-785. doi: 10.3892/etm.2013.1194

[15] Karzai, W., & Schwarzkopf, K. (2009). Hypoxemia during one-lung ventilation: Prediction, prevention, and treatment. *Anesthesiology,* 110(6), 1402-1411. doi: 10.1097/ALN.0b013e31819fb15d

[16] Lee, S.M., Kim, W.H., Ahn, H.J., Kim, J.A., Yang, M.K., Lee, C.H. … Choi, J.W. (2013). The effects of prolonged inspiratory time during one-lung ventilation: A randomised controlled trial. *Anaesthesia,* 68, 908-916. doi: 10.1111/anae.12318

[17] Licker, M., Fauconnet, P., Villiger, Y., & Tschopp, J.M. (2009). Acute lung injury and outcomes after thoracic surgery. *Curr. Opin. Anaesthesiol.*, 22(1), 61-67. doi: 10.1097/ACO.0b013e32831b466c

[18] Lohser, J., & Slinger, P. (2015). Lung injury after one-lung ventilation: a review of the pathophysiologic mechanisms affecting the ventilated and the collapsed lung. *Anesth. Analg.*, 121, 302-318. doi: 10.1213/ANE.0000000000000808

[19] Nieman, G.F., Satalin, J., Andrews, P., Aiash, H., Habashi, N.M., & Gatto, L.A. (2017). Personalizing mechanical ventilation according to physiologic parameters to stabilize alveoli and minimize ventilator induced lung injury (VILI). *Intensive Care Med. Exp.,* 5(8). doi: 10.1186/s40635-017-0121-x

[20] Riva, D.R., Contador, R.S., Baez-Garcia, C.S., Xisto, D.G., Cagido, V.R., Martini, S.V. … Zin, W.A. (2009). Recruitment maneuver: RAMP versus CPAP pressure profile in a model of acute lung injury. *Respir. Physiol. Neurobiol.,* 169, 62-68. doi: 10.1016/j.resp.2009.08.010

[21] Roz, H., Lafargue, M., & Ouattara, A. (2011). Case scenario: Management of intraoperative hypoxemia during one-lung ventilation. *Anesthesiology,* 114, 167-174. doi: 10.1097/ALN.0b013e3182023ed3

[22] Rzezinski, A.F., Oliveira, G.P., Santiago, V.R., Santos, R.S., Ornellas, D.S., Morales, M.M. … Rocco, P.R. (2009). Prolonged recruitment manoeuvre improves lung function with less ultrastructural damage in experimental mild acute lung injury. Respir. *Physiol. Neurobiol.*, 169, 271-281. doi: 10.1016/j.resp.2009.10.002

[23] Seo, J.H., Cho, C.W., Hong, D.M., Jeon, Y., & Bahk, J.H. (2016). The effects of thermal softening of double-lumen endobronchial tubes on postoperative sore throat, hoarseness and vocal cord injuries: A prospective double-blind randomized trial. *Br. J. Anaesth.,* 116(2), 282-288. doi: 10.1093/bja/aev414

[24] Shiva, S., Sack, M.N., Greer, J.J., Duranski, M., Ringwood,

L.A., Burwell, L. … Gladwin, M.T. (2007). Nitrite augments tolerance to ischemia/reperfusion injury via the modulation of mitochondrial electron transfer. *J. Exp. Med.,* 204(9), 2089-2102. doi: 10.1084/jem.20070198

[25] Silva, P.L., Moraes, L., Santos, R.S., Samary, C., Ornellas, D.S., Maron-Gutierrez, T. … Rocco, R.M.P. (2011). Impact of pressure profile and duration of recruitment maneuvers on morphofunctional and biochemical variables in experimental lung injury. *Crit. Care Med.,* 39(5), 1074-1081. doi: 10.1097/CCM.0b013e318206d69a

[26] Sinclair, S.E., Kregenow, D.A., Lamm, W.J., Starr, I.R., Chi, E.Y., & Hlastala, M.P. (2002). Hypercapnic acidosis is protective in an in vivo model of ventilator-induced lung injury. Am. J. Respir. *Crit. Care Med.,* 166, 403-408. doi: 10.1164/rccm.200112-117OC

[27] Tusman, G., Bohm S.H., Warner, D.O., & Sprung, J. (2012). Atelectasis and perioperative pulmonary complications in high-risk patients. *Curr. Opin. Anaesthesiol.,* 25, 1-10. doi: 10.1097/ACO.0b013e32834dd1eb

**МОРФОЛОГІЧНІ ЗМІНИ У ВЕНТИЛЬОВАНІЙ ЛЕГЕНІ ПІСЛЯ ТОРАКАЛЬНИХ ОПЕРАЦІЙ**

***Сидюк А.В., Сидюк О.Є., Кропельницький В.О., Клімас А.С.***

*Існує багато досліджень однолегеневої вентиляції (ОЛВ), котрі здебільшого обмежуються зменшенням пошкодження легень шляхом зміни стратегій вентиляції або порівняння відмінностей у пошкодженнях легень, спричинених різними пристроями ізоляції легень. Немає жодного дослідження, в якому би порівнювали морфологічні зміни вентильованих легень з використанням різних стратегій штучної вентиляції легень. Метою дослідження було вивчення патоморфологічних змін у вентильованій легені під час торакальної операції з використанням ОЛВ. Було проведено рандомізоване дослідження на 40 пацієнтах, котрі перенесли операції на грудній порожнині з використанням ОЛВ. Після підписання інформованої згоди пацієнти були розділені на дві групи. У контрольній групі (40 пацієнтів) з вентиляцією "за об'ємом" (VCV), у досліджуваній групі - вентиляцією "за тиском" (PCV) з додаванням PEEP 5 мм. Під час хірургічного втручання в грудній порожнині за допомогою ОЛВ виконали трансбронхіальну біопсію паренхіми вентильованої легені для вивчення патоморфологічних змін після штучної вентиляції легень з різними режимами. Біопсію виконували за допомогою бронхоскопу, котрий заводили крізь ендотрахеальну трубку в легеню, протилежну стороні оперативного втручання (після закінчення ОЛВ та "включення" колабованої легені). Досліджували морфологічні зміни, спричинені апаратом штучної вентиляції. Патоморфологічне дослідження легені, що не була колабована (котра брала участь в газообміні під час ОЛВ), було таким: контрольна група виявила значні зміни в альвеолярній стінці з її набряком, потовщенням інтерстиціальної легені, оклюзією судин, важкою запальною інфільтрацією клітин та пошкодженням альвеолярних структур. Альвеоли зруйнувались і зникли. Альвеолярні структури досліджуваної групи були кращими, ніж контрольної групи: легеневі інтерстиціальні та альвеолярні ексудати, а також запальна клітинна інфільтрація були значно зменшені порівняно з такими у контрольній групі. Результати дослідження дозволяють припустити, що використання PCV з "помірним" PEEP може значно покращити оксигенацію та зменшити гостру вентиляційну травму легень порівняно з VCV під час ОЛВ.*

**Ключові слова:** *морфологія легень, однолегенева вентиляція.*

**DOI: 10.31393/morphology-journal-2021-27(2)-03** **Reports of Morphology, Vol. 27, №2, Pages 16-22**

**ISSN 1818-1295 eISSN 2616-6194**

**REPORTS OF MORPHOLOGY**

***Official Journal of the Scientific Society of Anatomists, Histologists, Embryologists and Topographic Anatomists of Ukraine***

journal homepage: https://morphology-journal.com

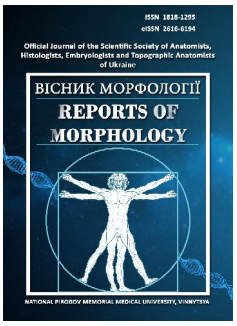


# Fractal dimension of external linear contour of human cerebellum (magnetic resonance imaging study)

***Maryenko N.I., Stepanenko O.Y.***
Kharkiv National Medical University, Kharkiv, Ukraine

**ARTICLE INFO**
Received: 12 February 2021
Accepted: 5 April 2021

**UDC:** 611.817.1:57.086:517:530.191

**CORRESPONDING AUTHOR**
e-mail: maryenko.n@gmail.com
Maryenko N.I.

*Fractal analysis is a method of mathematical analysis, which provides quantitative assessment of the spatial configuration complexity of the anatomical structures and may be used as a morphometric method. The purpose of the study was to determine the values of the fractal dimension of the outer linear contour of human cerebellum by studying the magnetic resonance images of the brain using the authors' modification of the caliper method and compare to the values determined using the box counting method. Brain magnetic resonance images of 30 relatively healthy persons aged 18-30 years (15 men and 15 women) were used in the study. T2-weighted digital magnetic resonance images were studied. The midsagittal MR sections of the cerebellar vermis were investigated. The caliper method in the author's modification was used for fractal analysis. The average value of the fractal dimension of the linear contour of the cerebellum, determined using the caliper method, was 1.513±0.008 (1.432¸ 1.600). The average value of the fractal dimension of the linear contour of the cerebellum, determined using the box counting method, was 1.530±0.010 (1.427¸ 1.647). The average value of the fractal dimension of the cerebellar tissue as a whole, determined using the box counting method, was 1.760±0.006 (1.674¸ 1.837). The values of the fractal dimension of the outer linear contour of the cerebellum, determined using the caliper method and the box counting method were not statistically significantly different. Therefore, both methods can be used for fractal analysis of the linear contour of the cerebellum. Fractal analysis of the outer linear contour of the cerebellum allows to quantify the complexity of the spatial configuration of the outer surface of the cerebellum, which is difficult to estimate using traditional morphometric methods. The data obtained from this study and the methodology of the caliper method of fractal analysis in the author's modification can be used for morphometric investigations of the human cerebellum in morphological studies, as well as in assessment of cerebellar MR images for diagnostic purposes.*

**Keywords:** *fractal analysis, caliper method, box counting method, cerebellum, magnetic resonance imaging.*

## Introduction

The human cerebellum has a rather complex spatial configuration, which is the most complex of all the structures of the central nervous system. At the base of the cerebellum is a white substance, which on sagittal and parasagittal sections has a tree-like branched shape. The cerebellar cortex covers the white matter from the outside, repeating the shape of the outer surface of the white matter and forming convolutions - cerebellar folia. Peculiarities of foliation (division of the cerebellar cortex into folia) and fissure of the cortex (delimitation of folia and lobes of the cerebellum by slits) reflect and determine the complexity of the spatial organization of the cerebellum as a whole [22]. In this case, disorders of foliation and fissure of the cortex, arising from disorders of cerebral morphogenesis, is one of the main morphological features of various malformations of the cerebellum [5]. These disorders underlie the classifications of cerebellar malformations and are used as their diagnostic criteria [5, 18, 21].

In addition, changes in the spatial configuration of the surface of the cerebellar cortex, probably, can be observed in other diseases and pathological conditions. For example, smoothing of the surface of the cortex of the cerebral hemispheres was observed in atrophic changes of the brain [10, 11, 12], similar changes can be observed in the

presence of atrophic changes of the cerebellum [6]. However, the characterization of foliation and fissuration of the cerebellar cortex is subjective and descriptive, without defining objective quantitative parameters. Therefore, the search for and development of techniques that could objectively characterize the complexity of the spatial configuration of the surface of the cerebellar cortex is an important area of research in modern neuroscience and morphology.

In recent years, fractal analysis has been increasingly used as a morphometric method. This type of mathematical analysis is used to estimate the complexity of the spatial configuration of different objects. The fractal dimension, which is determined in this case, characterizes the degree of filling of space with a certain object and increases with the complexity of the spatial configuration of this object. Values of fractal dimension, defined on two-dimensional images, vary from 1 to 2 [3, 4, 16]. For fractal analysis in morphology, neuroscience (including neuroimaging) use different methods of fractal analysis [3, 4, 7, 8, 9, 19], among which the most commonly used methods are box counting [1, 2, 10, 11, 15, 23, 24] and pixel dilatation [14, 17]. The caliper method is also sometimes used [13, 20]. For fractal analysis of various components of the cerebellar tissue most often use the method of box counting [1, 2, 23], less often - pixel dilatation in various modifications [14, 17]. Studies involving fractal analysis of the cerebellum using the caliper method have not been found in the available scientific literature. The method of caliper in the classical version in medicine is rarely used because of its routine. We have developed our own modification of the caliper method, which allows calculations to be performed automatically and more accurately than the classic version. For comparison, we chose the box counting method, which is most often used as a morphometric method in medicine and morphology.

*The aim* of the study was to determine the values of the fractal dimension of the external linear contour of the cerebellum by examining magnetic resonance imaging of the brain using the author's modification of the caliper method and compare with the values determined using the box counting method.

## Materials and methods

The study was conducted in compliance with the basic bioethical provisions of the Council of Europe Convention on Human Rights and Biomedicine (04.04.1997), the Helsinki Declaration of the World Medical Association on the ethical principles of scientific medical research with human participation (1964-2008), as well as the order The Ministry of Health of Ukraine №690 dated 23.09.2009. The conclusion of the Commission on Ethics and Bioethics of Kharkiv National Medical University confirms that the study was conducted in compliance with human rights, in accordance with current legislation in Ukraine, meets international ethical requirements and does not violate ethical standards for conducting biomedical research (Minutes of the meeting of the commission on ethics and bioethics of KNMU №10 from 07.11.2018).

In study used brain tomograms of 30 relatively healthy individuals (without detected structural changes in the brain) aged 18-30 years, including 15 men and 15 women.

Tomograms were obtained using a magnetic resonance imaging Siemens Magnetom Symphony with a magnetic induction value of 1.5 T. T2-weighted magnetic resonance (MR) images were used for the study. The parameters of magnetic resonance imaging were as follows: TE (echo time) 122 ms, TR (repetition time) 4520 ms, slice thickness - 5 mm. The median sagittal tomographic sections of the cerebellar worm were examined. For fractal analysis, the caliper method in the author's modification and the box counting method in the classical version were used.

Before fractal analysis, pre-processing of magnetic resonance (MR) images of the cerebellum was performed. To do this, a 128x128 pixel fragment was copied from the digital MR image, which completely contained a tomographic section of the cerebellum (Fig. 1A). Further processing and analysis of images was performed in Adobe Photoshop CS5.

To highlight the outer linear contour of the cerebellum, image segmentation was first performed. The areas of the digital image surrounding the cerebellum (background structures) were painted white (Fig. 1B). After that, the image was converted to binary format (Fig. 1C). The pixels of the binary raster image were of two colours: black (pixel brightness value 0; black pixels corresponded to the cerebellar tissue as a whole) or white (pixel brightness value 255; white pixels were background). The halftone image was converted to binary using the Adobe Photoshop CS5 "threshold" tool, which coloured all pixels darker than the specified threshold to black and lighter to white. The brightness thresholds ranged from 100 to 115 and were selected empirically so that the boundaries of the segmented area in the image corresponded to the outer contour of the cerebellar cortex.

After segmentation, fractal analysis was performed using the caliper method in the author's modification. This method included 5 stages. In the first stage of fractal analysis, the segmented area was selected using the "selection" tool of Adobe Photoshop CS5 (Fig. 1D) and the length of the contour (perimeter of the selected area) in pixels was measured using the "analysis" tool.

In the second stage of fractal analysis, a contour with a radius of 2 pixels was smoothed using the tool "selection - modification - smoothing" of Adobe Photoshop CS5 (Fig. 1E). In this case, all bends of the linear contour that had a radius less than the specified value of the smoothing radius were removed from the contour, replaced by a smooth line ("smoothed"). After smoothing, the contour length was measured again.

In the third to fifth stages of the fractal analysis, the

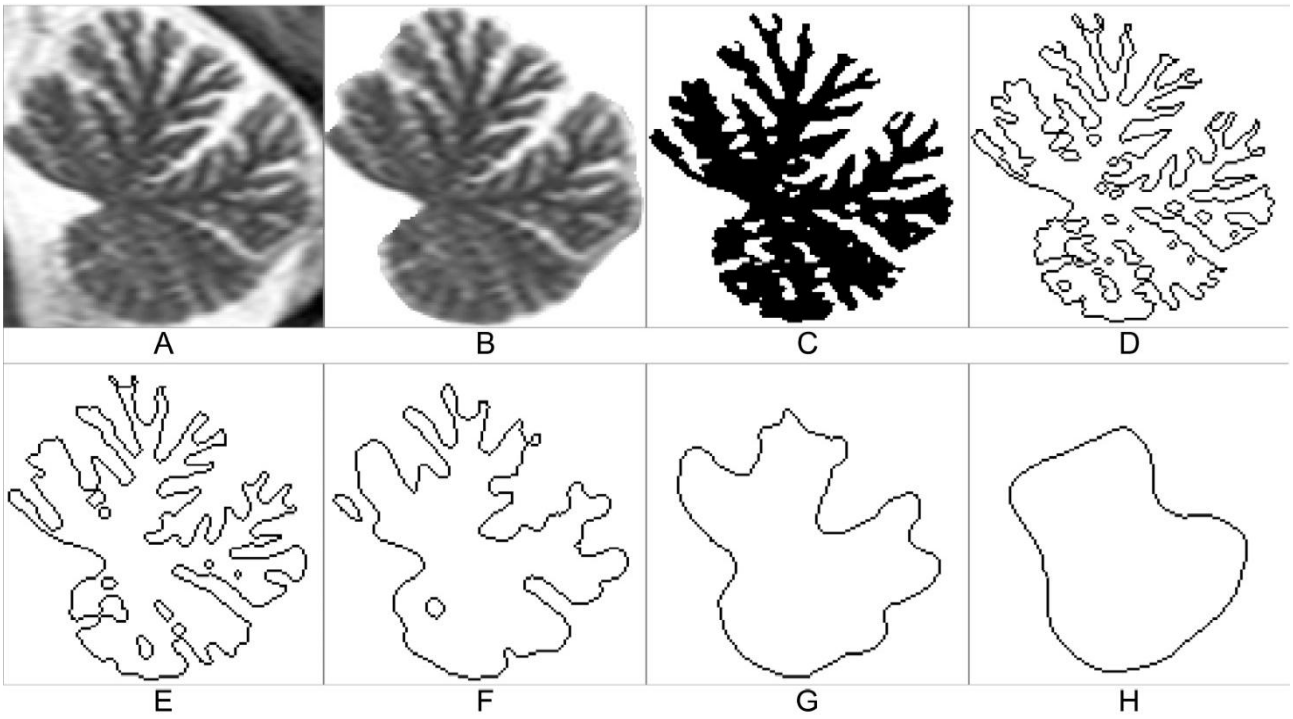


**Fig. 1.** Preliminary processing (A-C) and stages of MR images fractal analysis of the human cerebellum using the method of caliper (D-H). A - the original image; B - removal of background structures; C - segmented binary image (cerebellar tissue as a whole); D-H - external linear contour of the cerebellum at different stages of fractal analysis: D - 1st stage, contour smoothing is not used; E - 2nd stage, smoothing radius 2 pixels; F - 3rd stage, smoothing radius 4 pixels; G - 4th stage, smoothing radius 8 pixels; H - 5th stage, smoothing radius 16 pixels.

contour was smoothed again. In the third stage, the smoothing radius was 4 pixels, in the fourth - 8 pixels, in the fifth - 16 pixels (Fig. 1F-H). After each contour modification, the contour length was measured by smoothing it.

Then determined the value of the fractal dimension by the formula:

$$FD_a = \frac{\sum_{i=1}^{5}(Ln_{(1/R_i)} - \overline{Ln_{(1/R)}})(Ln_{(P_i/P_i)} - \overline{Ln_{(P/R)}})}{\sum (Ln_{(1/R_i)} - \overline{Ln_{(1/R)}})^2}$$

where $FD_a$ is the fractal dimension of the linear contour determined by the caliper method; R - contour smoothing radius (in pixels); P - length of the linear contour (in pixels), i - iteration (fractal analysis stage).

Since no smoothing was used in the first stage of fractal analysis, the value of $R_1$ was taken as 1 ($R_1$=1, $R_2$=2, $R_3$=4, $R_4$=8, $R_5$=16).

To compare the values of the fractal dimension of the linear contour of the cerebellum, determined by the author's modification of the caliper method with the values obtained by classical methods of fractal analysis, also performed fractal analysis using the method of box counting. Image J program was used for this method. Using this program, 2 values of fractal dimension were determined: $FD_b$ - fractal dimension of the linear contour of the cerebellum and $FD_c$ - fractal dimension of cerebellar tissue as a whole. To determine the $FD_b$, we used the contour of the selected area with a line width of 1 pixel (Fig. 1D), and then performed a fractal analysis of the linear contour using the method of box counting. $FD_c$ values were determined on segmented binary images (Fig. 1C). The following box size values were selected for box fraction analysis in Image J: 2, 4, 8, 16, 32 (1/64, 1/32, 1/16, 1/8, 1/4).

To identify factors associated with the values of the fractal dimension of the cerebellum, the following morphometric parameters and their ratio were determined: the length of the contour (perimeter) of the tomographic section of the cerebellum as a whole ($P_0$), which corresponded to the contour of the visible surface of the cerebellum; the area of the tomographic section of the cerebellum as a whole ($S_0$) (Fig. 1B), the length of the contour (perimeter) of the segmented area (Ps) and the area of the segmented area ($S_s$) (Fig. 1C). Based on these data for the tomographic section as a whole and for the segmented area, the values of the form factor ($SF_0$ and $SF_s$) were calculated by the formula:

$$SF = \frac{4p' S}{P^2}$$

where SF - shape factor, S - area, P - length of the contour (perimeter).

Statistical data processing was performed using Microsoft Excel 2010. For variation series, the following statistical parameters were calculated: arithmetic mean (M), its error ($m_M$), standard deviation (σ) and coefficient of

variation (CV). To determine the distribution of fractal dimension values, the median (Me), the values of the 25th and 75th percentiles, the minimum (min) and maximum (max) values were determined. The distribution of values for normality was checked using the Shaporo-Wilk W test. The significance of the statistical differences between the three values of the fractal dimension was assessed using the Kruskal-Wallis KW test with multiple Bonferroni correction for multiple comparisons. Pearson's correlation coefficient (r) was calculated to identify and characterize the correlations between the studied parameters. The significance of the correlation was assessed using the Student T test.

## Results

The average value of $FD_a$ (fractal dimension of the linear contour of the cerebellum, determined using the caliper method) was 1.513±0.008. The minimum value of $FD_a$ was 1.432, the maximum - 1.600. The standard deviation was 0.042, the coefficient of variation was 2.79%, which indicates low variability of fractal dimension values. $FD_a$ values were distributed normally ($p>0.05$).

The average value of $FD_b$ (fractal dimension of the linear contour of the cerebellum, determined by the method of box counting) was 1.530±0.010. The minimum value of $FD_b$ was 1.427, the maximum - 1.647. The standard deviation was 0.053, the coefficient of variation was 3.45%, which is slightly higher than the corresponding $FD_a$, but also indicates the low variability of this value of the fractal dimension. $FD_b$ values were also distributed normally ($p>0.05$).

The average value of $FD_c$ (fractal dimension of the cerebellar tissue as a whole, determined by the method of box counting) was 1.760±0.006. The minimum value of $FD_c$ was 1.674, the maximum - 1.837. The standard deviation was 0.030, the coefficient of variation was 1.73%, which also indicates the low variability of this value of the fractal dimension. $FD_c$ values were distributed normally ($p>0.05$). The statistical distribution of $FD_a$, $FD_b$ and $FD_c$ values is shown in Fig. 2.

The values of the fractal dimensions of the linear contour and the cerebellar tissue as a whole, determined by different methods ($FD_a$, $FD_b$ and $FD_c$) were compared with each other using the Kruskal-Wallis test. When checking the differences between the values of the three fractal dimensions, it was found that the values as a whole were statistically significantly different ($p»0$).

In a further pairwise comparison of values, it was found that the value of $FD_c$, which characterizes the cerebellar tissue as a whole, was statistically significantly different from the two values of the fractal dimension characterizing the linear contour of the cerebellum ($FD_a$ and $FD_b$) ($p»0$). But the two values of the fractal dimension that characterize the linear contour ($FD_a$ and $FD_b$) did not differ statistically significantly ($p>0.05$). Thus, the values of the fractal dimension of the linear contour of the cerebellum, determined using different methods of fractal analysis (caliper and box counting), had similar values, and the methods gave comparable results. Next, the magnitude of the difference was determined and the relationship between these values of the fractal dimension was investigated.

The difference between the two values of the fractal dimension that characterize the linear contour of the cerebellum ($FD_b$ - $FD_a$), ranged from -0.061 to 0.113; the median value of this parameter was 0.014; the value of the 25th percentile was -0.019; the value of the 75th percentile was 0.050. The value of the difference between the two values of the fractal dimension is associated with a statistically significant strong positive correlation with the value of the fractal dimension of the cerebellar tissue as a whole ($FD_c$) ($r=0.77$, $p<0.05$), a positive correlation of medium strength with the value of the fractal dimension of the linear contour, determined by the method of box counting ($FD_b$) ($r=0.64$, $p<0.05$), and with the area of the segmented area ($S_s$) ($r=0.54$, $p<0.05$). There was no statistically significant correlation with the value of the fractal dimension of the linear contour determined by the caliper ($FD_a$) method ($r=-0.28$, $p>0.05$). In 17 objects out of 30 (56.7%) the value of FDb was higher than FDa.

The ratio of the absolute value of the difference between the two values of the fractal dimension of the linear contour of the cerebellum ($|FD_b - FD_a|$) to the arithmetic mean of these two values ($(FD_a + FD_b) / 2$) varied from 0.07% to 7.08%; the average value was 2.56±0.34%. This value is associated with a statistically significant positive correlation of medium strength with the value of the fractal dimension of the cerebellar tissue as a whole ($FD_c$) ($r=0.60$, $p<0.05$),

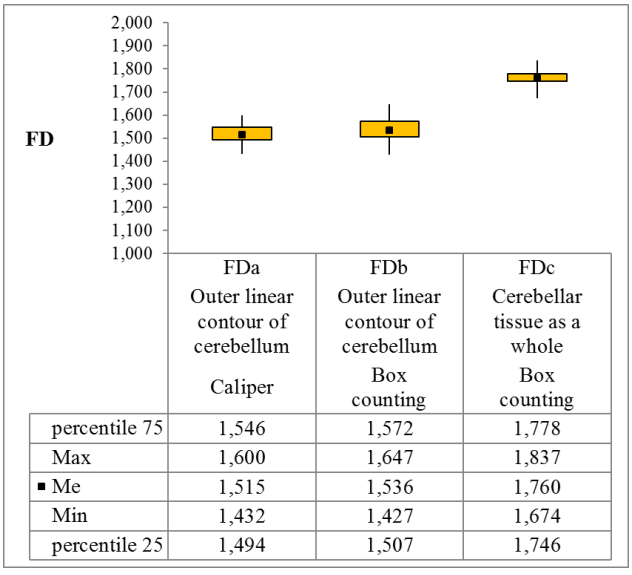


| | FDa Outer linear contour of cerebellum Caliper | FDb Outer linear contour of cerebellum Box counting | FDc Cerebellar tissue as a whole Box counting |
|---|---|---|---|
| percentile 75 | 1,546 | 1,572 | 1,778 |
| Max | 1,600 | 1,647 | 1,837 |
| Me | 1,515 | 1,536 | 1,760 |
| Min | 1,432 | 1,427 | 1,674 |
| percentile 25 | 1,494 | 1,507 | 1,746 |

**Fig. 2.** Distribution of fractal dimensions values of cerebellum external linear contour, determined by different methods of fractal analysis (caliper and box counting) and fractal dimensions of cerebellar tissue as a whole, determined by the method of box counting.

and with the area of the segmented area ($S_s$) (r=0.58, p<0.05), a negative correlation with the value of the fractal dimension of the linear contour, determined by the method of caliper ($FD_a$) (r=-0.39, p<0.05). No statistically significant correlation was found with the fractal dimension of the linear contour determined by the box counting ($FD_b$) method (r=0.24, p>0.05).

Therefore, the larger the area of the segmented portion of the image corresponding to the cerebellar tissue as a whole and the greater the fractal dimension characterizing the cerebellar tissue as a whole, the greater the fractal dimension of the linear contour determined by the box counting method exceeded the value determined by using the caliper method and the greater was the difference between these values in general.

When performing correlation analysis, it was found that between the two values of the fractal dimension of the external linear contour of the cerebellum, determined by different methods of fractal analysis ($FD_a$ and $FD_b$), there is a positive correlation of medium strength (r=0.56, p<0.05). No statistically significant correlation was found between $FD_a$ and $FD_c$ values (r=-0.17, p>0.05). There is a positive correlation of medium strength between the values of $FD_b$ and $FD_c$ (r=0.53, p<0.05).

The average value of the ratio of the length of the contour (perimeter) of the tomographic slice as a whole to the area of the slice ($P_0/S_0$) was (0.0358¸ 0.0455, σ=0.0027, CV=6.65%). The average value of the factor of the shape of the tomographic section as a whole ($SF_0$) was 0.69±0.01 (0.56¸ 0.75, σ=0.05, CV=6.75%).

The average value of the ratio of the length of the contour (perimeter) to the area of the segmented area ($P_s/S_s$) was 0.205±0.006 (0.161¸ 0.271, σ=0.031, CV=15.19%). The average value of the shape factor of the segmented area ($SF_s$) was 0.047±0.002 (0.028¸ 0.076, σ=0.012, CV=24.94%).

The average value of the ratio of the length of the contour (perimeter) of the segmented area to the length of the contour of the tomographic section as a whole ($P_s/P_0$) was 3.030±0.060 (2.400¸ 3.580, σ = 0.32, CV=10.69%). The average value of the ratio of the area of the segmented area to the area of the tomographic section as a whole ($S_s/S_0$) was 0.600±0.010 (0.510¸ 0.740, σ = 0.050, CV=8.34%).

A correlation analysis was also performed between the values of fractal dimensions of the cerebellum ($FD_a$, $FD_b$ and $FD_c$) and the above morphometric parameters. The values of the correlation coefficient are given in Table 1.

As can be seen from table 1, the values of the fractal dimension of the outer linear contour of the cerebellum, determined by the method of caliper ($FD_a$), are associated with a strong positive correlation with the length of the linear contour ($P_s$) and the shape factor of the segmented area ($SF_s$), the length of the contour to the area of the segmented area ($P_s/S_s$), the ratio of the length of the contour of the segmented area to the length of the contour of the tomographic section as a whole ($P_s/P_0$). $FD_a$ values are related by a negative correlation of the mean strength with the ratio of the area of the segmented area to the area of the tomographic section as a whole ($S_s/S_0$). Correlations between $FD_a$ and other morphometric parameters were not statistically significant (p>0.05).

**Table 1.** Correlation relationships of fractal dimension values and morphometric parameters of MR images of the human cerebellum.

| Fractal dimension | | $FD_a$ | $FD_b$ | $FD_c$ |
|---|---|---|---|---|
| Studied object | | Outer linear contour of cerebellum | | Cerebellar tissue as a whole |
| Method of fractal analysis | | Caliper | Box counting | |
| Morphometric parameters of MR images | $P_0$ | 0.244 | 0.252 | 0.354* |
| | $S_0$ | 0.176 | 0.388* | 0.607* |
| | $P_0/S_0$ | -0.084 | -0.347 | -0.561* |
| | $SF_0$ | -0.107 | 0.143 | 0.286 |
| | $P_s$ | 0.700* | 0.705* | 0.363* |
| | $S_s$ | -0.301 | 0.223 | 0.782* |
| | $P_s/S_s$ | 0.857* | 0.412* | -0.363* |
| | $SF_s$ | -0.885* | -0.666* | -0.019 |
| | $P_s/P_0$ | 0.738* | 0.745* | 0.313 |
| | $S_s/S_0$ | -0.648* | -0.060 | 0.598* |

**Notes:** * - p<0,05.

The values of the fractal dimension of the outer linear contour of the cerebellum, determined by the method of box counting ($FD_b$), are associated with a strong positive correlation with the length of the linear contour of the segmented section ($P_s$) and with the ratio of the contour length of the segmented section to the total contour ($P_s/P_0$), the positive correlation of the average force with the area of the tomographic section as a whole ($S_0$) and the ratio of the length of the linear contour to the area of the segmented area ($P_s/S_s$). $FD_b$ values are associated with a negative correlation between the mean force and the segmentation factor ($SF_s$). Correlations between $FD_b$ and other morphometric parameters were not statistically significant (p>0.05).

The values of the fractal dimension of the cerebellar tissue as a whole, determined by the method of box counting ($FD_c$), are associated with a strong positive correlation of medium strength with the area of the segmented area (Ss), a positive correlation of medium strength with the length of the linear contour of the tomographic section as a whole ($P_0$) and the segmented area ($P_s$), and with the area of the tomographic section as a whole ($S_0$). The FDc values are related by a negative correlation of the mean force with the ratio of the contour length to the area of the tomographic section as a whole ($P_0/S_0$) and the ratio of the contour length to the area of the segmented area ($P_s/S_s$). Correlations between $FD_c$ and other morphometric parameters were not statistically significant (p>0.05).

## Discussion

The cerebellum can be considered as a natural fractal object due to the complexity of the spatial configuration, self-repetition and self-similarity of the structure. However,

studies of the cerebellum using fractal analysis in the available scientific literature are not numerous [1, 2, 14, 23]. During the fractal analysis of cerebellum structures, scientists studied the white and grey matter of the cerebellum [1, 2, 23], or individual branches of the white matter of the cerebellum [14].

In our previous studies, using our own modification of the pixel dilatation method, we determined the values of the fractal dimension of the outer linear contour of the upper and lower cerebellar lobes, which were, respectively, 1.370±0.009 and 1.431±0.008 [17]. The values of the fractal dimension of the linear contour of the cerebellum obtained in this study slightly exceed these values, because previously only the values of the fractal dimension of individual parts of the cerebellum were determined, in contrast to this study, which studied the linear contour of the cerebellum completely. Differences and features of the studied areas, probably, also cause differences of the received values of fractal dimension.

Other scientists have not previously studied the linear contour of the cerebellum using fractal analysis. Some studies have included fractal analysis of the contour of the cerebral hemispheres (cortex) using the method of box counting, which allowed to quantify the degree of gyrification of the cortex and determine the presence of pathological atrophic changes in the brain [10, 11, 12]. Therefore, the study of the contour of the cerebellar cortex using fractal analysis allows to quantify the spatial configuration of its surface and assess the complexity of the shape of the cerebellum, which is clinically important for diagnosing cerebellar malformations and determining the presence and severity of atrophic cerebellar changes.

For fractal analysis it is important to select the optimal methods and their modifications, as well as the comparability of the results obtained using different methods of fractal analysis. The values of the fractal dimension of the linear contour of the cerebellum, obtained using the methods of caliper and box counting, are very close and do not differ statistically significantly. However, the correlation between these values is lower than expected (r=0.56). This feature can be explained by the very low variability of values: the coefficient of variation of both indicators does not exceed 3.5%. The average value of the difference between the two indicators is 2.5% and does not exceed 7.5%. Therefore, due to the closeness of the values in the sample, even a small difference between two values of the fractal dimension, determined by different methods of fractal analysis, significantly reduces the correlation between these values.

Therefore, given that the values of the fractal dimension of the linear contour of the cerebellum in the study sample (conditional norm) are distributed in a very small range, and there is no statistically significant difference between the two values of the fractal dimension, the obtained values can be used as normative criteria. using both methods - the caliper method in the author's modification and the box counting method.

## Conclusions

1. Fractal analysis of cerebellum outer linear contour allows you to quantify the complexity of the spatial configuration of the outer surface of the cerebellum, which is difficult to assess using traditional morphometric methods.

2. The values of the fractal dimension of cerebellum outer linear contour, determined using the methods of caliper and box counting, are not statistically significant. Therefore, both methods can be used for fractal analysis of the cerebellum linear contour.

3. The data obtained from this study and the method of fractal analysis using the caliper method in the author's modification can be used for morphometric examination of the human cerebellum during morphological studies, as well as to assess the state of the cerebellum on MR images for diagnostic purposes.

## References


[1] Akar, E., Kara, S., Akdemir, H., & Kiris, A. (2015). Fractal dimension analysis of cerebellum in Chiari Malformation type I. *Computers in Biology and Medicine,* 64, 179-186. https://doi.org/10.1016/j.compbiomed.2015.06.024

[2] Akar, E., Kara, S., Akdemir, H., & Kiris, A. (2017). 3D structural complexity analysis of cerebellum in Chiari malformation type I. *Medical & Biological Engineering & Computing,* 55(12), 2169-2182. https://doi.org/10.1007/s11517-017-1661-7

[3] Di Ieva, A., Esteban, F.J., Grizzi, F., Klonowski, W., & Martin-Landrove, M. (2015). Fractals in the neurosciences, Part II: clinical applications and future perspectives. *The Neuroscientist: a Review Journal Bringing Neurobiology, Neurology and Psychiatry,* 21(1), 30-43. https://doi.org/10.1177/1073858413513928

[4] Di Ieva, A., Grizzi, F., Jelinek, H., Pellionisz, A.J., & Losa, G.A. (2014). Fractals in the Neurosciences, Part I: General Principles and Basic Neurosciences. *The Neuroscientist: a review Journal Bringing Neurobiology, Neurology and Psychiatry,* 20(4), 403-417. https://doi.org/10.1177/1073858413513927

[5] Demaerel, P. (2002). Abnormalities of cerebellar foliation and fissuration: classification, neurogenetics and clinicoradiological correlations. *Neuroradiology,* 44(8), 639-646. https://doi.org/10.1007/s00234-002-0783-1

[6] Gellersen, H.M., Guo, C.C., O'Callaghan, C., Tan, R.H., Sami, S., & Hornberger, M. (2017). Cerebellar atrophy in neurodegeneration - a meta-analysis. *Journal of Neurology, Neurosurgery, and Psychiatry,* 88(9), 780-788. https://doi.org/10.1136/jnnp-2017-315607

[7] Grizzi, F., Castello, A., Qehajaj, D., Russo, C., & Lopci, E. (2019). The Complexity and Fractal Geometry of Nuclear Medicine Images. *Molecular Imaging and Biology,* 21(3), 401-409. https://doi.org/10.1007/s11307-018-1236-5

[8] Jelinek, H.F., & Fernandez, E. (1998). Neurons and fractals: how reliable and useful are calculations of fractal dimensions? *Journal of Neuroscience Methods,* 81(1-2), 9-18. https://

doi.org/10.1016/s0165-0270(98)00021-1
[9] John, A.M., Elfanagely, O., Ayala, C.A., Cohen, M., & Prestigiacomo, C.J. (2015). The utility of fractal analysis in clinical neuroscience. *Reviews in the neurosciences,* 26(6), 633-645. https://doi.org/10.1515/revneuro-2015-0011
[10] King, R.D., Brown, B., Hwang, M., Jeon, T., George, A.T., & Alzheimer's Disease Neuroimaging Initiative (2010). Fractal dimension analysis of the cortical ribbon in mild Alzheimer's disease. *NeuroImage,* 53(2), 471-479. https://doi.org/10.1016/j.neuroimage.2010.06.050
[11] King, R.D., George, A.T., Jeon, T., Hynan, L.S., Youn, T.S., Kennedy, D.N., & Dickerson, B. (2009). Characterization of Atrophic Changes in the Cerebral Cortex Using Fractal Dimensional Analysis. *Brain Imaging and Behavior,* 3(2), 154-166. https://doi.org/10.1007/s11682-008-9057-9
[12] Kiselev, V.G., Hahn, K.R., & Auer, D.P. (2003). Is the brain cortex a fractal? *NeuroImage*, 20(3), 1765-1774. https://doi.org/10.1016/s1053-8119(03)00380-x
[13] Lee, K.I., Choi, S.C., Park, T.W., & You, D.S. (1999). Fractal dimension calculated from two types of region of interest. Dentomaxillofac. *Radiology,* 28(5), 284-289. doi: 10.1038/sj/dmfr/4600458
[14] Liu, J.Z., Zhang, L.D., & Yue, G.H. (2003). Fractal dimension in human cerebellum measured by magnetic resonance imaging. *Biophysical Journal,* 85(6), 4041-4046. https://doi.org/10.1016/S0006-3495(03)74817-6
[15] Liu, S., Fan, X., Zhang, C., Wang, Z., Li, S., Wang, Y. … Jiang, T. (2019). MR imaging based fractal analysis for differentiating primary CNS lymphoma and glioblastoma. *European Radiology,* 29(3), 1348-1354. https://doi.org/10.1007/s00330-018-5658-x
[16] Mandelbrot, B.B. (1983). *The fractal geometry of nature*. N.Y.: W.H. Freeman & Co.
[17] Maryenko, N., & Stepanenko, O. (2020). Fractal dimension of phylogenetically different parts of the human cerebellum (magnetic resonance imaging study). *Reports of Morphology,* 26(2), 67-73. https://doi.org/10.31393/morphology-journal-2020-26(2)-10
[18] Patel, S., & Barkovich, A.J. (2002). Analysis and classification of cerebellar malformations. *AJNR. American Journal of Neuroradiology*, 23(7), 1074-1087.
[19] Ristanovic, D., & Milosevic, N.T. (2012). Fractal analysis: methodologies for biomedical researchers. *Theoretical Biology Forum*, 105(2), 99-118.
[20] Shrout, M.K., Potter, B.J., & Hildebolt, C.F. (1997). The effect of image variations on fractal dimension calculations. *Oral Surgery, Oral Medicine, Oral Pathology, Oral Radiology, and Endodontics,* 84(1), 96-100. https://doi.org/10.1016/s1079-2104(97)90303-6
[21] Soto-Ares, G., Delmaire, C., Deries, B., Vallee, L., & Pruvo, J.P. (2000). Cerebellar cortical dysplasia: MR findings in a complex entity. *AJNR. American Journal of Neuroradiology,* 21(8), 1511-1519.
[22] Welker, W.I. (1990). The significance of foliation and fissuration of cerebellar cortex. The cerebellar folium as a fundamental unit of sensorimotor integration. *Arch. Ital. Biol.*, 128(2-4), 87-109.
[23] Wu, Y.T., Shyu, K.K., Jao, C.W., Wang, Z.Y., Soong, B.W., Wu, H.M., & Wang, P.S. (2010). Fractal dimension analysis for quantifying cerebellar morphological change of multiple system atrophy of the cerebellar type (MSA-C). *NeuroImage*, 49(1), 539-551. https://doi.org/10.1016/j.neuroimage.2009.07.042
[24] Zaletel, I., Ristanovic, D., Stefanovic, B. D., & Puškaš, N. (2015). Modified Richardson's method versus the box-counting method in neuroscience. J*ournal of Neuroscience Methods,* 242, 93-96. https://doi.org/10.1016/j.jneumeth.2015.01.013

**ФРАКТАЛЬНА РОЗМІРНІСТЬ ЗОВНІШНЬОГО ЛІНІЙНОГО КОНТУРУ МОЗОЧКА ЛЮДИНИ (ЗА ДАНИМИ ДОСЛІДЖЕННЯ МАГНІТНО-РЕЗОНАНСНИХ ТОМОГРАМ)**

***Мар'єнко Н.І., Степаненко О.Ю.***

*Фрактальний аналіз є методом математичного аналізу, який дозволяє кількісно визначити складність просторової конфігурації анатомічних структур та може бути застосований в якості морфометричного методу. Мета дослідження - визначити значення фрактальної розмірності зовнішнього лінійного контуру мозочка шляхом дослідження магнітно-резонансних томограм головного мозку за допомогою авторської модифікації способу caliper та порівняти зі значеннями, визначеними за допомогою способу box counting. У дослідженні були використані томограми головного мозку 30 умовно здорових осіб віком 18-30 років (15 чоловіків та 15 жінок). Досліджували Т2-зважені цифрові магнітно-резонансні зображення. Були досліджені серединні сагітальні томографічні зрізи черв'яка мозочка. Для фрактального аналізу був використаний спосіб caliper в авторській модифікації. Середнє значення фрактальної розмірності лінійного контуру мозочка, визначеної за допомогою способу caliper, становило 1,513±0,008 (1,432¸ 1,600). Середнє значення фрактальної розмірності лінійного контуру мозочка, визначеної за допомогою способу box counting, становило 1,530±0,010 (1,427¸ 1,647). Середнє значення фрактальної розмірності тканини мозочка в цілому, визначеної за допомогою способу box counting, становило 1,760±0,006 (1,674¸ 1,837). Значення фрактальної розмірності зовнішнього лінійного контуру мозочка, визначені за допомогою способів caliper та box counting, статистично значуще не відрізняються. Тому обидва способи можуть бути використані для фрактального аналізу лінійного контуру мозочка. Фрактальний аналіз зовнішнього лінійного контуру мозочка дозволяє кількісно оцінити складність просторової конфігурації зовнішньої поверхні мозочка, котру важко оцінити за допомогою традиційних морфометричних методів. Дані, отримані в результаті даного дослідження та методика фрактального аналізу за допомогою способу caliper в авторській модифікації, можуть бути використані для морфометричного дослідження мозочка людини при проведенні морфологічних досліджень, а також для оцінювання стану мозочка на МР зображеннях із діагностичною метою.*

**Ключові слова:** *фрактальний аналіз, спосіб caliper, спосіб box counting, мозочок, магнітно-резонансна томографія.*

DOI: 10.31393/morphology-journal-2021-27(2)-04 Reports of Morphology, Vol. 27, №2, Pages 23-29

ISSN 1818-1295 eISSN 2616-6194

REPORTS OF MORPHOLOGY

*Official Journal of the Scientific Society of Anatomists, Histologists, Embryologists and Topographic Anatomists of Ukraine*

journal homepage: https://morphology-journal.com

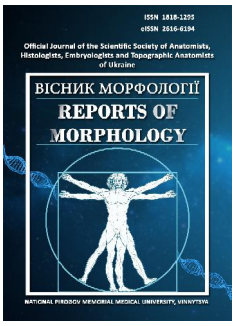


# Evaluation of embryotoxicity and fetotoxicity of Clindamycin phosphate under normal and elevated levels of serum Hydrogen sulfide in rats

***Taran I.V., Grebeniuk D.I., Voloshchuk N.I., Lozinska M.S., Nazarchuk O.A., Bodnarchuk O.V.***
National Pirogov Memorial Medical University, Vinnytsya, Ukraine

**ARTICLE INFO**
Received: 17 February 2021
Accepted: 7 April 2021

**UDC:** 577.18+546.221.1+615.099.092

**CORRESPONDING AUTHOR**
e-mail: doctor.svo@gmail.com
Grebeniuk D.I.

*Widespread use of antibiotics in clinical practice leads to the development of antibiotic resistance and encourages the search for new ways of modulation of their therapeutic effect. One of the potentially successful modulators may be Hydrogen sulfide, but the mechanisms of its action require careful studies, including toxicological. The aim of the study was to study the effect of Hydrogen sulfide levels on the embryotoxicity and fetotoxicity of oral and intravaginal Clindamycin phosphate administration. The experimental study was performed on 60 pregnant female rats, which were divided into 6 experimental groups: group 1 - control group; group 2 - high level of serum Hydrogen sulfide; group 3 - Clindamycin phosphate intravaginally; group 4 - Clindamycin phosphate intravaginally with high level of serum Hydrogen sulfide; group 5 - Clindamycin phosphate orally; group 6 - Clindamycin phosphate orally with high level of serum Hydrogen sulfide. We studied the dynamics of weight gain in pregnant rats, the number of corpora lutea, the number of implantation sites in the uterus, the number of live and dead fetuses, preimplantation and postimplantation mortality, as well as the dynamics of body weight gain and mental development of offspring. Artificially increasing the serum level of Hydrogen sulfide in pregnant rats led to an increase in maternal weight gain, an increase in the weight and cranio-caudal size of embryos, as well as a decrease in the number of resorbed fetuses and postimplantation mortality. The insignificant toxic effect of high doses of oral Clindamycin phosphate was leveled in the group with elevated indices of serum Hydrogen sulfide. Rats born to females with elevated levels of serum Hydrogen sulfide showed faster rates of weight gain and normal mental development according to the "open field" test.*

**Keywords:** *Clindamycin phosphate, Hydrogen sulfide, embryotoxicity, fetotoxicity.*

## Introduction

Treatment of patients with drugs from the group of antibiotics requires a balanced and professional approach, which is part of the concept of rational use of drugs. In turn, the rational use of antibiotics is an important part of the Ministry of Health's postulates, which should improve the prognosis of patients' recovery and reduce the length of hospital stay. However, despite the titanic efforts of the WHO and family doctors, the problem of controlling the circulation of antibiotics and their use by patients themselves remains. The main ones are uncontrolled intake, unauthorized discontinuation of antibiotics, self-increase or decrease in dose of drugs and, ultimately, the use of these potentially dangerous drugs without urgent need [8, 10, 19, 28].

All the principles of rational antibiotic therapy are divided into two major groups:

1. a group of principles and rules from the doctor and the manufacturer of the antibiotic;
2. a group of rules on the part of the patient.

If the second group can be little influenced by specialists, then the first group must be thoroughly studied, improved and create new approaches to antibiotic therapy.

In view of this, in recent years in the world literature there is information about the action of a number of endogenous factors that change the body's response to inflammation and septic conditions, which often use antibiotics. Such factors include the levels of vasoactive molecules, among which the most important is Hydrogen sulfide [9, 12, 13, 29, 31].

One of the most important issues in assessing the toxic effects of antibiotics on the human body is to determine the indicators of fetotoxicity and embryotoxicity.

One of the antibacterial agents widely used in gynecological practice, including for pregnant women, is a member of the group of lincosamides - the drug clindamycin [14, 15, 17, 21, 23, 25]. In the scientific literature there are reports of possible adverse effects of this drug on the course of labor and the condition of the fetus [1]. That is why, in our opinion, it is relevant both from a scientific and practical point of view to study the effect of Hydrogen sulfide on the reproductive toxicity of antibiotics, in particular clindamycin.

*The aim* of the research was to study the effect of Hydrogen sulfide levels on the indicators of embryotoxicity and fetotoxicity of Clindamycin phosphate under conditions of oral and intravaginal administration.

## Materials and methods

The experimental study was performed on 60 pregnant female rats weighing 200-240 grams (219.7±11.1 grams) and under 1 year of age.

All experiments were performed in accordance with the "Regulations on the use of animals in biomedical experiments" with the permission of the Bioethics Committee and in accordance with the provisions of Directive 2010/63/EU of the European Parliament and of the Council of 22 September 2010 "On the protection of animals used for scientific purposes".

Next, the experimental animals were divided into experimental groups as follows:

1 group (n=10) - control group - animals that received a solution of phosphate buffer.

Group 2 (n=10) - animals, which created an excess of serum Hydrogen sulfide.

Group 3 (n=10) - animals treated with Clindamycin phosphate intravaginally.

Group 4 (n=10) - animals injected with Clindamycin phosphate intravaginally on the background of excess serum Hydrogen sulfide.

Group 5 (n=10) - animals administered Clindamycin phosphate orally.

Group 6 (n=10) - animals administered Clindamycin phosphate orally on the background of excess serum Hydrogen sulfide.

All drugs were administered throughout pregnancy.

The phosphate buffer solution was administered orally through a 0.5 ml tube once a day.

Oral Clindamycin phosphate (Union Quimico Farmaceutica, S.A., Spain) was administered on a 1% starch gel via a tube once a day. The dose of the drug was equivalent to the maximum daily dose and according to the conversion tables was 500 mg/kg [22].

Intravaginally, Clindamycin phosphate (Pfizer Inc., USA) was administered to rats as micro-suppositories once daily. The dose of the drug according to the conversion tables was 1.5 mg [22]. Given that the suppository contains 100 mg of active substance and its weight is 2.5 grams, and based on the fact that the active substance is distributed evenly in the suppository, to provide an equivalent dose (1.5 mg of Clindamycin phosphate) we formed micro-suppositories weighing 37.5 mg.

Excess Hydrogen sulfide in animals was created by intraperitoneal administration of Hydrogen sulfide donor - sodium hydrosulfide (NaHS, Sigma-Aldrich, USA) at a dose of 1.5 mg/kg on 0.1 M phosphate buffer (pH 7.4), in the form of freshly made aqueous solution at the rate of 0.1 ml per 100 g of rat weight, 1 time per day [27].

On day 5 of the study, the content of Hydrogen sulfide in the serum was determined. To do this, all rats were bled from the tail vein. The serum of the obtained blood was examined by spectrophotometric method in the reaction between sulfide anion and para-phenylenediamine hydrochloride in an acidic environment in the presence of iron ions (III) [27].

Throughout the experiment, the general condition of the rats, behavior and dynamics of weight gain were observed. On days 7, 14 and 20, the weight gain of pregnant rats relative to baseline values was assessed.

On day 20, half of the 7 rats from each group were removed from the experiment by translocating the cervical vertebrae under ketamine anesthesia at the rate of 0.22 ml of ketamine per 100 grams of body weight of the experimental animal. A laparotomy was performed, after which the pregnant uterus was examined (Fig. 1).

The number of corpora lutea in the ovaries, the number of implantation sites in the uterus, the number of live and dead fetuses were recorded. Based on the obtained data, the term of fetal death was determined - before or after implantation.

Preimplantation (PreIL) and postimplantation (PostIL) mortality were determined by the formulas:

1. PreIL=(C- (A + B))/C*100%;
2. PostIL=B/(A + B)*100%,

where A is the number of live fetuses, B is the number of

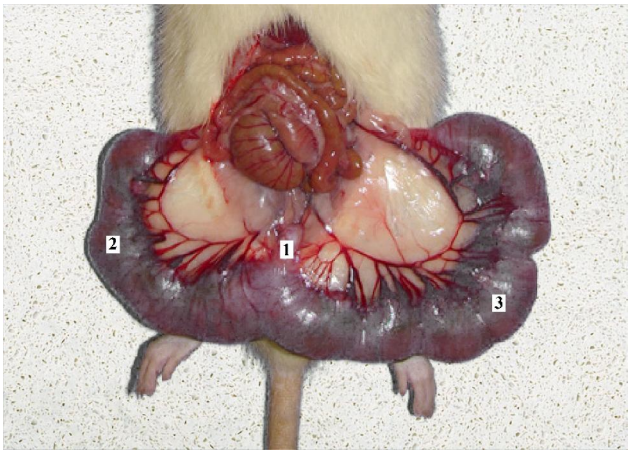


**Fig. 1.** Pregnant uterus removed into a laparotomy wound. 1 - cervix; 2, 3 - right and left uterine horns with embryos.

dead (resorbed) fetuses, C is the number of corpora lutea of pregnancy.

Fetuses were examined for visible mutations, sex, weight, and cranio-caudal size were determined. After that, part of the fetuses was fixed in Buen's solution to study the condition of the internal organs on serial sections. The rest of the fetuses was immersed in a solution of 96% ethanol and stained by the Dawson method to assess ossification points.

The rest of the rats were observed before birth. After birth, the number of newborn males and females was counted, and the weight of rats was measured at 5, 15, 30, and 50 days. In addition, for 30 days, 7 males and 7 females were randomly selected from rats born in each group, which were assessed for anxiety and mental development of offspring on the "open field" model.

The obtained data were processed using the statistical software package SPSS 20.0 for Windows.

## Results

In all groups and at all times of the study, no behavioral changes were observed in experimental animals. All rats maintained normal motor activity. Consumption of feed and water met the standards for this species.

The levels of serum Hydrogen sulfide in the groups of experimental animals are shown in Fig. 2.

In all groups where the excess of serum Hydrogen sulfide was artificially simulated, there was a significant increase ($p<0.01$) of this indicator by 11-12% compared to the groups that did not receive Hydrogen sulfide donors.

When assessing the dynamics of weight gain in pregnant female rats, the following data were obtained. During the first week, there was almost the same weight gain in all experimental animals.

In the second group (excess Hydrogen sulfide), the animals gained weight significantly faster than in the control group. Thus, the weight gain was higher compared to the control group by 15.35% in the second week and by 15.22% in 15-20 days of the study.

The studied indicator in the group with intravaginal administration of Clindamycin phosphate did not differ significantly from the control group at all terms of the study. At the same time, rats with intravaginal administration of Clindamycin phosphate on the background of excess Hydrogen sulfide gained weight in almost the same way as rats from group 2 - weight gain exceeded the control group by 14.47% in the second week and 14.33% in 15 -20 days of research, respectively.

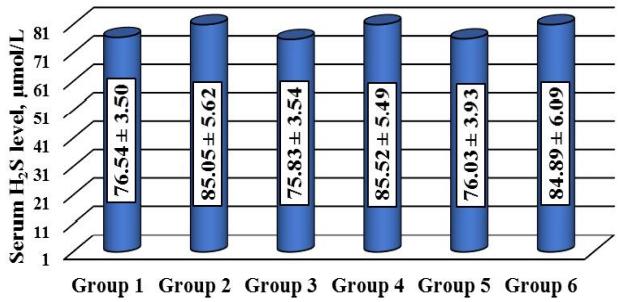


**Fig. 2.** Serum Hydrogen sulfide levels in groups of experimental animals.

Although in the group with oral Clindamycin phosphate the numerical values of weight gain were slightly lower than the value of this indicator in the control group, but statistically significant differences between the groups were not confirmed at any time in the study. Similarly, no statistically significant difference was found between the indicators of group 6 and the control group, although the numerical values in group 6 were slightly higher. In this case, both on the 14th and on the 20th day of the study, weight gain in rats of group 6 significantly exceeded the same indicator of group 5.

Detailed values of weight gain of experimental animals in all study groups are shown in Table 1.

The indicators we evaluated on the 20th day of the study are shown in Table 2.

At visual inspection of fetuses visible mutations were not defined by us, ossification points in groups 2-6 did not differ from group 1 (control group).

Fetuses had the largest mass and cranio-caudal size in groups 2 and 4, the smallest - in group 5, and the differences were statistically significant. In groups 1, 3 and 6 these indicators were almost identical.

The number of corpora lutea, as well as the number of live fetuses in the groups did not differ significantly. At the same time, the number of resorbed fetuses was significantly lower in groups 2 and 4. The largest number of resorbed fetuses was in group 5, although not statistically significantly higher than in the control group.

Regarding the indicators of intrauterine mortality, preimplantation mortality did not differ significantly in all groups. Postimplantation mortality was highest in the group with oral Clindamycin phosphate, although no significant differences from the control group were confirmed. The lowest rates of postimplantation mortality occurred in the groups with additional administration of sodium hydrosulfide, and the indicators of groups 2 and 4 were statistically significantly higher than the groups with the usual background level of Hydrogen sulfide.

The next stage of our study was to establish the effect of the studied substances on the physical and mental development of the offspring.

No fatalities were reported during the 50-day study. All rats were active, behavioral reactions, timing of hair, weight gain met age standards.

The dynamics of weight gain in rats are shown in Table 3.

In male rats born from animals of group 2, on the 15th and 30th day of life, body weight significantly exceeded those of groups 1 and 5, and on the 50th day - only a similar indicator of group 5. In female rats born from animals of group 2, body weight significantly exceeded that in groups 1 and 5 on days 15, 30 and 50 of the study.

**Table 1.** Estimation of weight gain of pregnant rats (M±m).

| Groups of animals | Initial weight, grams | Weight gain for the specified period, grams | | |
|---|---|---|---|---|
| | | 1-7 days | 8-14 days | 15-20 days |
| 1. Control (Phosphate buffer) | 219.0±14.9 | 15.20±3.77 | 22.80±3.43*[2,4] | 33.50±5.32*[2,4] |
| 2. NaHS | 219.6±12.7 | 16.20±1.62 | 26.30±3.27*[1,3,5] | 38.60±3.27*[1,3,5] |
| 3. Clindamycin phosphate intravaginally | 221.6±10.5 | 15.00±2.16 | 22.50±2.37*[2,4] | 33.10±4.23*[2,4] |
| 4. Clindamycin phosphate intravaginally + NaHS | 221.9±10.3 | 15.10±1.79 | 26.10±2.51*[1,3,5] | 38.30±3.40*[1,3,5] |
| 5. Clindamycin phosphate orally | 217.3±5.4 | 14.70±1.95 | 19.40±4.22*[2,4,6] | 31.60±2.99*[2,4,6] |
| 6. Clindamycin phosphate orally + NaHS | 218.8±12.5 | 15.20±3.55 | 23.80±3.16*[5] | 36.50±4.22*[5] |

**Notes** (hereinafter): * - statistically significant difference compared with the control group. The numbers indicate the group number, in comparison with which the differences are significant.

**Table 2.** Evaluation of the effect of the studied compounds on the embryonic development of rats (M±m).

| Groups of animals | Fetus weight, grams | Fetus size, cm | For 1 female | | | | |
|---|---|---|---|---|---|---|---|
| | | | Number of corpora lutea of pregnancy | Number of live fetus | Number of resorbed fetus | PreIL | PostIL |
| 1. Control (Phosphate buffer) | 3.086±0.367*[2,4] | 2.871±0.350*[2,4] | 13.43±1.27 | 10.86±1.07 | 1.429±0.787*[2] | 8.456±4.971 | 11.43±6.26*[2] |
| 2. NaHS | 3.457±0.207*[1,3,5] | 3.214±0.168*[1,3,5] | 13.29±0.95 | 11.29±1.11 | 0.571±0.535*[1,3,5] | 10.53±8.86 | 4.817±4.571*[1,3,5] |
| 3. Clindamycin phosphate intravaginally | 3.100±0.231*[2,4] | 2.886±0.204*[2,4] | 13.86±1.21 | 10.57±1.27 | 1.571±0.535*[2,4] | 12.48±3.82 | 12.93±4.21*[2,4] |
| 4. Clindamycin phosphate intravaginally + NaHS | 3.429±0.189*[1,3,5] | 3.186±0.135*[1,3,5] | 12.71±1.50 | 10.71±1.25 | 0.714±0.488*[3,5] | 9.810±5.487 | 6.294±4.330*[3,5] |
| 5. Clindamycin phosphate orally | 2.800±0.289*[2,4,6] | 2.614±0.261*[2,4,6] | 13.14±1.77 | 9.857±2.193 | 1.857±0.900*[2,4,6] | 11.35±5.36 | 16.22±9.00*[2,4,6] |
| 6. Clindamycin phosphate orally + NaHS | 3.200±0.306*[5] | 3.014±0.313*[5] | 13.43±1.27 | 11.00±1.41 | 0.857±0.690*[5] | 11.68±3.76 | 7.306±5.847*[5] |

**Notes:** PreIL - preimplantation mortality. PostIL - postimplantation mortality.

**Table 3.** Dynamics of weight gain of rats from 5 to 50 days of life (M±m).

| Groups of animals | Sex | Day of life | | | |
|---|---|---|---|---|---|
| | | 5 | 15 | 30 | 50 |
| 1. Control (Phosphate buffer) | Males | 11.37±0.89 | 22.21±1.19*[2] | 43.01±2.12*[2] | 76.71±2.47 |
| | Females | 11.44±0.85 | 22.37±1.25*[2] | 43.17±2.17*[2] | 76.59±2.59*[2] |
| 2. NaHS | Males | 12.24±1.10 | 23.80±1.30*[1,5] | 46.03±2.26*[1,5] | 78.81±2.81*[5] |
| | Females | 12.30±1.13 | 24.20±1.63*[1,5] | 46.19±2.20*[1,5] | 79.53±2.27*[1,5] |
| 3. Clindamycin phosphate intravaginally | Males | 11.87±0.71 | 22.83±1.02 | 45.40±2.09 | 77.03±2.09 |
| | Females | 12.01±0.74 | 23.03±1.16 | 45.53±1.97 | 77.03±2.09 |
| 4. Clindamycin phosphate intravaginally + NaHS | Males | 11.61±0.95 | 22.44±1.11 | 45.17±2.16 | 77.11±1.43 |
| | Females | 11,61±0,95 | 22,60±1,18 | 45,30±1,90 | 77,47±1,37 |
| 5. Clindamycin phosphate orally | Males | 11,26±1,12 | 22,30±1,24*[2] | 43,33±2,08*[2] | 75,23±2,26*[2] |
| | Females | 11,41±0,92 | 22,44±1,02*[2] | 43,49±2,21*[2] | 75,39±2,34*[2] |
| 6. Clindamycin phosphate orally + NaHS | Males | 11,34±0,86 | 22,31±1,29 | 44,04±1,76 | 76,16±2,24 |
| | Females | 11,56±0,71 | 22,63±1,17 | 44,20±1,90 | 77,07±2,18 |

**Table 4.** Evaluation of behavioral responses in the open field test model (M±m).

| Groups of animals | Sex | Ambulations | Grooming | Rering | Defecation |
|---|---|---|---|---|---|
| 1. Control (Phosphate buffer) | Males | 16.14±0.69 | 7.286±1.113 | 3.429±1.272 | 0.714±0.488 |
| | Females | 15.57±0.98 | 8.857±1.069 | 3.571±1.397 | 1.000±0.577 |
| 2. NaHS | Males | 15.86±0.90 | 7.429±1.134 | 3.143±1.345 | 0.857±0.690 |
| | Females | 15.43±1.27 | 9.143±0.690 | 2.571±0.976 | 0.571±0.535 |
| 3. Clindamycin phosphate intravaginally | Males | 15.71±0.76 | 8.000±1.155 | 3.143±1.215 | 0.714±0.756 |
| | Females | 15.29±0.95 | 8.143±1.069 | 2.857±1.215 | 1.143±0.690 |
| 4. Clindamycin phosphate intravaginally + NaHS | Males | 16.29±0.76 | 7.571±1.134 | 2.571±0.787 | 0.571±0.535 |
| | Females | 15.86±0.69 | 8.714±0.951 | 3.000±1.528 | 1.143±0.690 |
| 5. Clindamycin phosphate orally | Males | 16.14±0.90 | 7.714±1.254 | 3.143±0.690 | 0.857±0.900 |
| | Females | 16.29±0.95 | 8.571±1.134 | 3.286±1.254 | 0.714±0.756 |
| 6. Clindamycin phosphate orally + NaHS | Males | 16.43±0.79 | 8.286±1.113 | 3.714±1.380 | 0.429±0.535 |
| | Females | 15.71±1.50 | 8.429±1.397 | 3.143±0.900 | 0.857±0.378 |

An "open field" test was used to assess the behavioral responses of the offspring. The test results are shown in Table 4.

Thus, when evaluating the effect of the studied compounds on the offspring of rats, according to the "open field" test, we did not register any negative changes. All rats showed a sufficient level of resistance to stress, and indicators of interest (ambulation, ringing) and anxiety (grooming) did not go beyond the range of normal values.

## Discussion

In the body, Hydrogen sulfide acts as a signaling molecule, a gas transmitter for which no specific receptors have been found. H2S molecular targets are various ion channels, receptors, enzymes and proteins that regulate a wide range of biochemical and physiological processes [13].

The content of Hydrogen sulfide in the body often changes as a result of pathological conditions and the use of pharmacological drugs. Thus, Hydrogen sulfide deficiency is associated with ischemic heart and brain disorders, mental retardation, atherosclerosis, hyperhomocysteinemia, etc. [6, 30, 31]. On the other hand, excessive production of Hydrogen sulfide is involved in the pathogenesis of inflammatory diseases, septic shock, stroke, etc. [5, 31].

This involvement of Hydrogen sulfide in the pathogenesis of various pathological conditions is due to the fact that it is involved in the regulation of a wide range of physiological and pathophysiological processes, such as vascular tone, neuromodulation, cytoprotection, inflammation, apoptosis and others [9, 12, 13, 29, 31].

No less interesting is the ability of Hydrogen sulfide to stimulate angiogenesis by stimulating the proliferation of endothelial cells [19, 32].

In this study, by serial administration of sodium hydrosulfide, we were able to achieve an increase in the background level of Hydrogen sulfide in all experimental animals, as in our previous studies [27].

Clindamycin phosphate when administered intravaginally did not create toxic effects on the mother and the embryo. The absence of toxic effects was confirmed by similar to the control group indicators of weight gain of pregnant rats, as well as indicators of weight and size of embryos on the 20th day of the study. In addition, the number of live and resorbed fetuses, as well as pre-implantation and post-implantation mortality did not differ statistically from the control group. There were also no changes in body weight gain and mental development of rats born to females who received Clindamycin phosphate in the form of suppositories during pregnancy.

Administration of Clindamycin phosphate to pregnant female rats during pregnancy had a negligible adverse effect on females and embryos. However, it was not possible to prove the statistical significance of differences with the control group.

The creation of excess Hydrogen sulfide significantly improved the studied parameters in both rats with intravaginal administration of Clindamycin phosphate and in rats that were not administered the drug. This was manifested by a significant increase in body weight gain of pregnant rats and rats born from them, an increase in anthropometric indicators of embryos, as well as a decrease in the number of resorbed fetuses and post-implantation mortality. Mental development of rats was also characterized by better performance.

Additional administration of sodium hydrosulfide to rats treated with Clindamycin phosphate orally counteracted the slight adverse effects of the drug and significantly improved the studied parameters.

Such results of our researches can be explained by increase in a placental blood-groove and increase in trophism of embryos. On the one hand, the reason for this effect is the vasodilating effect of Hydrogen sulfide on the vessels of the placental circulation, which was previously described in the scientific literature [4, 11, 20]. On the other

hand, previous studies demonstrate the presence of Hydrogen sulfide in the ability to stimulate angiogenesis by stimulating the proliferation of endothelial cells [7, 18, 29, 32].

Further experimental studies will expand our understanding of the effects of Hydrogen sulfide on the morphological structure and development of the placenta, as well as a clearer understanding of its involvement in the pathogenesis of pathological conditions associated with placental blood flow.

Regarding the genotoxicity of Clindamycin phosphate against the background of excess Hydrogen sulfide, we did not conduct such studies for technical reasons. Literature data indicate the absence of genotoxicity in both oral and intravaginal forms of Clindamycin phosphate, which was confirmed by the results of the Ames mutation test for Salmonella typhimurium, as well as the micronucleus test in rats [1]. As for Hydrogen sulfide, as an exogenous agent, it has a genotoxic effect [2, 3]. At the same time, as an endogenous gas transmitter, Hydrogen sulfide has a protective and reparative effect on DNA [16, 24, 24, 26].

## Conclusions

1. Artificial increase in the background level of Hydrogen sulfide in pregnant rats leads to an increase in maternal weight gain, increased anthropometric indicators of embryos, as well as a decrease in the number of resorbed fetuses and postimplantation mortality and eliminates the small negative impact of high doses of Clindamycin phosphate administered orally.

2. Rats born from females with elevated levels of Hydrogen sulfide in the body show faster rates of weight gain and better mental development.

## References


[1] AHFS Drug Information 2018. McEvoy, G.K. (Ed.). (2018). Clindamycin Hydrochloride, Clindamycin Palmitate Hydrochloride, Clindamycin Phosphate. American Society of Health-System Pharmacists.

[2] Attene-Ramos, M.S., Nava, G.M., Muellner, M.G., Wagner, E.D., Plewa, M.J., & Gaskins, H.R. (2010). DNA damage and toxicogenomic analyses of hydrogen sulfide in human intestinal epithelial FHs 74 Int cells. *Environmental and Molecular Mutagenesis,* 51(4), 304-314. https://doi.org/10.1002/em.20546

[3] Attene-Ramos, M.S., Wagner, E.D., Plewa, M.J., & Gaskins, H.R. (2006). Evidence that hydrogen sulfide is a genotoxic agent. *Molecular Cancer Research: MCR,* 4(1), 9-14. https://doi.org/10.1158/1541-7786.MCR-05-0126

[4] Bhatia, M. (2005). Hydrogen sulfide as a vasodilator. *IUBMB Life,* 57(9), 603-606. https://doi.org/10.1080/15216540500217875

[5] Bhatia, M. (2019). Understanding Hydrogen Sulfide in Inflammation: Opportunities and Challenges. *Molecular and Cellular Therapies,* 7, 9-14. https://doi.org/10.13052/mct2052-8426.712

[6] Cai, H., & Wang, X. (2020). Effect of sulfur dioxide on vascular biology. *Histology and Histopathology*, 18290. Advance online publication. https://doi.org/10.14670/HH-18-290

[7] Chen, D.B., Feng, L., Hodges, J.K., Lechuga, T.J., & Zhang, H. (2017). Human trophoblast-derived hydrogen sulfide stimulates placental artery endothelial cell angiogenesis. *Biology of Reproduction,* 97(3), 478-489. https://doi.org/10.1093/biolre/iox105

[8] de With, K., Allerberger, F., Amann, S., Apfalter, P., Brodt, H.R., Eckmanns, T. … Kern, W.V. (2016). Strategies to enhance rational use of antibiotics in hospital: a guideline by the German Society for Infectious Diseases. *Infection,* 44(3), 395-439. https://doi.org/10.1007/s15010-016-0885-z

[9] Gadalla, M.M., & Snyder, S.H. (2010). Hydrogen sulfide as a gasotransmitter. *Journal of Neurochemistry,* 113 (1), 14-26. https://doi.org/10.1111/j.1471-4159.2010.06580.x

[10] Graham, K., Sinyangwe, C., Nicholas, S., King, R., Mukupa, S., Källander, K. … Hamade, P. (2016). Rational use of antibiotics by community health workers and caregivers for children with suspected pneumonia in Zambia: a cross-sectional mixed methods study. *BMC Public Health*, 16(1), 897. https://doi.org/10.1186/s12889-016-3541-8

[11] Greaney, J.L., Kutz, J.L., Shank, S.W., Jandu, S., Santhanam, L., & Alexander, L.M. (2017). Impaired Hydrogen Sulfide-Mediated Vasodilation Contributes to Microvascular Endothelial Dysfunction in Hypertensive Adults. *Hypertension* (Dallas, Tex.: 1979), 69(5), 902-909. https://doi.org/10.1161/HYPERTENSIONAHA.116.08964

[12] Kimura, H. (2011). Hydrogen sulfide: its production, release and functions. *Amino acids,* 41(1), 113-121. https://doi.org/10.1007/s00726-010-0510-x

[13] Kimura, H. (2014). Production and physiological effects of hydrogen sulfide. *Antioxidants & Redox Signaling,* 20(5), 783-793. https://doi.org/10.1089/ars.2013.5309

[14] Lamont, R.F., Keelan, J.A., Larsson, P.G., & Jørgensen, J.S. (2017). The treatment of bacterial vaginosis in pregnancy with clindamycin to reduce the risk of infection-related preterm birth: a response to the Danish Society of Obstetrics and Gynecology guideline group's clinical recommendations. *Acta Obstetricia et Gynecologica Scandinavica,* 96(2), 139-143. https://doi.org/10.1111/aogs.13065

[15] Larsson, P.-G., Poutakidis, G., Adolfsson, A., Charonis, G., Bauer, P., & Ekstrom, L. (2016). Treatment of Bacterial Vaginosis in Early Pregnancy and its Effect on Spontaneous Preterm Delivery and Preterm Premature Rupture of Membranes. *Clin. Microbiol.*, 5(5), 1-8. http://dx.doi.org/10.4172/2327-5073.1000259

[16] Li, S., & Yang, G. (2015). Hydrogen Sulfide Maintains Mitochondrial DNA Replication via Demethylation of TFAM. *Antioxidants & Redox Signaling,* 23(7), 630-642. https://doi.org/10.1089/ars.2014.6186

[17] Li, T., Wang, F., Zhang, Z., Zong, X., Bai, H., & Liu, Z. (2021). Treatment of Bacterial Vaginosis: A Comparison of Metronidazole and Clindamycin on Human Anaerobic Bacteria and Lactobacilli. Retrieved from: https://doi.org/10.21203/rs.3.rs-107727/v1

[18] Liao, W.X., Feng, L., Zhang, H., Zheng, J., Moore, T.R., & Chen, D.B. (2009). Compartmentalizing VEGF-induced ERK2/1 signaling in placental artery endothelial cell caveolae: a paradoxical role of caveolin-1 in placental angiogenesis in vitro. *Molecular Endocrinology* (Baltimore, Md.), 23(9), 1428-1444. https://doi.org/10.1210/me.2008-0475

[19] Mahmood, A., Elnour, A.A., Ali, A.A., Hassan, N.A., Shehab, A.,

& Bhagavathula, A.S. (2016). Evaluation of rational use of medicines (RUM) in four government hospitals in UAE. *Saudi Pharmaceutical Journal: SPJ: the official publication of the Saudi Pharmaceutical Society,* 24(2), 189-196. https://doi.org/10.1016/j.jsps.2015.03.003

[20] Materazzi, S., Zagli, G., Nassini, R., Bartolini, I., Romagnoli, S., Chelazzi, C. … Patacchini, R. (2017). Vasodilator activity of hydrogen sulfide (H2S) in human mesenteric arteries. *Microvascular Research,* 109, 38-44. https://doi.org/10.1016/j.mvr.2016.11.001

[21] Murphy, P.B., Bistas, K.G., & Le, J.K. (2020). *Clindamycin.* In StatPearls. StatPearls Publishing.

[22] Nair, A.B., & Jacob, S. (2016). A simple practice guide for dose conversion between animals and human. *Journal of Basic and Clinical Pharmacy,* 7(2), 27-31. https://doi.org/10.4103/0976-0105.177703

[23] Sexually Transmitted Diseases: Summary of 2015 CDC Treatment Guidelines. (2015). *Journal of the Mississippi State Medical Association,* 56(12), 372-375.

[24] Shackelford, R., Ozluk, E., Islam, M.Z., Hopper, B., Meram, A., Ghali, G., & Kevil, C.G. (2021). Hydrogen sulfide and DNA repair. *Redox Biology,* 38, 101675. https://doi.org/10.1016/j.redox.2020.101675

[25] Subtil, D., Brabant, G., Tilloy, E., Devos, P., Canis, F., Fruchart, A. … Dessein, R. (2018). Early clindamycin for bacterial vaginosis in pregnancy (PREMEVA): a multicentre, double-blind, randomised controlled trial. *Lancet* (London, England), 392(10160), 2171-2179. https://doi.org/10.1016/S0140-6736(18)31617-9

[26] Szczesny, B., Marcatti, M., Zatarain, J.R., Druzhyna, N., Wiktorowicz, J.E., Nagy, P. … Szabo, C. (2016). Inhibition of hydrogen sulfide biosynthesis sensitizes lung adenocarcinoma to chemotherapeutic drugs by inhibiting mitochondrial DNA repair and suppressing cellular bioenergetics. *Scientific Reports,* 6, 36125. https://doi.org/10.1038/srep36125

[27] Voloshchuk, N.I., Taran, I.V., & Melnik, A.V. (2015). Vascular mechanism in the formation of diclophenac induced gastrotoxicity: the association with the level of hydrogen sulfide. *Curierul Medical*, 58(1), 7-11.

[28] Walger, P. (2016). Rationaler Einsatz von Antibiotika [Rational use of antibiotics]. Internist (Berl)., 57(6), 551-568. doi: 10.1007/s00108-016-0071-5

[29] Wang, R. (2002). Two's company, three's a crowd: can H2S be the third endogenous gaseous transmitter? FASEB Journal: *Official Publication of the Federation of American Societies for Experimental Biology,* 16(13), 1792-1798. https://doi.org/10.1096/fj.02-0211hyp

[30] Whiteman, M., Le Trionnaire, S., Chopra, M., Fox, B., & Whatmore, J. (2011). Emerging role of hydrogen sulfide in health and disease: critical appraisal of biomarkers and pharmacological tools. *Clinical Science* (London, England: 1979), 121(11), 459-488. https://doi.org/10.1042/CS20110267

[31] Xiao, Q., Ying, J., Xiang, L., & Zhang, C. (2018). The biologic effect of hydrogen sulfide and its function in various diseases. *Medicine,* 97 (44), e13065. https://doi.org/10.1097/MD.0000000000013065

[32] Zhou, Y., Li, X.H., Zhang, C.C., Wang, M.J., Xue, W.L., Wu, D.D., … Zhu, Y.C. (2016). Hydrogen sulfide promotes angiogenesis by downregulating miR-640 via the VEGFR2/mTOR pathway. *American Journal of Physiology. Cell Physiology*, 310(4), C305-C317. https://doi.org/10.1152/ajpcell.00230.2015

**ОЦІНКА ЕМБРІОТОКСИЧНОСТІ ТА ФЕТОТОКСИЧНОСТІ КЛІНДАМІЦИНУ ФОСФАТУ ЗА УМОВИ НОРМАЛЬНОГО ТА ПІДВИЩЕНОГО РІВНЯ СИРОВАТКОВОГО ГІДРОГЕН СУЛЬФІДУ У ЩУРІВ**

***Таран І.В., Гребенюк Д.І., Волощук Н.І., Лозинська М.С., Назарчук О.А., Боднарчук О.В.***

*Широке використання антибіотиків в клінічній практиці веде до розвитку антибіотикорезистентності та спонукає до пошуку нових шляхів модуляції їх терапевтичного впливу. Одним із потенційно успішних модуляторів може бути гідроген сульфід, проте механізми його дії потребують ретельного дослідження в тому числі й токсикологічного. Мета дослідження - вивчити вплив рівнів гідроген сульфіду на показники ембріотоксичності та фетотоксичності кліндаміцину фосфату за умов перорального та інтравагінального введення. Експериментальне дослідження проводили на 60 вагітних самках щурів, які були розподілені на 6 дослідних груп: 1 група - група контролю; 2 група - надлишок сироваткового гідроген сульфіду; 3 група - кліндаміцину фосфат інтравагінально; 4 група - кліндаміцину фосфат інтравагінально на фоні надлишку сироваткового гідроген сульфіду; 5 група - кліндаміцину фосфат перорально; 6 група - кліндаміцину фосфат перорально на фоні надлишку сироваткового гідроген сульфіду. Вивчали динаміку набору маси вагітними самками, кількість жовтих тіл в яєчниках, кількість імплантаційних місць у матці, кількість живих та мертвих плодів, показники передімплантаційної та постімплантаційної летальності, а також динаміку набору маси тіла та психічний розвиток потомства за даними тесту "відкритого поля". Штучне підвищення фонового рівня гідроген сульфіду в організмі вагітних щурів призводило до збільшення приросту маси материнського організму, збільшення маси та краніо-каудальних розмірів ембріонів, а також знижувало кількість резорбованих плодів та показників постімплантаційної летальності. Незначний токсичний вплив високих доз кліндаміцину фосфату при його пероральному введенні нівелювався в групі з підвищеним рівнем фонового гідроген сульфіду. За даними тесту "відкритого поля" щурята, народжені від самок із підвищеним рівнем гідроген сульфіду в організмі, демонстрували більш швидкі темпи набору маси тіла та нормальні показники психічного розвитку.*

**Ключові слова:** *кліндаміцину фосфат, гідроген сульфід, ембріотоксичність, фетотоксичність.*

DOI: 10.31393/morphology-journal-2021-27(2)-05 Reports of Morphology, Vol. 27, №2, Pages 30-38

ISSN 1818-1295 eISSN 2616-6194

REPORTS OF MORPHOLOGY

*Official Journal of the Scientific Society of Anatomists, Histologists, Embryologists and Topographic Anatomists of Ukraine*

journal homepage: https://morphology-journal.com

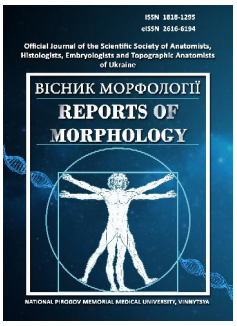


# Effect of exogenous melatonin and flaxseed oil on the expression state of MT1 receptors in rat skin under light deprivation

***Sobolevskaya I.S., Krasnobaeva M.I., Myadelets O.D.***

Vitebsk State Order of Friendship of Peoples Medical University, Vitebsk, Belarus

**ARTICLE INFO**

Received: 18 February 2021

Accepted: 9 April 2021

**UDC:** 619:612.821.014:612.018.2]: 303.447.3

**CORRESPONDING AUTHOR**

e-mail: irinasobolevskaya1986@gmail.com

Sobolevskaya I.S.

*Most of the skin cells have their own autonomous functional circadian system, which is able to control physiological and biochemical processes in the general integument. A special role in these processes is assigned to the "clock" hormone of the pineal gland, melatonin, which acts on target cells through specific receptors (MT1, MT2, MT3 and RORα). Any disturbance of circadian rhythms can lead to rearrangements (disturbances) in the receptor apparatus of the cells of the general cover, which require a certain correction. Consequently, there is a need to search for effective and reliable drugs that will prevent the negative consequences caused by chronodestruction. In the present work, we studied the effectiveness of the effect of exogenous melatonin and flaxseed oil on the expression of MT1 receptors in the general coat of rats under light deprivation. An experimental study was carried out on 130 white outbred male rats (170-220 g), which were randomly divided into 5 groups: intact, light deprivation animals, light deprivation animals, which were injected intragastrically with flaxseed oil and melatonin. On days 7, 14 and 21, histological material was taken (fragments of the skin of the interscapular region of the back). For immunohistochemical studies, serial sections were stained using MTNR1A polyclonal antibodies. For morphometric data analysis, the Image Scope Color and ImageJ computer programs were used. All statistical data processing was performed using the Statistica 10.0 software. Differences were considered significant at a significance level of less than 0.01 (p <0.01). In the course of the experiment, it was found that light deprivation contributes to a change in the activity of expression of the MT1 melatonin receptors in the epidermis, sebaceous glands and hair follicles. Studies have shown that the administration of flaxseed oil, melatonin, and their combination to rats with desynchronosis is accompanied by the leveling of the adverse effect of desynchronosis on the studied parameters of MT1 receptors. The most pronounced corrective effect on the expression of MT1 receptors is observed with the introduction of exogenous melatonin on the 21st day of the experiment.*

**Keywords:** *melatonin MT1 receptors, epidermis, sebaceous glands, hair follicles, melatonin, flaxseed oil, light deprivation.*

## Introduction

Circadian rhythms have a significant impact on many structures of the skin. Any shifts in circadian rhythms lead to a disruption in the production of the hormone - melatonin, which contributes to serious changes in the work of the general and local circadian systems in the body. Since melatonin affects target cells through receptors (MT1, MT2, MT3 and RORα), any quantitative fluctuations in it can lead to modulation of reactions and changes in the state of the receiving part [4, 12, 13, 15].

The MT1 and MT2 melatonin receptors are expressed in skin cells, which are involved in the regulation of many of its physiological processes and defense mechanisms. MT1 receptors have the highest sensitivity and degree of binding. Their distinctive feature is their high sensitivity to melatonin. The MT1 receptor also plays a key role in the regulation of the cutaneous circadian clock [3, 4, 7, 12, 13, 15].

Although constant darkness (light deprivation) is rarely considered as a cause of changes in the state of the circadian clock (compared to exposure to constant light), its effect on humans and animals is no less dangerous. Consequently, any disturbance of circadian rhythms can lead to rearrangements in the receptor apparatus of the cells of the general cover, cause disturbances in its

morphofunctional state and, as a consequence, lead to skin diseases [4, 12].Consequently, there is a need to search for effective and reliable drugs that will prevent the negative consequences caused by chronodestruction. So, first of all, to restore a specific response, replacement therapy with an appropriate agonist is required [8, 10, 22]. Considering that melatonin synthesis changes under constant darkness, the use of its synthetic analogs should have a direct effect on the body. At the same time, the amino acid nature of the hormone ensures its bioavailability, and absorption occurs at the level of substrates.

In recent years, much attention has also been paid to the search for an alternative natural source of melatonin. Thus, this hormone has been identified and quantified both in products of animal and plant origin [14]. It has been established that the highest concentration of this phytohormone is possessed by some plant seeds, from which vegetable oils are subsequently obtained (flaxseed, olive, amaranth, walnut oil, etc.) In this regard, linseed oil is the most economically available and effective. In addition, this vegetable oil is of great interest because of the high content of essential fatty acids that are not synthesized in the human body: linoleic, α-linolenic and γ-linolenic [2, 14, 16, 18].

At the same time, there is practically no information on the features of the effect of melatonin and flaxseed oil on changes in the number (occupied area) and density of MT1 receptors on target cells, and the question of such a relationship remains open.

The efficacy of flaxseed oil and melatonin can be enhanced and side effects mitigated when they are combined wisely. Moreover, the nature and direction of their joint action may differ significantly from the impact of individual components [19].

At present, the prevention and correction of disorders caused by desynchronosis in the body in general and in the general cover in particular require increased attention, and the possibility of stimulating MT1 receptors can be considered as a promising strategy for improving the general condition of the skin.

*The aim* of the study was to substantiate the possibility of correction by exogenous melatonin and flaxseed oil of changes in the expression of MT1 receptors in the skin of white male rats, caused by light deprivation.

## Materials and methods

An experimental study was carried out on 130 white outbred male rats (170-220 g), which were randomly divided into 5 groups (Table 1). All animals were kept in standard vivarium conditions on an optimal diet. Morphological changes in the general cover of the animals were assessed on days 7, 14 and 21.

All manipulations with rats were carried out in accordance with the following regulatory documents: "European Convention for the Protection of Vertebrate Animals used for Experiments or Other Scientific Purposes (Strasbourg, 03/18/1986, ETS No. 123), EEC Council Directives (11/24/1986), FELASA (1994-1996), TCP 125-2008 and "Rules of Laboratory Practice of the Republic of Belarus", Protocol-design of the experiment (approved by the VSMU Commission on Bioethics and Humane Treatment of Laboratory Animals).

**Table 1.** Characteristics of animals experimental groups.

| Group | Description |
|---|---|
| Intact (n=10) | Animals exposed to standard fixed lighting (12 h light/12 h dark) |
| Light deprivation (n=30) | Animals kept in constant darkness around the clock (24 hours darkness) |
| Light deprivation + linseed oil (n=30) | Animals kept in constant darkness around the clock (24 hours dark), which were injected orally through a tube in the morning with flaxseed oil in an amount of 0.2 ml/day from day 1 of the experiment. |
| Light deprivation + melatonin (n=30) | Animals kept in constant darkness around the clock (24 h darkness), which were injected orally through a tube in the morning hours through a tube with melatonin (Melason 3 mg, Rubicon, Republic of Belarus), dissolved in 1% starch solution from day 1 of the experiment. The equivalent dose was calculated taking into account the weight of the rat by the formula [15]: ED (rat) = TD (human)*MC (human)/MC (rat), where ED is the equivalent dose (mg/kg); TD - therapeutic dose for humans (mg/kg), MC - metabolic coefficient (human = 39; rat = 6.0). |
| Light deprivation + melatonin + flaxseed oil (n=30) | Animals kept in constant darkness around the clock (24 hours dark), which were injected orally through a tube in the morning with melatonin and flaxseed oil from day 1 of the experiment. |

For immunohistochemical studies, skin fragments (interscapular region of the back) were fixed in a 10% solution of neutral buffered formalin (24 hours). Then the histological material was embedded in paraffin and serial sections were made. The preparations were stained immunohistochemically using polyclonal antibodies MTNR1A (Elabscience, USA). For immunohistochemical staining, a fully automated Leica Microsystems Bond-maX immunohistostainer was used. As a result of the reaction, MT1-positive areas were stained brown or yellowish.

Histological changes in the preparations were assessed at x200, x400 magnifications. The morphological assessment of the expression of MT1 receptors was carried out using a computerized image analysis system (licensed software Leica Aplication Suite, Version 3.6.0). For morphometric analysis of the data, we used the licensed computer program for image analysis Image Scope Color, as well as the image processing software ImageJ. An automatic assessment was made of the percentage of MT1-positive sites (filling factor, %) and the nature of cytoplasmic expression in immunopositive sites (expression intensity factor, standard units).

Statistical data processing was performed using the Statistica 10.0 software. Methods of nonparametric statistics were used. Statistical hypotheses of equality of

the general population means were tested using the U (Mann-Whitney), W (Wilcoxon), and H (Kruskal-Wallis) tests with the accepted significance level α=0.05.

## Results

According to previous studies, the 24-hour stay of experimental animals in the dark led to significant changes in the expression of MT1 receptors [1]. Thus, on the 7th day, in the keratinocytes of the epidermis and sebocytes of the sebaceous glands, the filling factor of MT1 receptors decreased with a simultaneous increase in the intensity factors of their expression in these structures (Fig. 1, 2). Along with this, an increase in all the studied parameters was observed in the hair follicles. At the same time, the level of immunopositive cells and the intensity of their expression increased (Fig. 1, 2).

Intragastric administration of flaxseed oil, melatonin and their combination to experimental animals for 7 days in constant darkness was accompanied by changes in the expression of membrane melatonin receptors in the general cover. Thus, in the cells of the epidermis and sebaceous glands, the use of flaxseed oil, as well as melatonin, prevented a sharp decrease in the level of MT1-positive cells, compared with rats in the light deprivation group ($p<0.001$) (see Fig. 1, 2). Higher efficacy was observed in animals that were injected with exogenous melatonin. At the same time, the combined use of the oil and the hormone led to a much significant decrease in the filling factors of MT1 receptors in these skin structures relative to animals in complete darkness (Fig. 1, 2, 3).

The change in the intensity of MT1 immunohistochemical staining on the 7th day of the experiment in the epidermis, sebaceous glands and hair follicles was observed only in animals that were simultaneously injected with flaxseed oil and melatonin (Fig. 4, 5, 6). Thus, in rats of this group, the values of the expression intensity coefficients corresponded to the control parameters. In other animals, there were no significant changes in the indicator.

The study of histological skin preparations obtained on the 14th day of exposure to light deprivation showed a further decrease in the filling factors of MT1 receptors in comparison with intact animals in the epidermis and sebaceous glands. A similar pattern was observed in hair

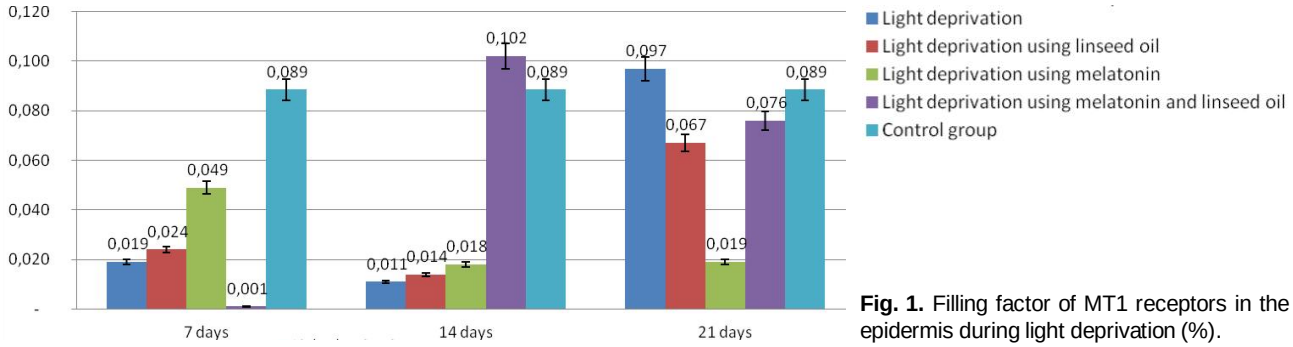


**Fig. 1.** Filling factor of MT1 receptors in the epidermis during light deprivation (%).

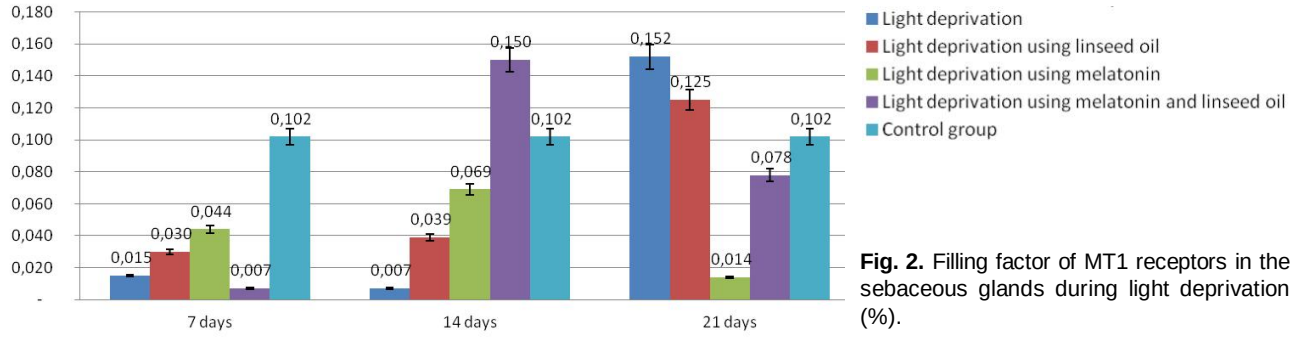


**Fig. 2.** Filling factor of MT1 receptors in the sebaceous glands during light deprivation (%).

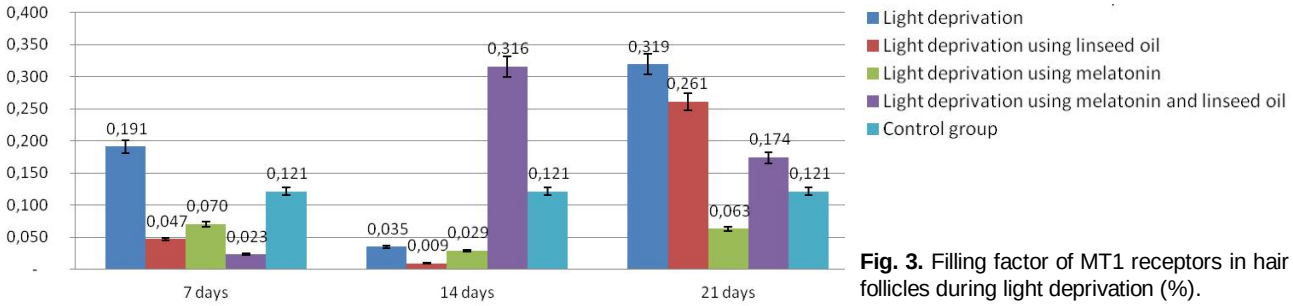


**Fig. 3.** Filling factor of MT1 receptors in hair follicles during light deprivation (%).

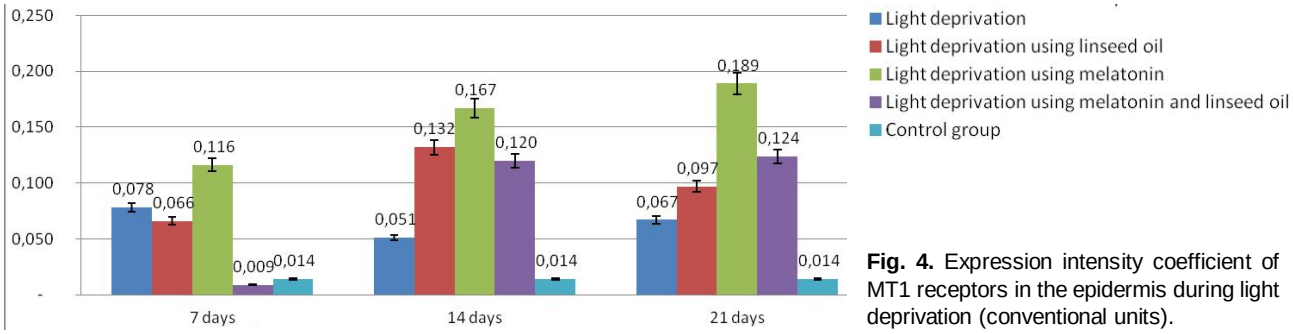


**Fig. 4.** Expression intensity coefficient of MT1 receptors in the epidermis during light deprivation (conventional units).

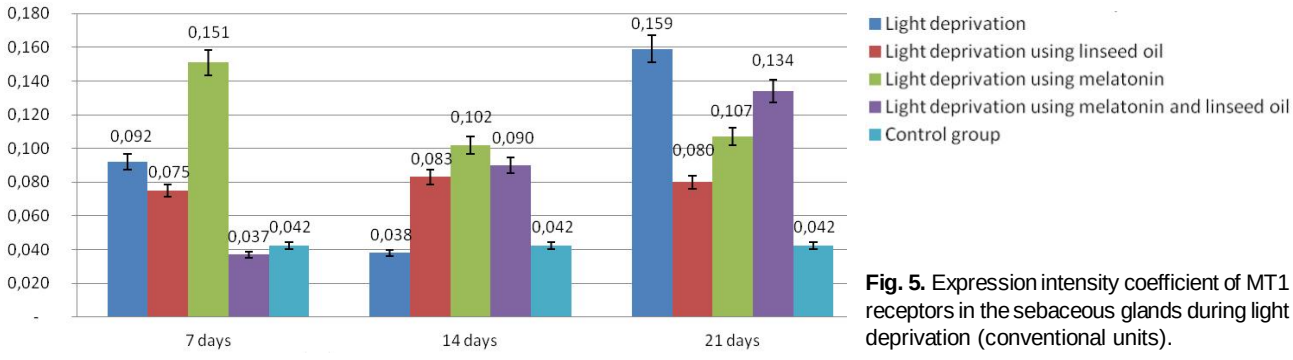


**Fig. 5.** Expression intensity coefficient of MT1 receptors in the sebaceous glands during light deprivation (conventional units).

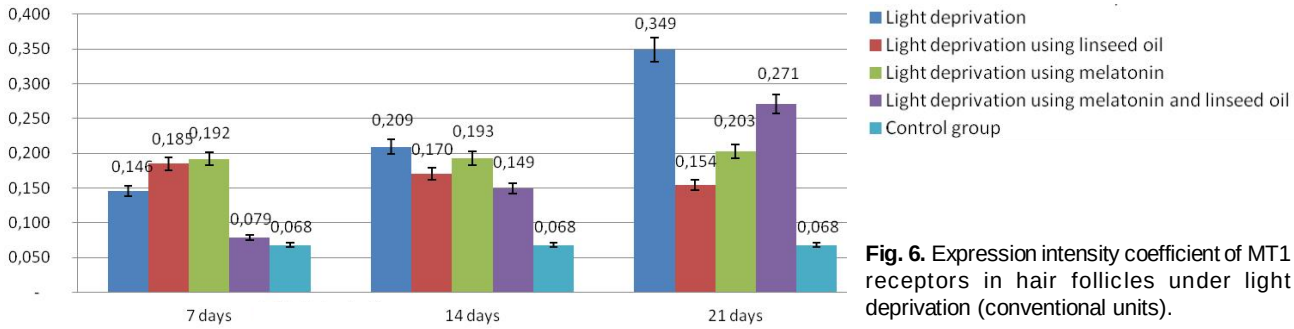


**Fig. 6.** Expression intensity coefficient of MT1 receptors in hair follicles under light deprivation (conventional units).

follicles. At this stage of the experiment, there was a significant decrease in the percentage of MT1-positive cells. At the same time, the indicators of MT1 immunoreactivity remained elevated in all the studied structures of the rat skin as compared with the control values [20].

Intragastric administration of flaxseed oil and exogenous melatonin to animals for 14 days of the experiment did not have a significant effect on the level of immunopositive cells in the epidermis and hair follicles compared to the light deprivation group. However, the melatonin receptors of sebaceous gland sebocytes were found to be more sensitive to exogenous melatonin. This was manifested in a sharp increase (above the control figures) of the MT1 fill factors. At the same time, the combined administration of the oil and the hormone at this observation period contributed to a sharp increase (17.5 times, $p<0.001$) in MT1-positive areas in all skin structures compared to the light deprivation group (see Fig. 1-3). As for the severity of the intensity of immunohistochemical staining, on the 14th day there was a significant increase in the coefficients of the expression intensity of MT1 receptors in all groups of animals, both in relation to the group without the use of substances and the intact group ($p<0.001$). At the same time, the most pronounced effect was observed in animals that were injected only with melatonin (see Fig. 4, 5, 6).

As can be clearly seen from Figures 1-3, on the 21st day of the rats being in constant darkness, there was a significant increase in the percentage of receptor-positive cells and the severity of the intensity of immunohistochemical staining in all three studied structures [6]. However, the administration of flaxseed oil, melatonin, and a combination of oil and a hormone to experimental animals for 21 days led to a decrease in the filling factors of MT1 receptors in the epidermis, sebaceous glands and hair follicles in comparison with the light deprivation group (Fig. 1-6). At the same time, the intragastric intake of melatonin contributed to the fall of the studied indicator in all studied structures below the control values.

Three-week administration of flaxseed oil and

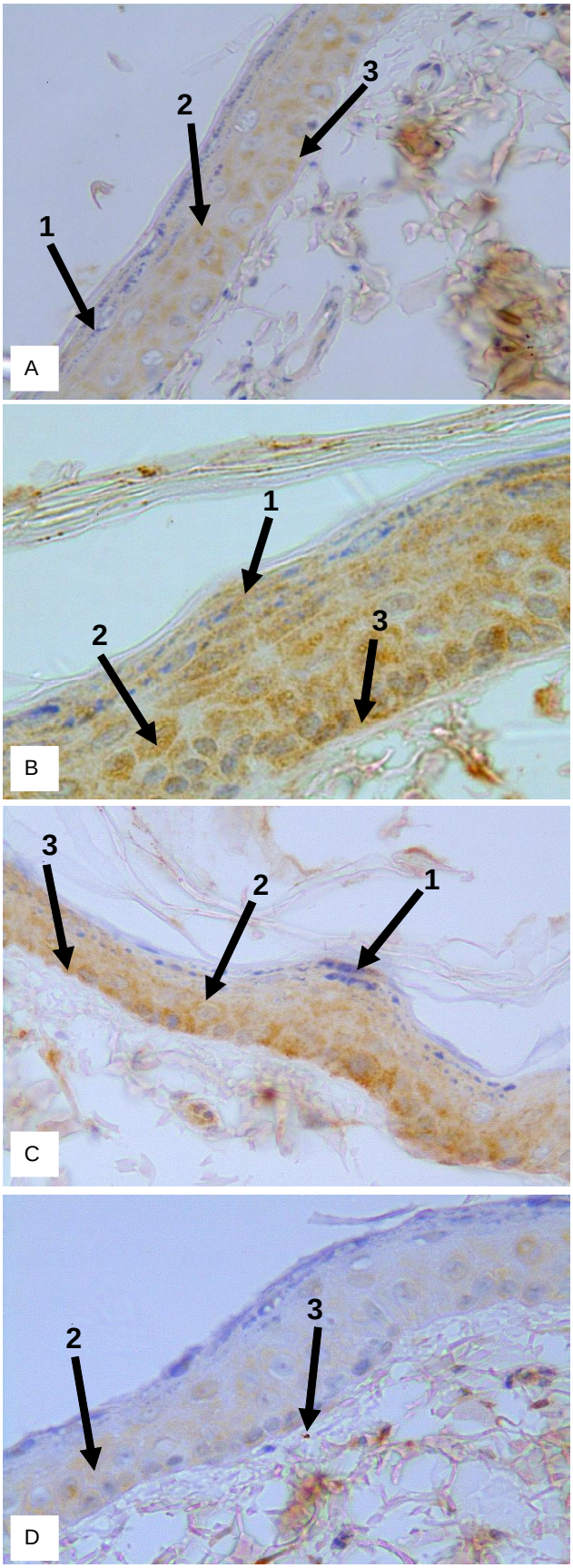


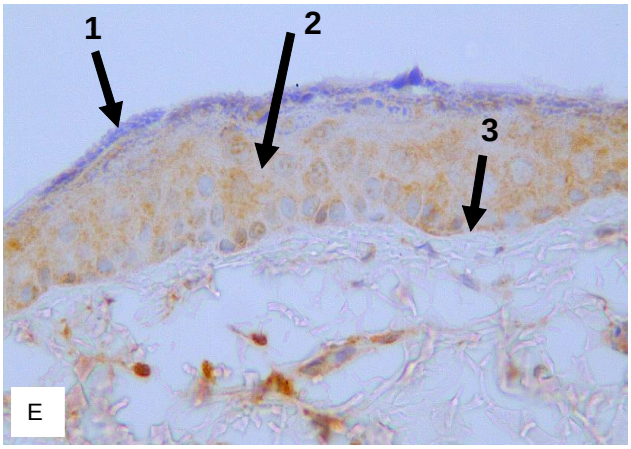


**Fig. 7.** Immunohistochemical detection of MT1 receptors in the cells of rats' skin epidermis during light deprivation (arrow). x400. Intact Animals (A); increased immunohistochemical response after 21 days of light deprivation (B); decrease in MT1 expression after administration of flaxseed oil (C) and combined use of flaxseed oil and melatonin (D); minimal MT1 expression after melatonin administration (E). The arrow shows MT1-positive cells of the granular (1), prickly (2) and basal (3) layers of the epidermis.

melatonin led to a slight decrease in the severity of the intensity of immunohistochemical staining relative to the light deprivation group. At the same time, the expression

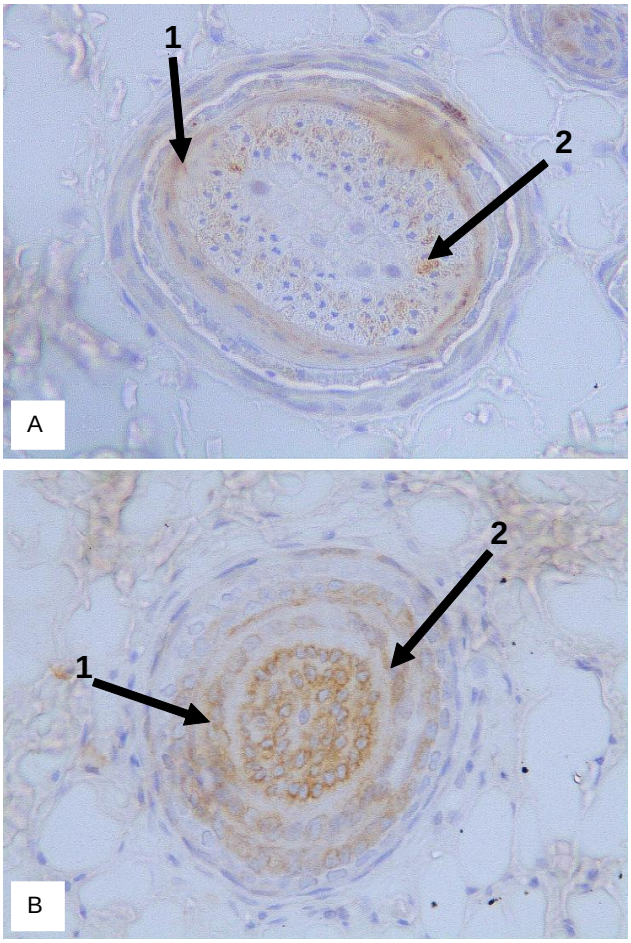

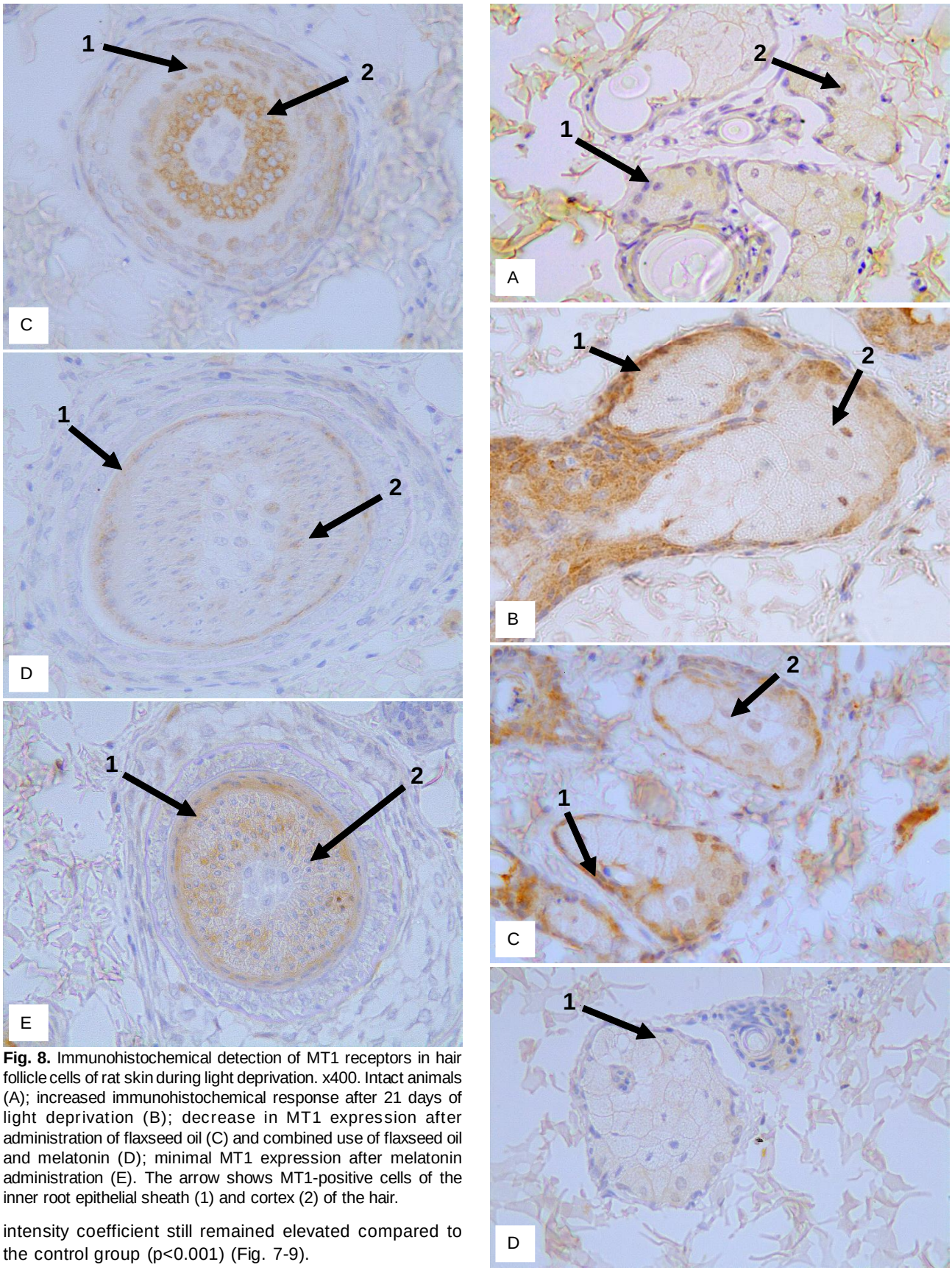


**Fig. 8.** Immunohistochemical detection of MT1 receptors in hair follicle cells of rat skin during light deprivation. x400. Intact animals (A); increased immunohistochemical response after 21 days of light deprivation (B); decrease in MT1 expression after administration of flaxseed oil (C) and combined use of flaxseed oil and melatonin (D); minimal MT1 expression after melatonin administration (E). The arrow shows MT1-positive cells of the inner root epithelial sheath (1) and cortex (2) of the hair.

intensity coefficient still remained elevated compared to the control group ($p<0.001$) (Fig. 7-9).

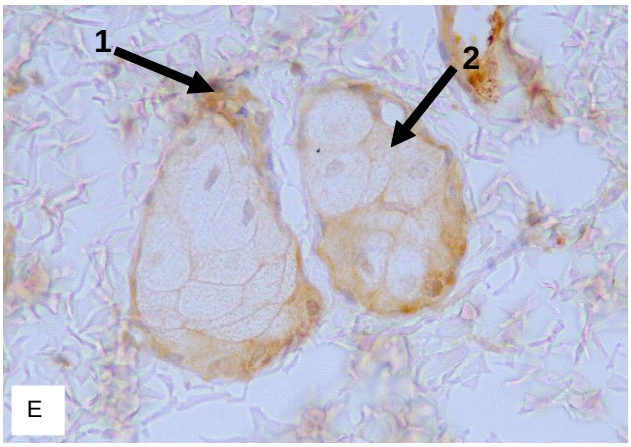


**Fig. 9.** Immunohistochemical detection of MT1 receptors in the cells of the sebaceous glands of rat skin during light deprivation. x400. Intact animals (A); increased immunohistochemical response after 21 days of light deprivation (B); decrease in MT1 expression after administration of flaxseed oil (C) and combined use of flaxseed oil and melatonin (D); minimal MT1 expression after melatonin administration (E). The arrow shows MT1-positive, poorly differentiated (1) and mature (2) sebocytes of the terminal sections of the sebaceous glands.

## Discussion

Thus, MT1 receptors serve to bind melatonin in the skin, and their expression directly affects the effectiveness of the hormone [3, 4, 7, 12, 13, 15, 16].

The data obtained in this work provide evidence that light deprivation contributes to some destabilization of the local circadian system in the epidermis, sebaceous glands and hair follicles of experimental animals against the background of the absence of periodicity in the production of melatonin. Taking into account the fact that the most intense expression of this hormone is observed at night, in response to 24-hour darkness in animals, the level of melatonin in tissues and peripheral blood should strongly increase. The signs of this process in the present study were the destabilization of MT1 receptors in keratinocytes and sebocytes on days 7 and 14, which consisted in a decrease in their number, while the proportion of highly positive cells increased. It can be assumed that these changes occur due to qualitative (structural) and quantitative disorders of cell receptors, against the background of excessive chronic exposure to the hormone. According to the literature, a similar decrease in the number of melatonin receptors is observed with age-related changes in the skin. This leads to an increase in the proportion of damaged keratinocytes and sebocytes, and the loss of their ability to normal regeneration [3].

It is known that circulating melatonin is able to influence its own concentration according to the principle of negative feedback [4, 12]. Therefore, it is natural to assume that a longer stay of animals in the dark (for 21 days) induces a decrease in melatonin production and promotes an increase in the expression of cytoplasmic MT1 receptors in keratinocytes and sebocytes. The cells compensate for the hormonal deficiency by increasing the number of receptors on their surface, which is necessary for binding its minimal amounts.

The corrective effect of the introduction of flaxseed oil can most likely be explained by several reasons. First, it contains large amounts of essential fatty acids linoleic, α-linolenic (maximum amount) and γ-linolenic. This oil also contains oleic, palmitic, linoleic and stearic acids [6, 14, 18]. Moreover, only linseed oil contains linoleic and α-linolenic acids in a ratio of 1:1 that is optimal for the human body [6]. It has been proven that omega-3 fatty acids increase the content of this indole in the blood due to the synergistic regulation of the pineal gland [11, 14, 22]. Secondly, flaxseed oil is a natural source of melatonin (phytomelatonin), which may also have an effect on hormonal status [14]. Third, flaxseed oil has a high content of lignans, which act as antioxidants and phytoestrogens [5]. Thus, flaxseed oil is generally referred to as a functional food, which has high physiological benefits and reduces the risk of developing many diseases, as well as increases the protective properties of the body [11].

Consequently, with the introduction of flaxseed oil to rats against the background of light deprivation, a clear tendency to a decrease in the severity of disorders in the expression of MT1 receptors and a tendency to its normalization were manifested. This was especially pronounced on days 7 and 21 of the study.

Melatonin replacement therapy has also been shown to be effective during light deprivation. Some smoothing of the effect of an unfavorable environmental factor on melatonin receptors of epidermal cells and hair follicles was observed, but only on days 7 and 21 [2, 4, 5, 10, 12, 15]. At the same time, in sebocytes of the sebaceous glands, this effect persisted throughout the study. This phenomenon can be explained by the fact that the sebaceous glands do not belong to the structures of extrapineal synthesis of melatonin, in contrast to the keratinocytes of the skin and, therefore, sebocytes may be more sensitive to the exogenous hormone. According to studies on the effect of exogenous melatonin on rodents using various stress models, it was found that this hormone has a powerful and long-term anti-stress effect [9, 17, 23].

At the same time, the activity of flaxseed oil and melatonin increases when they are combined. So, it was found that melatonin protects omega-3 from lipid peroxidation, and also promotes the absorption of these fatty acids in the body. This increases both the level of fatty acids and the optimization of the ratio of omega-6 and omega-3. However, omega-3 fatty acids contribute to the production of melatonin in the body. It is assumed that melatonin and omega-3 enhance mitochondrial protection against free radical damage [21].

## Conclusions

The results obtained in the course of the study lead to the following conclusions:

1. Light deprivation is accompanied by destabilization of the expression of MT1 melatonin receptors in the epidermis, sebaceous glands and hair follicles

2. The use of flaxseed oil and melatonin as a corrector helps to level the adverse effect of desynchronosis on the studied parameters of MT1 receptors in the epidermis, sebaceous glands and hair follicles.

3. The most pronounced effect on the expression of MT1 receptors is observed with the introduction of exogenous melatonin on the 21st day of the experiment.

## References


[1] Arzamastsev, E.V., Guskova, T.A., Berezovskaya, I.V., Lyubimov, B.I., Lieberman, S.S., & Verstakova, O.L. (2005). *Методические указания по изучению общетоксического действия фармакологических веществ. Руководство по экспериментальному (доклиническому) изучению новых фармакологических веществ [Guidelines for the study of the general toxic effect of pharmacological substances. Guidelines for experimental (preclinical) study of new pharmacological substances].* Под ред. Р.У.Хабриева, Ed. R.U.Khabrieva. M.: Медицина - M.: Medicine.

[2] Bykov, M.I., Esaulenko, E.E., & Basov, A.A. (2015). Экспериментальное обоснование использования льняного масла и масла из плодов грецкого ореха в гастроэнтерологической практике [Experimental substantiation of the use of flaxseed oil and walnut oil in gastroenterological practice]. *Экспериментальная и клиническая гастроэнтерология - Experimental and Clinical Gastroenterology,* 118(6), 53-56.

[3] Dong, K., Goyarts, E., Rella, A., Pelle, E., Wong, Y.H., & Pernodet, N. (2020). Age associated decrease of MT-1 melatonin receptor in human dermal skin fibroblasts impairs protection against UV-induced DNA damage. *Int. J. Mol. Sci.*, 21(1), 326. doi: 10.3390/ijms21010326

[4] Emet, M., Ozcan, H., Ozel, L., Yayla, M., Halici, Z., & Hacimuftuoglu, A.A. (2016). Review of melatonin, its receptors and drugs. *Eurasian J. Med.*, 48(2), 135-141. doi: 10.5152/eurasianjmed.2015.0267

[5] Goyal, A., Sharma, V., Upadhyay, N., Gill, S., Sihag, M. (2014) Flax and flaxseed oil: an ancient medicine & modern functional food. *J. Food Sci. Technol.,* 51(9), 1633-1653. doi: 10.1007/s13197-013-1247-9

[6] Han, Y., Deng, X., Zhang, Y., Wang, X., Zhu, X., Mei, S., & Chen, A. (2020). Antidepressant-like effect of flaxseed in rats exposed to chronic unpredictable stress. *Brain Behav.*, 10(6), e01626. doi: 10.1002/brb3.1626

[7] Isola, M., Ekstrom, J., Lilliu, M.A., Isola, R., & Loy, F. (2016). Dynamics of the melatonin MT1 receptor in the rat parotid gland upon melatonin administration. *J. Physiol. Pharmacol.,* 67(1), 111-119. doi: 10.1111/j.1600-079X.2007.00470.x

[8] Keskin, E., & Uluisik, D. (2019). The protective effect of melatonin on plasma lipid profile in rats with cerulein-induced acute pancreatitis. *Turkish Journal of Sport and Exercise,* 21(2), 332-336. doi: 10.15314/tsed.541829

[9] Khan, R., Morley, S., Daya, S., & Potgieter, B. (1990). *The evaluation of melatonin as a possible anti-stress hormone.* In: Lubec G., Rosenthal G.A. (eds) Amino Acids. Springer, Dordrecht. doi: 10.1007/978-94-011-2262-7_120

[10] Kim, T.K., Lin, Z., Tidwell, W.J., Li, W., & Slominski, A.T. (2015). Melatonin and its metabolites accumulate in the human epidermis in vivo and inhibit proliferation and tyrosinase activity in epidermal melanocytes in vitro. *Mol. Cell. Endocrinol.*, 404, 1-8. doi: 10.1016/j.mce.2014.07.024

[11] Lavialle, M., Champeil-Potokar, G., Alessandri, J.M., Balasse, L., Guesne, T.P., Papillon, C. … Denis, I. (2008) An (n-3) polyunsaturated fatty acid-deficient diet disturbs daily locomotor activity, melatonin rhythm, and striatal dopamine in Syrian hamsters. *J. Nutr.,* 138(9), 1719-1724. doi: 10.1093/jn/138.9.1719

[12] Liu, J., Clough, S.J., Hutchinson, A.J., Adamah-Biassi, E.B., Popovska-Gorevski, M., & Dubocovich, M.L. (2016). MT1 and MT2 melatonin receptors: a therapeutic perspective. *Ann. Rev. Pharmacol. Toxicol.,* 56, 361-383. doi: 10.1146/annurev-pharmtox-010814-124742

[13] Mathes, A.M., Heymann, P., Ruf, C., Huhn, R., Hinkelbein, J., Volk, T., & Fink, T. (2019). Endogenous and exogenous melatonin exposure attenuates hepatic MT1 melatonin receptor protein expression in rat. *Antioxidants,* 8(9), 408. doi:10.3390/antiox8090408

[14] Peuhkuri, K., Sihvola, N., & Korpela, R. (2012). Dietary factors and fluctuating levels of melatonin. *Food & Nutrition Research,* 56. doi: 10.3402/fnr.v56i0.17252

[15] Plikus Bogi, M.V. (2018). Skin as a window to body-clock time. *Proceedings of the National Academy of Sciences*, 115(48), 12095-12097. doi: 10.1073/pnas.1817419115

[16] Plikus Bogi, M.V., Van Spyk, E.N., & Pham, K. (2015). The circadian clock in skin: implications for adult stem cells, tissue regeneration, cancer, aging, and immunity. *J. Biol. Rhythms,* 30(3), 163-182. doi: 10.1177/0748730414563537

[17] Reiter, R.J., Tan, D.X., & Maldonado, M.D. (2005). Melatonin as an antioxidant: physiology versus pharmacology. *Journal of Pineal Research,* 39, 215-216. doi: 10.1111/j.1600-079X.2005.00261.x

[18] Slominski, A.T., Hardeland, R., Zmijewski, M.A., Slominski, R.M., Reiter, R.J., & Paus, R. (2018). Melatonin: a cutaneous perspective on its production, metabolism, and functions. *J. Invest. Dermatol.,* 138(3), 490-499. doi: 10.1016/j.jid.2017.10.025

[19] Sobolevskaya, I.S., Myadelets, O.D., & Yarotskaya, N.N. (2020). Состояние липидного обмена у крыс при световой депривации на фоне коррекции льяным маслом и мелатонином [The state of lipid metabolism in rats during light deprivation against the background of correction with linseed oil and melatonin]. *Вестник Казанского национального медицинского университета - Bulletin of Kazan National Medical University,* 2, 404-409. ISSN: 2524 - 0692.

[20] Sobolevskaya, I.S., Krasnobaeva, M.I., & Myadelets, O.D. (2020). Особенности экспрессии рецепторов мелатонина MT1 в кожном покрове крыс при световой депривации [Peculiarities of expression of MT1 melatonin receptors in the skin of rats under light deprivation]. *Морфологія - Morphology,* 14(4), 64-71. doi: 10.26641/1997-9665.2020.4.64-71

[21] Xu, J., Yang, W., & Deng, Q. (2012). Flaxseed oil and α-lipoic acid combination reduces atherosclerosis risk factors in rats fed a high-fat diet. *Lipids Health Dis.*, 11, 148. doi: 10.1186/1476-511X-11-148

[22] Zhao, M., Tuo, H., Wang, S., & Zhao, L. (2020). The effects of dietary nutrition on sleep and sleep disorders. *Mediators of Inflammation*, 2020(3142874), 1-7. doi: 10.1155/2020/3142874

[23] Zhong, J., & Liu, Y. (2018). Melatonin and age-related cardiovascular diseases. *Aging Med.* (Milton), 1(2), 197-203. doi: 10.1002/agm2.12036

**ВПЛИВ ЕКЗОГЕННОГО МЕЛАТОНІНА ТА ЛЛЯНОГО МАСЛА НА СТАН ЕКСПРЕСІЇ РЕЦЕПТОРІВ MT1 У ШКІРІ ЩУРІВ ЗА УМОВИ СВІТЛОВОЇ ДЕПРИВАЦІЇ**

***Соболевська І.С., Краснобаєва М.І., Мяделець О.Д.***

*Більшість клітин шкіри володіють власною автономною функціональною циркадною системою, яка здатна контролювати фізіологічні та біохімічні процеси в загальному покрові. Особлива роль у цих процесах відводиться "вартовому" гормону епіфіза мелатоніну, котрий впливає на клітини-мішені за допомогою специфічних рецепторів (MT1, MT2, MT3 і RORα). Будь-який розлад добових ритмів може призводити до перебудов (порушень) у рецепторному апараті клітин загального покриву, що вимагає певної корекції. Отже, виникає необхідність у пошуку дієвих і надійних препаратів, що дозволять запобігти негативним наслідкам, викликаних хронодеструкцією. У даній роботі проведено дослідження ефективності впливу екзогенного мелатоніну і лляного масла на експресію рецепторів MT1 в загальному покриві щурів при світловій депривації. Експериментальне дослідження було проведено на 130 білих безпородних щурах-самцях (170-220 г), яких випадковим чином розподілили на 5 груп: інтактна, тварини з моделюванням світлової депривації, тварини з моделюванням світлової депривації, яким внутрішньошлунково вводили лляне масло і мелатонін. На 7, 14 і 21 добу забирали гістологічний матеріал (фрагменти шкіри міжлопаткової області спини). Для іммунногістохімічних досліджень серійні зрізи фарбували з використанням поліклональних антитіл MTNR1A. Для морфометричного аналізу даних застосовували комп'ютерні програми Image Scope Color і ImageJ. Всю статистичну обробку даних проводили за допомогою програми Statistica 10.0. Відмінності вважали достовірними за умови p<0,01. В ході експерименту було встановлено, що світлова депривація сприяє зміні активності експресії рецепторів мелатоніну MT1 в епідермісі, сальних залозах і волосяних фолікулах. Проведені дослідження показали, що введення щурам з десинхронозом лляної олії, мелатоніну, а також їх комбінації супроводжується нівелюванням несприятливого впливу десинхроноза на досліджувані параметри рецепторів MT1. Найбільш виражений корекційний ефект на експресію рецепторів MT1 спостерігається при введенні екзогенного мелатоніну на 21 добу експерименту.*

**Ключові слова:** *рецептори мелатоніну MT1, епідерміс, сальні залози, волосяні фолікули, мелатонін, лляне масло, світлова депривація.*

**DOI: 10.31393/morphology-journal-2021-27(2)-06** **Reports of Morphology, Vol. 27, №2, Pages 39-46**

**ISSN 1818-1295 eISSN 2616-6194**

**REPORTS OF MORPHOLOGY**

***Official Journal of the Scientific Society of Anatomists, Histologists, Embryologists and Topographic Anatomists of Ukraine***

journal homepage: https://morphology-journal.com

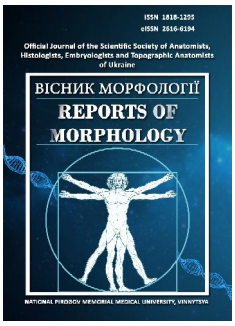


# Regression models of teleroentgenograhic indicators of the position of teeth and the profile of face soft tissues in juvenile aged persons with different face types according to Schwarz A.M.

***Prokopenko O.S.***
National Pirogov Memorial Medical University, Vinnytsya, Ukraine

**ARTICLE INFO**
Received: 22 February 2021
Accepted: 12 April 2021

**UDC:** 617.52:616-073.756.3-053.7

**CORRESPONDING AUTHOR**
e-mail: prokopenko.stom@gmail.com
Prokopenko O.S.

*Considering the differences in the values of teleroentgenograhic (TRG) indicators in different racial, gender, ethnic, age, population, geographical population groups and numerical methods of TRG analysis, determination of normative values of cephalometric, gnatometric TRG-indicators, their interdependencies in the population of different countries is extremely important both for human anatomy and for the practice of dentists. This fully applies to residents of Ukraine of different age groups. The aim of the work is to develop and analyze regression models of teleroentgenograhic indicators of tooth position and facial soft tissue profile according to Schwarz A.M. in Ukrainian young men and young women with different facial types. Lateral teleroentgenograms of 49 young men (aged 17 to 21 years) and 76 young women (aged 16 to 20 years) with physiological occlusion as close as possible to orthognathic were analyzed. In the license package "Statistica 6.0" regression models of indicators of position of teeth and profile of soft tissues of the face according to the method of Schwarz A.M. depending on basic cephalometric and gnatometric indicators separately for boys and for girls with different types of the face are constructed. In young men, 16 of the 24 possible reliable regression models were constructed, in which the coefficient of determination is greater than 0.6 ($R^2$=from 0.609 to 0.998). For young men with 1st (back face type) and 3rd (front face type) face types, the following models were created with respect to 5 indicators from 8 possible (respectively, angles Max1-SpP S-arz, distances Sn-Pn and Pog'-Por, angles Gl'LsPog' and SnPog'-Pn; $R^2$ = from 0.609 to 0.998 and angles Max1-SpP S-arz and Mand1-MP Schwars, distances Sn-Pn and Pog'-Por, angle Gl'LsPog'; $R^2$ = from 0.609 to 0.946), and for young men with 2nd face types (average face type according to Schwarz AM) - for 6 indicators (angles Max1-SpP S-arz and Mand1-MP Schwars, distances Sn-Pn and Pog'-Por, angles Gl'LsPog'and SnPog'-Pn; $R^2$ = from 0.690 to 0.990). In young women, 17 of the 24 possible reliable models with $R^2$ greater than 0.6 ($R^2$ = 0.628 to 0.958) were constructed. For young women with 1st type of face 6 indicators are modeled - angles Max1-SpP S-arz, distances Sn-Pn and Pog'-Por, angles Gl'LsPog'and SnPog'-Pn, the distance of Li-SnPog'($R^2$= from 0.663 to 0.958). For young women with 2nd face type, the following models were created for 7 indicators - angles Max1-SpP S-arz and Mand1-MP Schwars, distances Sn-Pn and Pog'-Por, angles Gl'LsPog' and SnPog'-Pn, distances Li-SnPog'($R^2$= from 0.628 to 0.891). For young women with 3rd face type the smallest number of models with $R^2$ larger than 0.6 was built, compared to all groups of persons with different face types - only 4 models for Max1-SpP S-arz angle, Pog'-Por distance, angles Gl'LsPog' and SnPog'-Pn ($R^2$ from 0.718 to 0.847).*

**Keywords:** *young men, young women, teleroentgenograhic indicators, regression models, indicators of teeth location, indicators of facial soft tissues, facial types according to Schwarz A.M.*

## Introduction

Determination of cephalometric parameters, morphometry of parameters of craniofacial structures, indicators of the human dental apparatus have always occupied an important place both in anatomical research

and in the practice of dentists, surgeons, cosmetologists, etc. The most valuable, informative and accessible method for determining such indicators was X-ray cephalometric analysis using lateral teleroentgenography. The method of teleroentgenography allows to obtain a lifetime image of the head and its bone structures, soft tissues of the face in full accordance with their actual size and location, allows to obtain both qualitative and quantitative linear and angular morphometric parameters [1, 16, 18]. But there are still a number of unresolved problems in determining and interpreting the results of teleroentgenography - there are dozens of author's methods of such research, which are used by researchers and practitioners intuitively, based on their own experience and preferences, or the priorities of their choice in a particular country or medical institution; frequent discrepancy between the author's indicators established on certain samples of the population and the indicators received by researchers on other samples depending on racial [2, 14, 17], ethnic [21, 25, 32], population [13, 22] features of the population of different geographical zones, different countries [12, 20, 23].

Therefore, determining the features of cephalometric, gnatometric teleroentgenograhic (TRG) indicators of the population of different countries is extremely important for both human anatomy and practice, especially dentists, orthopedists, orthodontists, specialists in maxillofacial surgery. In recent years, a number of scientific and practical developments in this direction have appeared in Ukraine [8, 9, 27]. An important place among such studies is occupied by works on mathematical modeling of individual teleroentgenograhic indicators of various methods of cephalometric analysis, inherent in persons with orthognathic occlusion, which is necessary primarily for practical use in dentistry [5, 6, 10, 15, 24].

*The aim* of the work is to develop and analyze regression models of teleroentgenograhic indicators of tooth position and facial soft tissue profile according to Schwarz A.M. in Ukrainian young men and young women with different face types.

## Materials and methods

We analyzed lateral teleroentgenograms in residents of Ukraine of the youth age group - 49 young men (aged 17 to 21 years) and 76 young women (aged 16 to 20 years) with a physiological bite that was as close as possible to orthognathic (hereinafter "orthognathic bite"). Teleroentgenograms were obtained on a dental cone-beam tomograph Veraviewepocs 3D Morita (Japan). Some of the primary indicators of teleroentgenograms were obtained from the database of the research center of National Pirogov Memorial Medical University, Vinnytsya.

Determination of teleroentgenograhic parameters was performed using licensed medical software OnyxCeph$^{3}$™, version 3DPro (Image Instruments GmbH, Germany). Measurements were performed according to the recommendations of Schwarz A.M. [29, 30]. Cephalometric points were determined according to the recommendations of Phulari B.S. [26] and S.I. Doroshenko and E.A. Kulginsky [11].

The obtained teleroentgenograhic indicators were divided into 3 groups [6, 7]. Indicators of group 1 - metric characteristics of the skull, defined in the classical methods of A. Bjork [3], C.J. Burstone [4], J.R. Jarabak [19], R.M. Ricketts [28], A.M. Schwarz [29, 30] and S.S. Steiner [31] and which in the process of surgical and orthodontic treatment usually do not change, but act as basic indicators of cephalometric analysis in relation to which the lateral radiographs determine the inclination, position of the upper and lower jaws, closing plane and individual teeth. The second group of indicators - teleroentgenograhic indicators of the upper and lower jaws, inter-jaw indicators according to the method of A.M. Schwarz [29, 30], the definition of which is most often focused during orthodontic surgery when necessary to correct the length, width, angles and position of the upper and lower jaws.

The third group of indicators included teleroentgenograhic indicators of the position of the teeth and the profile of the soft tissues of the face according to the method of A.M. Schwarz [29, 30]: angle Max1-SpP S-arz (°) - is formed by lines Ap1u-Is1u (inclination of the central axis of the upper medial incisor) and ANS-PNS (palatal plane, SpP); angle Mand1-MP Shwars (°) - is formed by lines Ar1L-Is1L and Me-Im and determines the position of the axes of the mandibular incisors relative to the mandibular plane according to A.M. Schwarz; angle II (°) - inter-cutter angle, formed by lines Ap1u-Is1u (central axis of the upper medial incisor) and Ar1L-Is1L (central axis of the lower medial incisor); distance Sn-Pn (mm) - determines the position of the point Sn relative to the perpendicular Pn; Pog'-Por distance (mm) - the distance from the Pog' point to the orbital perpendicular Por (determines the position of the chin relative to the perpendicular to the Frankfurt plane, drawn through the orbit); angle GI'LsPog' (°) - formed by lines GI'-Ls and LsPog' (determines the convexity of the face); the angle SnPog'-Pn (°) - formed by the lines SnPog' and the perpendicular Pn and the distance Li-SnPog' (mm) - determines the position of the point Li relative to the line SnPog'.

Young men and young women were divided into separate groups with different face types according to A.M. Schwarz [29] depending on the values of the facial angle F, which is determined between the Se-N lines (line from the constructive point Se) (sellia turcica entru) in the middle of the distance between back and front inclined wedge-shaped processes to point N (nasion)) and N-A ((line from point N (nasion) to point A (subspinale), the most posterior point of the anterior contour of the upper jaw)): 1 type (back face type according to Schwarz A.M.) - 13 young men or 23 young women, angle F up to 83°; 2 type (average face type according to Schwarz A.M.) - 18 young men or 24 young women, angle F from 84° to 87°; 3 type (front face type according to Schwarz A.M.) - 18 young men, or 29 young

women, angle F>87°.

Conducted mathematical modeling of teleroentgenograhic indicators of 3 groups depending on TRG indicators of 1 or 2 groups in young men and young women with different face types according to Schwarz A.M. using the method of step-by-step regression analysis in the license package "Statistica 6.0". The following conditions were observed during the regression analysis: the final version of the obtained model must have a coefficient of determination ($R^2$) of not less than 0.60; the value of the F-criterion is not less than 3.0; the number of independent variables of the equation should be as small as possible.

The Biomedical Ethics Commission of National Pirogov Memorial Medical University, Vinnytsya, Ukraine has established that the conducted research and applied research methods correspond to the international and domestic bioethical and moral and legal requirements and laws of Ukraine (protocol №8 dated 5.10.2017).

## Results

The results of simulation of teleradiographic indicators of the position of the teeth and the profile of the soft tissues of the face in adolescents with different types of faces according to Schwarz A.M. have the form of the following regression equations.

For young men with 1 face type:

Max1-SpP S-arz (young men type 1) =38.09 + 0.515 x MM - 0.633 x N-Se + 0.595 x Max ($R^2$=0.839; $F_{(3,9)}$=15.59; p<0.0007; Error of estimate=1.671);

Sn-Pn (young men type 1) = - 41.32 + 0.148 x B + 0.320 x H + 0.303 x T + 0.199 x R.asc ($R^2$=0.946; $F_{(4,8)}$=34.84; p<0.0000; Error of estimate=0.7564);

Pog'-Por (young men type 1) = - 159.8 - 1.017 x T + 1.598 x H + 0.608 x N-S ($R^2$=0.968; $F_{(3,9)}$=90.76; p<0,0000; Error of estimate=1.199);

Gl'LsPog' (young men type 1) =159.6 - 1.705 x T - 1.269 x R.asc. + 0.932 x H + 0.927 x S-E ($R^2$=0.933; $F_{(4,8)}$=27.78; p<0.0001; Error of estimate=2.288);

SnPog'-Pn (young men type 1) =100.3 + 1.013 x T - 1,002 x H - 0.125 x F ($R^2$=0.998; $F_{(3,9)}$=1755; p<0.0000; Error of estimate=0.248),

where here and in the future: $R^2$ - coefficient of determination; $F(_{I,II})$=!!,!! - critical (!,!!) and received (!!,!!) the value of the Fisher test; St. Error of estimate - standard error of the standardized regression coefficient; MM - maxillary-mandibular angle, determines the angle at which the upper jaw is located relative to the lower jaw in the sagittal plane and is formed by lines A-B and ANS-PNS (°); N-Se (the length of the front of the skull base by Schwarz A.M.) - the distance from point Se to point N (mm); Max (length of the upper jaw) - distance from the constructive point apMax to point PNS (mm); B (basal angle) - indicates the angle between the upper and lower jaws and is formed by lines ANS-PNS (palatal plane SpP) and Im-Me (mandibular plane MPS by Schwarz) (°); H - angle H by Schwarz A.M., formed by the lines Po-Or and Pn, determines the angle of inclination of the Frankfurt plane to the base of the skull (°); T (profile angle T) - formed by lines Sn-Pog' and Pn (nasal perpendicular) (°); R.asc (the length of the branch of the mandible) - the distance from the constructive point R.asc to the constructive point tGoS (mm); N-S (the length of the anterior cranial base by Jarabak J.R.) - the distance from point N to point S (mm); S-E (the length of the back of the skull base by Steiner C.C.) - the distance from point S to the constructive point E (mm); F (facial angle) - formed by lines Se-N and N-A and determines the location of the anterior contour of the upper jaw in the sagittal plane to the base of the skull (°).

In young men with 1 type of face, the coefficients of determination of regression equations ($R^2$) of Mand1-MP Schwars, II angles and Li-SnPog' distances are from 0.312 to 0.590 and therefore are not relevant for practical use by dentists.

For young men with 2 face type:

Max1-SpP S-arz (young men type 2) =60.25 + 0.780 x MM - 0.508 x N-S-Ba ($R^2$=0,690; $F_{(2,15)}$=16,70; p<0.0002; Error of estimate=3.073);

Mand1-MP Schwars (young men type 2) =103.7 - 0.996 x T + 0.436 x G - 0.849 x I + 0.202 x S-ar:ar-Go ($R^2$=0.807; $F_{(4,13)}$=13.57; p<0.0001; Error of estimate=3.641);

Sn-Pn (young men type 2) = - 42.73 - 0.295 x P-PTV + 0.422 x POr-NBa + 0.345 x H ($R^2$=0.930; $F_{(3,14)}$=62.12; p<0.0000; Error of estimate=1.106);

Pog'-Por (young men type 2) = - 63.93 + 0.377 x R.asc. - 0.645 x T + 0.736 x H ($R^2$=0.972; $F_{(3,14)}$=165.0; p<0.0000; Error of estimate=1.524);

Gl'LsPog' (young men type 2) =175.8 - 1,323 x T + 0.444 x POr-NBa - 2.645 x N-S:S-Ar' ($R^2$=0.892; $F_{(3,14)}$=38.72; p<0.0000; Error of estimate=2.554);

SnPog'-Pn (young men type 2) = 83.53 + 1.013 x T - 0.934 x H ($R^2$=0.990; $F_{(2,15)}$=765.2; p<0.0000; Error of estimate=0.613),

where here and in the future: N-S-Ba (by Bjork A.) - the angle formed by the S-N lines (front of the skull base) and S-Ba (°); G (gonial angle, angle of the lower jaw) - is formed by lines ppCond-MT2 and T2-Me, which intersect at a point tGoS (°); I (inclination angle) - determines the angle of inclination of the upper jaw (spinal plane) to the nasal perpendicular (°); S-ar:ar-Go (by Jarabak J.R.) - indicator of the ratio of distances S-ar and ar-Go; P-PTV (by Ricketts R.M.) - the distance from point Po to point Pt, parallel to the Frankfurt plane (mm); POr-NBa (cranial inclination angle (deflection) by Ricketts R.M.) - the angle formed by the lines Po-Or and Ba-N (°); N-S:S-Ar' (by Bjork A.) - indicator of the ratio of distances ar'-S and N-S.

In young men with facial type 2, the coefficients of determination of the regression equations ($R^2$) of the angle II and the distance Li-SnPog' are equal to 0.515 and 0.574, respectively, and such models are impractical for practical use.

For young men with 3 face type:

Max1-SpP S-arz (young men type 3) =17.23 + 1.692 x MM - 1.370 x I - 0.623 x T + 3.347 x N-S:S-Ar' ($R^2$=0.609; $F_{(4,13)}$=5.063; p<0.0111; Error of estimate=3.615);

Mand1-MP Schwars (young men type 3) =198.7 - 1.455 x MM + 0.986 x B + 0.615 x N-CC - 0.641 x Max ($R^2$=0.848; $F_{(4,13)}$=18.13; p<0.0000; Error of estimate=3.146);

Sn-Pn (young men type 3) = - 174.3 + 0.794 x H + 0.845 x F - 0.653 x B + 0.440 x POr-NBa + 0.342 x T + 0.425 x I ($R^2$=0.946; $F_{(6,11)}$=32.05; p<0.0000; Error of estimate=1.241);

Pog'-Por (young men type 3) = - 207.3 + 0.958 x F + 1.397 x H - 0.815 x T + 0.451 x N-CC ($R^2$=0.889; $F_{(4,13)}$=26.16; p<0.0000; Error of estimate=2.170);

Gl'LsPog' (young men type 3) = 147.1 - 0.780 x T + 0.569 x B + 0.981 x R.asc. - 1.103 x Max ($R^2$=0.807; $F_{(4,13)}$ = 13.57; p<0.0001; Error of estimate=3.272),

where here and in the future: N-CC (by Ricketts R.M.) - anterior length of the skull base, the distance from point N to point CC (mm).

In young men with 3 type face, the coefficients of determination of regression equations ($R^2$) of angles II, SnPog'-Pn and distance Li-SnPog' are from 0.237 to 0.518 and therefore do not matter for practical use by dentists.

For young women with 1 face type:

Max1-SpP S-arz (young women type 1) = 113.7 - 1.168 x H + 0.781 x MM + 0.566 x R.asc. - 0.557 x Length of Mandible ($R^2$=0,699; $F_{(4,17)}$=9.874; p<0.0003; Error of estimate=3.284);

Sn-Pn (young women type 1) = - 165.8 + 1.271 x H + 1.132 x F - 0.215 x G - 0.114 x N-S-Ar ($R^2$=0.899; $F_{(4,17)}$=37.78; p<0.0000; Error of estimate=1.342);

Pog'-Por (young women type 1) = - 106.0 - 1.145 x MM + 0.877 x I + 0.934 x H - 0.598 x P-PTV + 0.599 x F ($R^2$=0.895; $F_{(5,16)}$=27.40; p<0.0000; Error of estimate=1.856);

Gl'LsPog' (young women type 1) =180.0 - 1.760 x T + 0.599 x R.asc. - 0.376 x N-CC - 0.576 x I + 0.431 x MM ($R^2$=0.925; $F_{(5,16)}$=39.58; p<0.0000; Error of estimate=1.931);

SnPog'-Pn (young women type 1) =103.2 + 0.698 x T - 0.743 x H - 0.402 x N-CC + 0.150 x R.asc. - 0.412 x F + 0.288 x Max ($R^2$=0.958; $F_{(6,15)}$=56.53; p<0.0000; Error of estimate = 0.839);

Li-SnPog' (young women type 1) = - 8.556 + 0.315 x B + 0.368 x T + 0.394 x P-PTV + 0.299 x Max ($R^2$=0.663; $F_{(4,17)}$=8.350; p<0.0006; Error of estimate=1.525),

where here and in the future: Length of Mandible - the length of the mandible (the distance from the projection of the Pog point on the line tGo-Me to the point tGo) (mm); N-S-Ar (sella angle by Bjork A.) - the angle between the anterior cranial base and the lateral cranial base, which determines the position of the temporomandibular joint and glenoid fossae and is formed by the lines N-S and S-ar (°).

In young women with 1 type face, the coefficients of determination of regression equations ($R^2$) of Mand1-MP Schwars and II angles are equal to 0.121 and 0.481, respectively, so such models are impractical for practical use.

For young women with 2 face type:

Max1-SpP S-arz (young women type 2) =186.5 + 1.360 x MM - 0.680 x S-ar:ar-Go - 1.156 x I - 7.242 x N-S:S-Ar' - 0.553 x N-S-Ba ($R^2$=0.863; $F_{(5,17)}$=21.36; p<0.0000; Error of estimate = 2.395);

Mand1-MP Schwars (young women type 2) =174.6 - 1.086 x MM + 0.726 x B ($R^2$=0.648; $F_{(2,20)}$=18.42; p<0.0000; Error of estimate=3.667);

Sn-Pn young women type 2) = - 213.6 + 0.971 x H + 1.544 x F + 0.245 x N-S + 0.294 x B - 0.156 x MM - 0.284 x POr-NBa ($R^2$=0.891; $F_{(6,16)}$=21,75; p<0.0000; Error of estimate=1.194);

Pog'-Por (young women type 2) = - 110.8 + 0.262 x Length of Mandible - 0.709 x T + 1.278 x H ($R^2$=0.880; $F_{(3,19)}$=46.51; p<0.0000; Error of estimate=2.118);

Gl'LsPog' (young women type 2) =244.5 - 0.894 x T - 0.538 x N-S-Ba ($R^2$=0.660; $F_{(2,20)}$=19.42; p<0.0000; Error of estimate=3.827);

SnPog'-Pn (young women type 2) =91.49 + 0.583 x T - 1.529 x H + 0.341 x N-S-Ba + 0.158 x N-CC ($R^2$=0.807; $F_{(4,18)}$=18.85; p<0.0000; Error of estimate = 2.011);

Li-SnPog' (young women type 2) =2.919 + 0.221 x T - 0.169 x ar-Go + 0.233 x S-E ($R^2$=0.628; $F_{(3,19)}$=10.68; p<0.0002; Error of estimate=1.324),

where here and in the future: ar-Go (by Burstone C.J.) - the length of the branch of the mandible, the distance from point Ar to point Go (mm).

The coefficient of determination of the regression equation ($R^2$) of the angle II in young women with 2 type face is equal and such a model has no practical significance.

For young women with 3 face type:

Max1-SpP S-arz (young women type 3) = - 214.9 + 1.005 x MM + 0.934 x N-Se + 1.371 x H - 0.822 x Max + 0.632 x I + 0.498 x P-PTV ($R^2$=0.718; $F_{(6,22)}$=9.332; p<0.0000; Error of estimate=3.727);

Pog'-Por (young women type 3) = - 84.28 + 0.294 x R.asc. - 0.806 x T + 1.152 x H - 0.214 x ar-Go ($R^2$=0.844; $F_{(4,24)}$=32.54; p<0.0000; Error of estimate=2.013);

Gl'LsPog' (young women type 3) =417.6 - 1.177 x T - 1.341 x F - 4.469 x N-S:S-Ar' - 0.538 x N-CC - 0.297 x S-ar:ar-Go - 0.478 x N-S-Ar ($R^2$=0.847; $F_{(6,22)}$=20.34; p<0.0000; Error of estimate=2.411);

SnPog'-Pn (young women type 3) = 40.28 + 0.633 x T - 0.655 x H + 0.223 x MM ($R^2$=0.822; $F_{(3,25)}$=38.50; p<0.0000; Error of estimate=1.654).

In young women with 3 type face, the coefficients of determination of the regression equations ($R^2$) of the Mand1-MP Schwars angle and the distances Sn-Pn and Li-SnPog' are from 0.494 to 0.597 and therefore do not matter for practical use in dentistry. The regression equation for angle II in young women with 3 type face was not constructed at all.

## Discussion

A number of works have proved the fundamental possibility of modeling teleroentgenograhic parameters of the dental apparatus in Ukrainian young men and young women depending on cephalometric parameters. However,

the coefficients of determination $R^2$, which in the evaluation of regression models are interpreted as the conformity of the model to the data and indicate the efficiency of the model in different researchers differ significantly. I.V. Gunas and co-authors [15] constructed and analyzed regression models of TRG parameters used in the method of C.J. Burstone in young men and young women with normal occlusion and a harmonious face. Moreover, the authors managed to obtain regression models with $R^2$>0.6 for all 6 studied indicators of the second group and for all 7 indicators of the third group, depending on the indicators of the first group.

A.V. Chernysh and co-authors [6] built regression models of individual cephalometric parameters in young men and young women used in the method of E.P. Harvold: young men have all possible models of TRG-indicators, which are included in the second group, depending on the indicators of the first group with $R^2$ from 0.616 to 0.940, and young women have built such models only for indicators of the length of the upper and lower jaws with $R^2$, respectively, 0.857 and 0.792. Also, these researchers built reliable models of the third group (angle Ap1uAp1l-DOP) depending on the indicators of the first and second groups, both for young men (R2 = 0.626) and for young women ($R^2$ = 0.584).

A.V. Chernysh also performed simulations of the cephalometric parameters used in the R.M. Ricketts method [5]. The author constructed for both young men and young women by 2 possible models of indicators of the second group (distances Go-CF and Xi-Pm) depending on the indicators of the first group (respectively, $R^2$ = 0.884 and 0.928 and $R^2$ = 0.735 and 0.719) and 7 of the 8 possible reliable models in young men of the indicators included in the third group (distances 6u-6l, Overjet, Overbite, 6u-PTV, 1l-APog, 1u-APog and Xi-OcP) depending on the indicators of the first and second groups and only 5 such models in young women (distances 6u-PTV, 1l-APog, 1u-APog and Xi-OcP and angle Max1-APog).

Instead, M.O. Dmitriev and co-authors [10], modeled gnatometric TRG parameters used in methods by A.M.Schwarz, J.Mc Namara, B.B.Downs, R.A.Holdway, P.F.Schmuth, C.C.Steiner and C.H.Tweed, depending on the parameters of basal cranial structures in young Ukrainian residents with orthognathic occlusion. In young men out of 43 possible regression models, the authors obtained only 4 reliable models with a coefficient of determination greater than 0.5 (for indicators of effective upper jaw length, upper jaw length, SND angle and distance S_L), and in young women, no models with a coefficient of determination greater than 0.5 were constructed at all.

According to the results of our mathematical modeling by stepwise regression analysis of eight teleroentgenograhic indicators of the position of the teeth and soft tissues of the face, which were included in the third group according to the method of A.M. Schwarz depending on the first group (basic cephalometric TRG-indicators) and the second group of indicators (gnatometric TRG-indicators of the upper and lower jaws) according to the method of A.M. Schwarz in young men with orthognathic occlusion and with different face types according to A.M. Schwarz, constructed 16 of the 24 possible reliable regression models in which the coefficient of determination is greater than 0.6 ($R^2$ = from 0.609 to 0.998). For young men with the first and third face types, the following models were created for five indicators (respectively, the angle Max1-SpP S-arz, the distances Sn-Pn and Pog'-Por, the angles Gl'LsPog' and SnPog'-Pn; $R^2$ = from 0.839 to 0.998 and angles Max1-SpP S-arz and Mand1-MP Schwars, distances Sn-Pn and Pog'-Por, angle Gl'LsPog'; $R^2$ = from 0.609 to 0.946), and for a group of young men with the second type face - about 6 indicators (angles Max1-SpP S-arz and Mand1-MP Schwars, distances Sn-Pn and Pog'-Por, angles Gl'LsPog' and SnPog'-Pn; $R^2$ = from 0.690 to 0.990).

For young women built almost the same number of models - 17 of the 24 possible reliable regression models in which the coefficient of determination is greater than 0.6 ($R^2$ = from 0.628 to 0.958). But the number of models for certain groups of people with different face types, as well as the indicators for which such models were created in young women differed slightly. For young women with the first type of face, the following models were created for 6 indicators - in addition to the same five indicators ($R^2$ = from 0.699 to 0.958), as for young men of the first group, a model was built for the distance Li-SnPog' ($R^2$ = 0.663). For young women with the second type of face, the following models were created for 7 indicators - in addition to the same six indicators ($R^2$ = from 0.660 to 0.891), as for young men with the second type of face, a model was also built for the distance Li-SnPog' ($R^2$ = 0.628). Instead, for young women with the third type of face, the smallest number of models with coefficients of determination greater than 0.6, compared to all groups, both young men and young women with different facial types - only 4 models for the angle Max1-SpP S-arz, Pog'-Por distances, Gl'LsPog' and SnPog'-Pn angles (with $R^2$ from 0.718 to 0.847). Compared with the group of young men with the third type of face, young women with this type of face were not built models with a coefficient of determination greater than 0.6 for the angle Mand1-MP Schwars and the distance Sn-Pn, instead - such a model was created for the angle SnPog'-Pn.

It should be noted that for Max1-SpP S-arz, Gl'LsPog' and Pog'-Por distances, models with a coefficient of determination greater than 0.6 have been developed for both young men and young women of all face types. For the Sn-Pn distance, such models are designed for young men of all face types and for young women of all face types except the third type, and for the SnPog'-Pn angle, on the contrary, for young women of all face types and for young men of all face types except the third type. The Mand1-MP Schwars angle was modeled with a coefficient of determination greater than 0.6 in young men with the second and third facial types and in young women with the

second facial type, and the Li-SnPog' distance was modeled only in young men with the first and second facial types.

The inter-incisor angle II in all models of young men with different face types and young women with the first and second face types was modeled with coefficients of determination less than 0.6, and in young women with the third face type the model of this indicator was not built at all.

Regression equations of Li-SnPog' distance values had coefficients of determination less than 0.6 in young men of all face types ($R^2$ from 0.312 to 0.574) and in young women with 3 face types ($R^2$ = 0.494), and coefficients of determination of regression equations of Mand1-MP Schwars angle values were less than 0.6 in young men with 1 facial type ($R^2$ = 0.569) and in young women with 1 and 3 facial types (respectively, $R^2$ = 0.121 and $R^2$ = 0.597).

In young men with different types of faces to the constructed models of teleroentgenograhic indicators, which were included in the third group according to the method of Schwarz A.M. most often includes the following TRG indicators of the first and second groups: profile angle T (21.4%), angle H according to A.M. Shwars (16.1%) and angles MM (maxillary-mandibular angle), B (basal angle, angle between upper and lower jaws) and distance R.asc. (length of the branch of the mandible) (7.1%).

In young women models of teleroentgenograhic indicators of the third group according to the method of A.M. Schwarz most often includes the following TRG indicators of the first and second groups: profile angle T and angle H according to A.M. Shwars (13.9% each), angle MM (maxillary-mandibular angle) (11.1%) and angle F (facial angle) (6.9%).

In our opinion, the practical application of the created regression models of teleroentgenograhic indicators of tooth position and soft tissue profile of the face depending on the basic cephalometric indicators and gnatometric indicators of the upper and lower jaws based on sex, face type will provide an individual approach to the patient and the best consequences of treatment in case of need of surgical correction of these indicators at inhabitants of Ukraine of youthful age.

## Conclusions

1. In young men, residents of Ukraine with orthognathic occlusion and with different types of faces according to A.M. Schwarz, constructed 16 of 24 possible reliable regression models with coefficients of determination greater than 0.6 ($R^2$ = from 0.609 to 0.998) groups of teleroentgenograhic indicators of the position of the teeth and the profile of soft tissues of the face, which can be corrected during surgery, orthopedic interventions in dentistry depending on the group of basic, invariable cephalometric indicators and the group of teleroentgenograhic indicators of the upper and lower jaws. In young women with different face types, 17 of the 24 possible models in which the coefficient of determination is greater than 0.6 ($R^2$ = from 0.628 to 0.958) were constructed.

2. The created models are suitable for use in the practice of dentists, cosmetologists in order to provide an individualized approach to determining the tactics, scope and improvement of the consequences of interventions when necessary to correct these indicators in adolescents.

## References


[1] Amini, F., Razavian, Z.S., & Rakhshan, V. (2016). Soft tissue cephalometric norms of Iranian class I adults with good occlusions and balanced faces. *International Orthodontics,* 14(1), 108-122. doi: 10.1016/j.ortho.2015.12.003

[2] Behbehani, F., Hicks, E.P., Beeman, C., Kluemper, G.T., & Rayens, M.K. (2006). Racial variations in cephalometric analysis between Whites and Kuwaitis. *Angle Orthod.,* 76(3), 406-411. doi: 10.1043/0003-3219(2006)076[0406:RVICAB]2.0.CO;2

[3] Björk, A. (1966). Sutural growth of the upper face studied by the implant method. *Acta Odontologica Scandinavica,* 24(2), 109-27. doi: 10.3109/00016356609026122

[4] Burstone, C.J., James, R.B., Legan, H., Murphy, G.A., & Norton, L.A. (1978). Cephalometrics for orthognathic surgery. *Journal of Oral Surgery (American Dental Association),* 1965, 36(4), 269-277. PMID: 273073

[5] Chernysh, A.V. (2018). Regression models of individual cephalometric indicators used in the method of R.M. Ricketts. *Biomedical and Biosocial Anthropology,* 32, 56-62. doi.org/10.31393/bba32-2018-08

[6] Chernysh, A.V, Hasiuk, P.A, Yasko, V.V, & Smolko, D.G. (2018). Regression models of individual cephalometric indicators used in the method of E.P. Harvold. *Reports of Morphology,* 24(4), 29-34. https://doi.org/10.31393/morphology-journal-2018-24(4)-04

[7] Dmitriev, M.O. (2017). Зв'язки основних краніальних показників з характеристиками положення зубів верхньої і нижньої щелеп та профілем м'яких тканин обличчя в юнаків і дівчат [Relationships of the main cranial indicators with the characteristics of the position of the teeth of the upper and lower jaws and the profile of the soft tissues of the face in boys and girls]. *Вісник морфології - Reports of Morphology,* 23(1), 125-31.

[8] Dmitriev, M.O. (2017). Визначення нормативних цефалометричних параметрів за методикою Г.Шмута для українських юнаків та дівчат [Identification of normative cephalometric parameters based on G.Schmuth method for young male and female ukrainians]. *Вісник морфології - Reports of Morphology,* 23(2), 288-292.

[9] Dmitriev, M.O., Chernysh, A.V., & Chugu, T.V. (2018). Cephalometric studies of Ukrainian boys and girls with physiological bite by the method of Charles J. Burstone. *Biomedical and Biosocial Anthropology,* 30, 62-67. doi: 10.31393/bba30-2018-09

[10] Dmitriev, M.O, Dudik, O.P, Chugu, T.V, & Cherkasova, O.V. (2018). Modeling of gnatometric indices depending on parameters of basal cranial structures in boys and girls with orthognathic bite. *Bulletin of Scientific Research*, 90(1), 110-113. doi.org/10.11603/2415-8798.2018.1.8764]

[11] Doroshenko, S.I., & Kulginsky, E.A. (2007). *Fundamentals of Teleradiography.* Kyiv: Health.

[12] Drevensek, M., Farcnik, F., & Vidmar, G. (2006). Cephalometric

standards for Slovenians in the mixed dentition period. *Eur. J. Orthod.,* 28(1), 51-57. doi: 10.1093/ejo/cji081

[13] Gonzalez, M.B., Caruso, J.M., Sugiyama, R.M., & Schlenker, W.L. (2013). Establishing cephalometric norms for a Mexican population using Ricketts, Steiner, Tweed and Arnett analyses. *APOS Trends Orthod.,* (3), 171-177. doi: 10.4103/2321-1407.121437

[14] Gueye, M., Dieng, L., Mbodj, E.B., Seck, A.K., Toure, A., Thioune, N., & Ngom, P.I. (2014). Relationship between bizygomatic width and the size of maxillary anterior teeth among young Senegalese black people recruited in army. *Odontostomatol. Trop.*, 37(148), 5-12. PMID: 25980092

[15] Gunas, I.V, Chernysh, A.V, Cherkasov, V.G., & Cherkasova, O.V. (2018). Modeling by using regression analysis of teleroentgenographic individual indicators used in the method of Charles J. Burstone. *Biomedical and Biosocial Anthropology,* 31, 59-65. doi: 10.31393/bba31-2018-08

[16] Hashim, H.A., & AlBarakati, S.F. (2003). Cephalometric soft tissue profile analysis between two different ethnic groups: a comparative study. *J. Contemp. Dent. Pract.,* 4(2), 60-73. doi: 10.5005/jcdp-4-2-60

[17] Huang, W.J., Taylor, R.W., & Dasanayake, A.P. (1998). Determining cephalometric norms for Caucasians and African Americans in Birmingham. *Angle Orthod.,* 68(6), 503-511. doi: 10.1043/0003-3219(1998)068<0503:DCNFCA>2.3.CO;2

[18] Jacobson, A., & White, L. (2007). Radiographic cephalometry: from basics to 3-D imaging. *American Journal of Orthodontics and Dentofacial Orthopedics,* 131(4), S133. doi: 10.1016/j.ajodo.2007.02.038

[19] Jarabak, J.R., & Fizzell, J.A. (1972). T*echnique and treatment with light-wire edgewise appliances.* Ed.2, St. Louis. The CV Mosby Company.

[20] Johannsdottir, B., Thordarson, A., & Magnusson, T.E. (2004). Craniofacial skeletal and soft tissue morphology in Icelandic adults. *European Journal of Orthodontics,* 26, 245-250. doi: 10.1093/ejo/26.3.245

[21] Kalha, A.S., Latif, A., & Govardhan, S.N. (2008). Soft-tissue cephalometric norms in a South Indian ethnic population. *Am. J. Orthod. Dentofacial. Orthop.,* 133(6), 876-881. doi: 10.1016/j.ajodo.2006.05.043

[22] Kumari, L., & Das, A. (2017). Determination of Tweed's cephalometric norms in Bengali population. *Eur. J. Dent.*, 11(3), 305-310. doi: 10.4103/ejd.ejd_274_16

[23] Liang, C., Liu, S., Liu, Q., Zhang, B., & Li, Z. (2014). Norms of McNamara's Cephalometric Analysis on Lateral View of 3D CT Imaging in Adults from Northeast China. *Journal of Hard Tissue Biology*, 23(2), 249-254. doi: 10.2485/jhtb.23.249

[24] Marchenko, A.V., Prokopenko, O.S., Dzevulska, I.V., Zakalata T.R., & Gunas, I.V. (2021). Mathematical modeling of teleroentgenographic parameters according to the method of Schwarz A.M. depending on the basic cephalometric parameters in Ukrainian young men and young women with different face types. *Wiadomosci Lekarskie,* 74(6), 1488-1492. doi: 10.36740/WLek202106137

[25] Mohammad, H.A., Abu Hassan, M.I., & Hussain, S.F. (2011). Academic Journals Cephalometric evaluation for Malaysian Malay by Steiner analysis. *Scientific Research and Essays,* 6(3), 627-634. doi: 10.5897/SRE10.869

[26] Phulari, B. (2013). *An atlas on cephalometric landmarks*. JP Medical Ltd. doi: 10.5005/jp/books/11877

[27] Prokopenko, O.S., Beliaiev, E.V., Dmitriev, M.O., Cherkasova, O.V., & Skoruk R.V. (2020). Features of cephalometric parameters, which usually do not change during surgery and orthodontic interventions, in Ukrainian young men and women with orthognathic occlusion and different types and profiles of the face according to Schwarz A.M. *Вісник морфології - Reports of Morphology,* 26(3), 37-45. doi: 10.31393/bba39-2020-10

[28] Ricketts, R.M. (1961). Cephalometric analysis and synthesis. *The Angle Orthodontist.*, 31(3):141-56.

[29] Schwarz, A.M. (1960). *Rontgenostatics; Practical Evaluation of the Tele-X-ray-photo (study-head-plate)* (Vol.1). Leo L. Bruder.

[30] Schwarz, A.M. (1961). Roentgenostatics: a practical evaluation of the x-ray headplate. *American Journal of Orthodontics,* 47(8), 561-585. doi: 10.1016/0002-9416(61)90001-X

[31] Steiner, C.C. (1959). Cephalometrics in clinical practice. *Angle Orthod.,* 29(1), 8-29. doi: 10.1043/0003-3219(1959)029<0008:CICP>2.0.CO;2

[32] Wu, J., Hägg, U., & Rabie, A.B. (2007). Chinese norms of McNamara's cephalometric analysis. *Angle Orthod.,* 77(1), 12-20. doi: 10.2319/021606-62R.1

**РЕГРЕСІЙНІ МОДЕЛІ ТЕЛЕРЕНТГЕНОГРАФІЧНИХ ПОКАЗНИКІВ ПОЛОЖЕННЯ ЗУБІВ ТА ПРОФІЛЮ М'ЯКИХ ТКАНИН ОБЛИЧЧЯ В ОСІБ ЮНАЦЬКОГО ВІКУ З РІЗНИМИ ТИПАМИ ОБЛИЧЧЯ ЗА SCHWARZ A.M.**

***Прокопенко О.С.***

*Зважаючи на існування відмінностей значень телерентгенографічних (ТРГ) показників в різних расових, статевих, етнічних, вікових, популяційних, географічних за місцем проживання групах населення та чисельних методик ТРГ аналізу, визначення нормативних значень цефалометричних, гнатометричних ТРГ-показників, їх взаємозалежностей у населення різних країн є вкрай важливим як для анатомії людини, так і для практичної діяльності лікарів-стоматологів. Це в повній мірі стосується і мешканців України різних вікових груп. Мета роботи - розробка та аналіз регресійних моделей телерентгенографічних показників положення зубів та профілю м'яких тканин обличчя за Schwarz A.M. в українських юнаків і дівчат з різними типами обличчя. Проаналізовані бокові телерентгенограми 49 юнаків (вік від 17 до 21 року) та 76 дівчат (вік від 16 до 20 років) з фізіологічним прикусом, максимально наближеним до ортогнатичного. В ліцензійному пакеті "Statistica 6.0" побудовані регресійні моделі показників положення зубів та профілю м'яких тканин обличчя за методикою Schwarz A.M. в залежності від базових цефалометричних та гнатометричних показників окремо для юнаків і для дівчат з різними типами обличчя. В юнаків побудовані 16 із 24 можливих достовірних регресійних моделей, в яких коефіцієнт детермінації є більшим, ніж 0,6 ($R^2$= від 0,609 до 0,998). Для юнаків з 1 (задній тип обличчя) та з 3 (передній тип обличчя) типами обличчя створені такі моделі щодо 5 показників з 8 можливих (відповідно, кута Max1-SpP S-arz, відстаней Sn-Pn і Pog'-Por, кутів Gl'LsPog' і SnPog'-Pn; $R^2$ = від 0,609 до 0,998 та кутів Max1-SpP S-arz і Mand1-MP Schwars, відстаней Sn-Pn і Pog'-Por, кута Gl'LsPog'; $R^2$ = від 0,609 до 0,946), а для юнаків з 2 типом обличчя (середній тип обличчя за Schwarz A.M.) - щодо 6 показників (кутів Max1-SpP S-arz і Mand1-MP Schwars, відстаней Sn-Pn і Pog'-Por, кутів Gl'LsPog' і SnPog'-Pn; $R^2$ = від 0,690 до 0,990). В дівчат побудовано 17 з 24 можливих достовірних моделей з $R^2$ більшими, ніж 0,6 ($R^2$= від 0,628 до 0,958). Для дівчат з 1 типом обличчя змодельовані 6 показників - кута Max1-SpP S-arz, відстаней Sn-Pn і Pog'-Por, кутів Gl'LsPog' і SnPog'-Pn, відстані Li-SnPog'*

*($R^2$ = від 0,663 до 0,958). Для дівчат з 2 типом обличчя створені такі моделі щодо 7 показників - кутів Max1-SpP S-arz і Mand1-MP Schwars, відстаней Sn-Pn і Pog'-Por, кутів Gl'LsPog' і SnPog'-Pn, відстані Li-SnPog' ($R^2$ = від 0,628 до 0,891). Для дівчат з 3 типом обличчя побудована найменша кількість моделей з $R^2$ більшими, ніж 0,6, порівняно з усіма групами осіб з різними типами обличчя - всього 4 моделі для показників кута Max1-SpP S-arz, відстані Pog'-Por, кутів Gl'LsPog' та SnPog'-Pn ($R^2$ від 0,718 до 0,847).*

**Ключові слова:** *юнаки, дівчата, телерентгенографічні показники, регресійні моделі, показники розташування зубів, показники м'яких тканин обличчя, типи обличчя за Schwarz A.M.*

DOI: 10.31393/morphology-journal-2021-27(2)-07 Reports of Morphology, Vol. 27, №2, Pages 47-52

ISSN 1818-1295 eISSN 2616-6194

REPORTS OF MORPHOLOGY

*Official Journal of the Scientific Society of Anatomists, Histologists, Embryologists and Topographic Anatomists of Ukraine*

journal homepage: https://morphology-journal.com

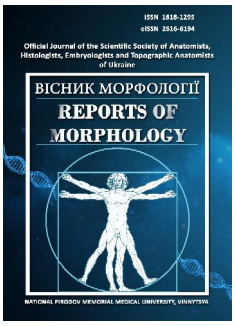


# Comparative characteristics of changes in central hemodynamics during early recovery after different exercise regimes

***Lukyantseva H.V., Bakunovsky O.M., Malyuga S.S., Oliinyk T.M., Manchenko N.R., Manchenko Y.R., Korolyova D.O.***

National University of Ukraine on Physical Education and Sport, Kyiv, Ukraine

**ARTICLE INFO**

Received: 24 February 2021

Accepted: 14 April 2021

**UDC:** 612.13:613.73(045)

**CORRESPONDING AUTHOR**

e-mail: lukjantseva@gmail.com

Lukyantseva H.V.

*The cardiovascular system is one of the most important functional systems of the body, which determine the level of physical performance of the body. Insufficient study of the response of the circulatory system to the combination of strength training with endurance exercises requires more detailed comparative studies of the impact of dynamic and static loads on the indicators of central hemodynamics. Accordingly, the aim of our study was to study the characteristics of the reaction of the cardiovascular system in the period of early recovery after dosed exercise of a dynamic and static nature. The study examined the response of the central hemodynamics of young men in the period of early recovery after dynamic loading (Martine functional test) and static loading (holding on the stand dynamometer DS-200 force with a power of 50% of maximum standing force). The change in circulatory system parameters was recorded using a tetrapolar thoracic impedance rheoplethysmogram on a computerized diagnostic complex "Cardio +". It is established that the dynamic load in the period of early recovery does not cause a significant positive chronotropic effect, leads to a decrease in vascular resistance of blood flow, to an increase in pulse blood pressure. The increase in cardiac output is mainly due to the increase in stroke volume, which indicates a fairly high functional reserves of the heart. It is revealed that under conditions of static loading the reaction of central hemodynamics and the course of early recovery are radically different from the changes of indicators under dynamic loading. In persons with a normodynamic type of reaction to dynamic load, there are no significant changes in the minute volume of blood at a similar volume of active muscle mass static load. Meeting the metabolic needs of working skeletal muscles and compensating for the oxygen debt is realized by increasing the total peripheral vascular resistance and increasing systolic blood pressure in the postpartum period. The physiological meaning of this phenomenon is to maintain a sufficient level of venous return of blood to ensure the pumping function of the heart.*

**Keywords:** *cardiovascular system, dynamic loading, static loading, recovery.*

## Introduction

One of the most important functional systems of the body, which largely determines and limits the physical performance of the body, is the circulatory system. Adaptation of the cardiovascular system (CVS) to different modes of physical activity is one of the central issues of the whole problem of adaptation because the ability of this system to increase its function often becomes the link that significantly limits the intensity and duration of adaptive responses [9, 10, 18, 24].

Modern non-professional areas of physical fitness, as well as sports of higher achievements are characterized by a significant increase in the intensification of training loads, which is dictated by the desire of athletes to achieve the highest sports results [13, 14, 15]. However, the marked increase in volume, duration and intensity of physical activity without proper consideration of individual features of adaptation to them can lead to prepathological and, sometimes, even to pathological changes of activity of heart and blood vessels (arrhythmia, hypertrophic cardiomyopathy, myocardial dystrophy, coronary artery pathology, myocarditis, etc.) [16, 20], which without proper consideration of the functional aspects of the adaptation of

the cardiovascular system can cause deaths during sports [6, 19].

Intense muscular work leads to a significant increase in the load on the circulatory system, resulting in the formation of structural and functional changes in the heart, which are combined into the general concept of "sports heart". The establishment of diagnostic criteria for this syndrome continues to this day, due to the search for markers of myocardial damage, risk factors for cardiac pathology and predictors of sudden cardiac death, etc. [8, 10, 19, 22].

Regular physical activity of static, static-dynamic and dynamic nature causes specific adaptive changes in the circulatory system. Electro-morphological remodeling of the sports heart, which occurs, together with its functional restructuring inevitably lead to changes in the injection function and, as a consequence, to systemic changes in a number of indicators of central and peripheral hemodynamics [1, 6, 8].

Fitness training as a type of physical activity, optimally combines dynamic and strength training loads. This approach involves testing the level of physical performance of a person, in particular, determining the parameters of the response of central hemodynamics to the combination of a set of strength loads with endurance exercises. Insufficient study of these issues requires more detailed comparative studies of the impact of dynamic and static loads on the performance of the circulatory system.

*The aim* of our study was to study the features of the central hemodynamic response in the period of early recovery after dosed physical activity of dynamic and static nature.

## Materials and methods

The presented work is a fragment of research work of the Department of Medical and Biological Disciplines of the National University of Physical Education and Sport of Ukraine "Influence of exogenous and endogenous factors on the course of adaptive reactions of the body to physical activity of varying intensity" (state registration number 012U108187).

The study involved practically healthy male adolescents (21 years) without bad habits, 4th year students of NUUPES, direction of training "Sports" (examined 24 volunteers, average height - 175.0±4.0 cm, average body weight 69.20±1.10 kg). The study of the subjects was performed in the morning 1-2 hours after a meal, after the arrival of the subject to the laboratory at least 15 minutes of passive rest (in order to eliminate potential stress effects on the cardiovascular system). The examination protocol included information on the date and time of the examination, sex and age (date of birth) of the subject, features of physical activity for the last 3 months.

The study was conducted in two stages. In the first stage, the course of changes in central hemodynamics in the period of early recovery after dynamic loading (DL) and determined the type of response of the cardiovascular system to the functional Martine test (test with 20 squats for 30 seconds), modified for use as a functional test with dynamic load. Before exercise, the heart rate (HR) was counted for 10 seconds by palpation on the left carotid artery, blood pressure was measured in the right upper extremity by the method of Korotkov and, simultaneously with blood pressure measurement, recorded tetrapolar thoracic impedance rheoplethysmogram (TRP) "Cardio+" complex (Ukraine). For the first ten seconds after exercise, the heart rate in the left carotid artery was counted. In the next 40 seconds, blood pressure was measured and TRP was recorded. Next, during the last 10 seconds of the first minute of recovery, heart rate was counted. The above examination was repeated in the second and third minutes of recovery. During the examination, the subject was in a standing position.

The second stage of the study began 15 minutes after the first. In the second stage, the response of the cardiovascular system to the dosed static load (SL) was determined. For the second stage of the study, only individuals with a normotonic type of reaction were selected. The students (20 people) involved in this stage were randomly (randomly) divided into 2 groups: control (Gr.1, 10 people) and main (Gr.2, 10 people). In both groups with the help of a stand-up dynamometer DS-500, 5 minutes before the functional test with static load, determined the maximum arbitrary standing force. As a sample with a static load in Gr.2 used the hold on the stand dynamometer DS-200 for 15 seconds, the force level, which corresponded to 50% of the maximum standing force. The countdown of the holding time began from the moment of fixing the force on the corresponding mark of the dynamometer. In Gr.1 - simulated the corresponding static force by holding on the stand dynamometer DS-200 for 15 seconds, the level of effort, which corresponded to 10% of the maximum standing force, which should not cause significant force and shifts in the visceral systems of the body [3, 20, 18]. Subjects in both groups and researchers who recorded CVS performance were not informed about the level of effort held by a particular subject. The dynamometer readings were monitored by a separate researcher-controller. Registration of CVS performance indicators was performed in the same sequence and by the same methods as in the sample with dynamic loading until full recovery.

The following indicators of central hemodynamics were evaluated: heart rate (HR), systolic blood pressure (sBP), diastolic blood pressure (dBP), pulse blood pressure (pBP), mean dynamic blood pressure (adBP), stroke volume (SV), minute blood volume (MVB), total peripheral vascular resistance (TPVR).

Statistical data processing was performed in the license package "Statistica 5.5" using non-parametric methods of evaluation of the obtained results.

## Results

At the first stage of the study, 24 volunteers were examined. A normotonic reaction to a functional test was found in 20 people, a hypotonic type of reaction was

**Table 1.** The average values of central hemodynamics in the period of early recovery (M±σ).

| indicator | Before DL | 1 min after DL | 2 min after DL | 3 min after DL |
|---|---|---|---|---|
| HR, b/s | 74.11±3.02 | 86.08±2.04* | 77.06±2.03 | 77.15±1.02 |
| sBP, mm Hg | 121.3±3.2 | 130.3±3.1* | 132.2±1.14* | 125.1±2.15 |
| dBP, mm Hg | 67.09±2.18 | 63.60±2.21 | 64.05±1.09 | 66.04±2.08 |
| pBP, mm Hg | 55.08±2.11 | 67.39±1.08* | 67.01±1.02* | 57.23±2.13 |
| adBP, mm Hg | 84.31±3.14 | 85.16±2.03 | 86.06±1.04 | 85.11±2.03 |
| SV, ml | 79.14±3.11 | 92.13±2.08* | 80.08±2.06 | 78.06±3.04 |
| MVB, l/min | 5.632±0.224 | 7.902±0.092* | 6.052±0.152 | 5.821±0.122 |
| TPVR, dyn *s/cm$^5$ | 1213±14 | 888.2±11.1* | 1159±12 | 1196±13 |

**Notes:** * - reliable in relation to the condition before load (p<0,05).

established in 3 people, and a hypertensive in one. For the analysis of changes in central hemodynamics after dynamic exercise, only the data obtained in the study of individuals with a normotonic response to the Martin test were selected. The average values of central hemodynamics in the period of early recovery are shown in Table 1.

Immediately after exercise in a dynamic mode, an increase in heart rate by 15%, as well as a moderate increase in systolic blood pressure and a slight decrease in diastolic pressure, which, in turn, caused an increase in pulse blood pressure by 22%. No statistically significant changes in mean dynamic pressure were recorded. Stroke volume increased by an average of 16% during dynamic exercise and minute blood volume increased by 40%. The total peripheral resistance during physical activity in the dynamic mode decreased and at the first minute of recovery was 73% of the value of TPVR to the load. In all surveyed students, the recovery of the circulatory system to its original state occurred 2-3 minutes after dynamic exercise.

The response of central hemodynamics to static load was analyzed by comparing the course of early recovery in Gr2 and Gr1. The average values of central hemodynamics in the period corresponding to the period of early recovery after dosed static exercise are shown in table 2.

In the main group (Gr.2) immediately after static load, the level of sBP increased by an average of 15 mm Hg, which led to an increase in pulse blood pressure by 35% and a tendency to increase TPVR. In Gr1 in the corresponding period after static loading there was only a statistically insignificant tendency to increase sBP, pBP and adBP. In the first minute after exercise, the changes in sBP and pBP that took place in Gr.2 were significant relative to the values of these indicators in Gr1. Complete recovery of blood pressure in Gr2 occurred 4 minutes after SL.

At 1 and 2 minutes after static loading, there were no statistically significant changes in heart rate, SV and MVB in both groups. However, in Gr.2 in the first minute there was a tendency to decrease SV along with tendencies to increase heart rate and MVB, and in the third minute - in Gr.2 registered a statistically significant increase in heart rate and decrease SV relative to the initial state of Gr.2 and values in Gr.1 at the specified time. These changes in heart rate and SV were combined with a tendency to decrease MVB compared with the value of the indicator at 1 and 2 minutes. However, at the third minute, the value of MVB in Gr2 approached the initial level and did not differ from the value of MVB in the control.

In Gr.1 TPVR remained unchanged. In Gr.2 registered progressive from 1 to 3 minutes growth of TPVR. As a result, the total vascular resistance of blood vessels increased by 7% relative to the state to static load and exceeded the value of the indicator in Gr.1 in the corresponding recovery period by 6%. Recovery in terms of heart rate, SV and TPVR in Gr. 2 occurred in the 5th minute after SL.

## Discussion

Dosed physical activity during a standard functional Martin test did not cause a significant positive chronotropic effect, and the growth of MVB was provided mainly by an increase in SV, which is a manifestation of a high degree of

**Table 2.** The average values of central hemodynamics in the period of early recovery after dosed static exercise (M±σ).

| | | HR | sBP | dBP | pBP | adBP | SV | MVB | TPVR |
|---|---|---|---|---|---|---|---|---|---|
| | | b/s | mm Hg | | | | ml | l/min | dyn *s/cm$^5$ |
| Before DL | Gr 1 | 73.27±3.12 | 125.2±3.1 | 81.04±1.08 | 45.07±3.07 | 95.04±2.04 | 80.07±2.02 | 5.682±0.104 | 1290±12 |
| | Gr 2 | 74.11±3.09 | 128.1±3.2 | 80.09±1.02 | 47.11±2.08 | 96.04±2.03 | 79.13±3.04 | 5.682±0.206 | 1283±13 |
| 1 min after DL | Gr 1 | 74.09±2.09 | 130.2±4.8 | 79.05±2.04 | 50.03±2.03 | 98.02±1.02 | 79.01±1.02 | 5.683±0.203 | 1303±11 |
| | Gr 2 | 80.04±2.03 | 143.2±3.2*+ | 78.09±2.04 | 65.07±1.08*+ | 100±1 | 75.06±3.04 | 5.963±0.202 | 1326±10* |
| 2 min after DL | Gr 1 | 72.04±3.03 | 130.2±3.2 | 80.07±2.06 | 50.05±3.04 | 98.03±2.02 | 77.02±3.02 | 5.792±0.201 | 1302±11 |
| | Gr 2 | 77.04±3.14 | 135.2±2.4* | 80.14±1.09 | 55.12±2.07 | 98.09±1.05 | 76.07±1.03 | 5.842±0.202 | 1347±9*+ |
| 3 min after DL | Gr 1 | 73.17±2.13 | 126.4±3.4 | 80.07±1.08 | 46.06±3.07 | 95.04±3.05 | 78.07±1.03 | 5.653±0.203 | 1298±12 |
| | Gr 2 | 83.16±1.09*+ | 130.6±2.1 | 79.14±2.1 | 51.12±3.07 | 96.19±3.04 | 68.09±3.07*+ | 5.612±0.202 | 1370±9*+ |

**Notes:** * - reliable in relation to the condition before loading (p<0.05); + - reliably relative to the control group (p<0.05).

functional reserves of the heart [1, 4]. These reserves are due to increased heart rate (due to physiological hypertrophy of the left ventricular myocardium with a sufficient degree of capillarization) and physiological dilatation of the heart chambers, in particular, the left ventricle, which provides the required end-diastolic volume [2, 12].

In our study, students with a normotonic type of response to the Martin test showed an increase in minute blood volume corresponding to the intensity of the load due to both an increase in SV and heart rate. However, heart rate remained within normocardia, which indicates a fairly high functional reserves of the heart. It should be noted that bradycardia was not observed at rest in the subjects.

Significant growth of sBP, too, may be evidence of increased left ventricular pumping function in trained students. The tendency to decrease the level of diastolic blood pressure, which was observed in response to dynamic loading, is the result of a decrease in the tone of resistive vessels, which may be due to the release of biologically active substances - vasodilators, more beta- than alpha-adrenoreceptors and local temperature rise in actively working skeletal muscles [3, 9]. Reducing the tone of resistive vessels leads to their expansion in working muscles, which when performing dynamic physical exercises of a global nature (involving more than 50% of muscle mass) leads to a decrease in total peripheral vascular resistance [7, 11]. In our study, a significant decrease in TPVR was detected in the first minute after dynamic loading. From the second minute of recovery, the level of TPVR corresponding to the appropriate value of the indicator was registered. Note that rheography does not actually register the resistance of blood vessels; TPVR is defined as the ratio of mean-dynamic blood pressure (adBP) to cardiac output (ie, to MVB). During the Martin test, we did not find any significant changes in adBP. However, cardiac output increased, and TPVR, respectively, decreased, which is a physiologically appropriate response of the cardiovascular system to exercise [5, 17, 23].

Based on the analysis of the data obtained at the first stage of the study, we have reason to believe that the registration of TRP during the Martine test allowed a deeper study of the nature of the central hemodynamic response to DL and describe the physiological picture of hemodynamic response in normotonic response as follows: muscles, in particular, oxygen demand, should be provided by increase in MVB; reduction of vascular resistance of blood flow and increase of pulse blood pressure improve the state of perfusion of the capillary bed of working muscles, and the stability of adBP ensures optimal conditions for metabolism of water, nutrients and other components between blood and tissue fluid [1, 3, 13, 17, 21].

Under conditions of static loading lasting 15 seconds, the reaction of CG and the course of early recovery were radically different from the dynamics of CG during DL and in the control group. In individuals with a normodynamic type of response to DL, there were no significant changes in MVB at a similar volume of active muscle mass static load, which is 50% of maximum strength. The dynamics of blood pressure indicators, which was characterized by a significant increase in sBP, was indicative. In our opinion, this may be due to the fact that with sufficient force of static load, the working muscles create external pressure on the vessels that pass through them. This primarily applies to the exchange vessels, where blood flow may stop altogether. In this case, some volume of blood can circulate through arterio-venous shunts [13, 14, 15]. The result will be a redistribution of circulating blood volume with an increase in blood volume in the arteries of the great circle of circulation, which is usually no more than 15% of the total circulating blood volume. Thus, it can be assumed that sBP increases in response to postload due to arterial hyperemia caused by mechanical obstruction of blood flow in tense muscles. The growth of TPVR in the first minute after SL can be explained by the same reasons as the growth of sBP.

However, in contrast to sBP, TPVR after the cessation of mechanical interference continues to grow within 2 and 3 minutes of the early recovery period. The probable reason for this, seemingly paradoxical fact, may be reactive hyperemia in ischemic muscles with significant static tension. It can be assumed that this increase in TPVR causes overflow of the microcirculatory region of the vascular bed, the cause of which lies, firstly, in the sharp relaxation of precapillary sphincters under the action of muscle metabolism and, secondly, increased venous tone as a compensatory response to limitation. blood flow into the venous bed during SL [3, 6, 7, 10]. The latter is aimed at maintaining a sufficient level of venous return to ensure the pumping function of the heart. Confirmation of our assumption that SL may lead to such a decrease in blood volume in the venous area of the great circle of circulation, which will require compensation, can be registered in the third and first minutes of the recovery period increase in heart rate in response to decreased SV. This is observed in orthostatic reactions, the cause of which is known to be a sharp decrease in venous return.

## Conclusions

1. Dynamic loading during the Martin test in the period of early recovery leads to a decrease in vascular resistance of blood flow, to an increase in pulse blood pressure and to an increase in cardiac output, mainly due to the positive inotropic effect.

2. Under conditions of static load, the reaction of central hemodynamics and the course of early recovery are radically different from changes in dynamic loading.

3. In persons with a normotonic type of reaction to dynamic load, there were no significant changes in the minute volume of blood at a similar volume of active muscle mass static load. Meeting the metabolic needs of working muscles and compensating for oxygen debt are realized through post-work growth of total peripheral vascular resistance and increase in systolic blood pressure.

## References


[1] Badano, L., Kolias, J., Muraru, D., Abraham, T., Aurigemma, G., Edvardsen, T. … Voigt, Jens-U. (2018). Standardization of left atrial, right ventricular, and right atrial deformation imaging using two-dimensional speckle tracking echocardiography: a consensus document of the EACVI/ASE/industry task force to standardize deformation imaging. *Eur. Hear J. Cardiovasc. Imaging*, 19(6), 591-600. doi: 10.1093/ehjci/jey042

[2] Boraita, A., Heras, M., Morales, F., Marina-Breysse, M., Canda, A., Rabadan, M. … Tunon, J. (2016). Reference values of aortic root in male and female white elite athletes according to sport. *Circ Cardiovasc Imaging,* 9(10), e005292. doi: 10.1161/CIRCIMAGING.116.005292.

[3] D'Andrea, A., Formisano, T., Riegler, L., Scarafile, R., America, R., Martone, F. … Calabro, R. (2017). Acute and Chronic Response to Exercise in Athletes: The "Supernormal Heart". *Adv Exp Med Biol,* 999, 21-41. doi: 10.1007/978-981-10-4307-9_2.

[4] D'Ascenzi, F., Pisicchio, C., Caselli, S., Di Paolo, F., Spataro, A., & Pelliccia, A. (2017). RV remodeling in Olympic athletes. *JACC Cardiovasc Imaging,* 10(4), 385-393. doi: 10.1016/j.jcmg.2016.03.017

[5] De la Garza, M., Carro, A., & Caselli, S. (2020). How to interpret right ventricular remodeling in athletes. *Clin. Cardiol.*, 43(8), 843-851. doi: 10.1002/clc.23350

[6] Doleeb, S., Kratz, A., Salter, M., & Thohan, V. (2019). Strong muscles, weak heart: testosterone-induced cardiomyopathy. *ESC Heart Failure,* 6(5), 1000-1004. https://doi.org/10.1002/ehf2.12494

[7] Domenech-Ximenos, B., la Garza, M., & Prat-Gonzalez, S. (2019). Exercise-induced cardio-pulmonary remodelling in endurance athletes: not only the heart adapts. *Eur. J. Prev. Cardiol.,* 27(6), 651-659. doi: 10.1177/2047487319868545

[8] Fagerberg, P. (2018). Negative Consequences of Low Energy Availability in Natural Male Bodybuilding: A Review. *Int. J. Sport Nutr. Exerc. Metab.,* 28(4), 1, 385-402. doi: 10.1123/ijsnem.2016-0332

[9] Fluck, M., Kramer, M., Fitze, D., Kasper, S., Franchi, M., & Valdivieso, P. (2019). Cellular Aspects of Muscle Specialization Demonstrate Genotype - Phenotype Interaction Effects in Athletes. *Front. Physiol.*, 8(10), 526. doi: 10.3389/fphys.2019.00526

[10] Franchi, M., Reeves, N., & Narici, M. (2017). Skeletal Muscle Remodeling in Response to Eccentric vs. Concentric Loading: Morphological, Molecular, and Metabolic Adaptations. *Front. Physiol.*, 8, 447. doi: 10.3389/fphys.2017.00447

[11] Gati, S., Sharma S., & Pennell, D. (2018). The role of cardiovascular magnetic resonance imaging in the assessment of highly trained athletes. *JACC Cardiovasc. Imaging*, 11(2P1), 247-259. doi: 10.1016/j.jcmg.2017.11.016

[12] Koshy, S., Koshy, G., & Lekha, G. (2018). Changes in right ventricular morphology and function in athletes. *Echocardiography,* 35(6), 767-768. doi: 10.1111/echo.14027

[13] Longstrom, J., Colenso-Semple, L., Waddell, B., Mastrofini, G., Trexler, E., & Campbell, B. (2020). Physiological, Psychological and Performance-Related Changes Following Physique Competition: A Case-Series. *J. Funct. Morphol. Kinesiol.*, 5(2), 27-35. doi: 10.3390/jfmk5020027

[14] Korytko, Z., Kulitka, E., Bas, O., Chornenka, C., Zahidnyy, V., & Yakubovskyi T. (2020). Adequacy criteria of physical loadings and their use in sports, physical education, and physical rehabilitation. *Physical Education, Sport and Health Culture in Modern Society,* 50(2), 68-77. https://doi.org/10.29038/2220-7481-2020-02-68-77

[15] Maden-Wilkinson, T., Balshaw, T., Massey, G., & Folland, J. (2020). What makes long-term resistance-trained individuals so strong? A comparison of skeletal muscle morphology, architecture, and joint mechanics. *J. Appl. Physiol,* 128(4), 1000-1011. doi: 10.1152/japplphysiol.00224.2019

[16] Marrakchi, S., Kammoun, I., Bennour, E., Laroussi, L., Ben Miled M., & Kachboura S. (2020). Inherited primary arrhythmia disorders: cardiac channelopathies and sports activity. *Herz,* 45(2), 142-157. doi: 10.1007/s00059-018-4706-2

[17] Martinez, V., la Garza M., & Grazioli, G. (2019). Cardiac performance after an endurance open water swimming race. *Eur. J. Appl. Physiol.,* 119(4), 961-970. doi: 10.1007/s00421-019-04085-x

[18] Martino, F., Perestrelo, A., Vinarsky, V., Pagliari, S., & Forte, G. (2018). Cellular Mechanotransduction: From Tension to Function. *Front. Physiol.*, 5(9), 824. doi: 10.3389/fphys.2018.00824

[19] Mont, L., Pelliccia, A., Sharma, S., Biffi, A., Borjesson, M., Terradellas, J. … La Gerche, A. (2017). Pre-participation cardiovascular evaluation for athletic participants to prevent sudden death: position paper from the EHRA and the EACPR, branches of the ESC. Endorsed by APHRS, HRS, and SOLAECE. *Eur. J. Prev. Cardiol.*, 24, 41-69. doi.org/10.1093/europace/euw243.

[20] Pelliccia, A., Sharma, S., Gati, S., Back, M., Borjesson, M., Caselli, S. … Wilhelm, M. (2021). Corrigendum to: 2020 ESC Guidelines on Sports Cardiology and Exercise in Patients with Cardiovascular Disease. *European Heart Journal,* 42(1), 17-96. doi: 10.1093/eurheartj/ehaa605

[21] Qasem, M., George, K., Somauroo, J., Forsythe, L., Brown, B., & Oxborough, D. (2019). Right ventricular function in elite male athletes meeting the structural echocardiographic task force criteria for arrhythmogenic right ventricular cardiomyopathy. *J. Sports Sci.,* 37(3), 306-312. doi: 10.1080/02640414.2018.1499392

[22] Radmilovic, J., D'Andrea, A., D'Amato, A., Tagliamonte, E., Sperlongano, S., Riegler, L., & Scarafile, R. (2019). Echocardiography in Athletes in Primary Prevention of 2Sudden Death. *J. Cardiovasc. Echogr.*, 29(4), 139-148. doi: 10.4103/jcecho.jcecho_26_19

[23] Sanz, M., Garza, D., & Giraldeau, G. (2017). Influence of gender on right ventricle adaptation to endurance exercise: an ultrasound two-dimensional speckle-tracking stress study. *Eur. J. Appl. Physiol.,* 117(3), 389-396. doi: 10.1007/s00421-017-3546-8

[24] Schoenfeld, B., & Grgic, J. (2018). Evidence-Based Guidelines for Resistance Training Volume to Maximize Muscle Hypertrophy. *Strength Cond. J.,* 40(4), 107-112. doi: 10.1519/SSC.0000000000000363


**ПОРІВНЯЛЬНА ХАРАКТЕРИСТИКА ЗМІН ЦЕНТРАЛЬНОЇ ГЕМОДИНАМІКИ В ПЕРІОД РАННЬОГО ВІДНОВЛЕННЯ ПІСЛЯ РІЗНИХ РЕЖИМІВ ФІЗИЧНОГО НАВАНТАЖЕННЯ**

***Лук'янцева Г.В., Бакуновський О.М., Малюга С.С., Олійник Т.М., Манченко Н.Р, Манченко Я.Р., Корольова Д.О.***

*Серцево-судинна система є однією з найважливіших функціональних систем організму, які визначають рівень фізичної працездатності організму. Недостатня вивченість реакції системи кровообігу на поєднання комплексу силових навантажень*

*із вправами на витривалість вимагає більш докладних порівняльних досліджень впливу динамічних і статичних навантажень на показники центральної гемодинаміки. Відповідно, метою нашого дослідження стало вивчення особливостей реакції серцево-судинної системи у період раннього відновлення після дозованих фізичних навантажень динамічного і статичного характеру. У дослідженні вивчали реакцію центральної гемодинаміки юнаків у період раннього відновлення після динамічного навантаження (функціональна проба Мартіне) і статичного навантаження (утримання на становому динамометрі ДС-200 зусилля потужністю 50% від максимальної станової сили). Зміну показників системи кровообігу реєстрували за допомогою тетраполярної грудної імпедансної реоплетизмограми на комп'ютеризованому діагностичному комплексі "Кардіо+". Встановлено, що динамічне навантаження у період раннього відновлення не викликає значного позитивного хронотропного ефекту, призводить до зменшення опору судин току крові, до збільшення пульсового артеріального тиску. Зростання хвилинного об'єму крові відбувається переважно за рахунок зростання ударного об'єму крові, що свідчить про достатньо високі функціональні резерви серця. Виявлено, що за умов статичного навантаження реакція центральної гемодинаміки і перебіг раннього відновлення кардинально відрізняються від змін показників при динамічному навантаженні. В осіб з нормодинамічним типом реакції на динамічне навантаження не відбувається суттєвих змін хвилинного об'єму крові при аналогічному за об'ємом активної м'язової маси статичному навантаженні. Забезпечення метаболічних потреб працюючих скелетних м'язів і компенсація кисневого боргу реалізуються за рахунок зростання загального периферичного опору судин і збільшення систолічного артеріального тиску у післяробочий період. Фізіологічний сенс означеного явища полягає у підтриманні належного рівня венозного повернення крові для забезпечення насосної функції серця.*

**Ключові слова:** *серцево-судинна система, динамічне навантаження, статичне навантаження, відновлення.*

DOI: 10.31393/morphology-journal-2021-27(2)-08 Reports of Morphology, Vol. 27, №2, Pages 53-62

ISSN 1818-1295 eISSN 2616-6194

**REPORTS OF MORPHOLOGY**

***Official Journal of the Scientific Society of Anatomists, Histologists, Embryologists and Topographic Anatomists of Ukraine***

journal homepage: https://morphology-journal.com

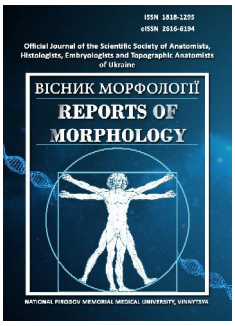


# Lumbar intervertebral disks: morphometric parameters and indices

***Danylevych V.P.[1], Guminskyi Yu.Y.[1], Hryhorieva O.A.[2], Danylevych S.H.[3]***

[1]National Pirogov Memorial Medical University, Vinnytsya, Ukraine
[2]Zaporizzhya State Medical University, Zaporizzhya, Ukraine
[3]Medical radiological center, Vinnytsia, Ukraine

**ARTICLE INFO**
Received: 26 February 2021
Accepted: 19 April 2021

**UDC:** 611.721.1

**CORRESPONDING AUTHOR**
e-mail: vidanlet@gmail.com
Danylevych V.P.

*An important element of evidence-based medicine is to take into account the individual variability of the indicators of the norm of intervertebral discs, which is undoubtedly the basis for early preclinical detection of their pathology. Mathematical modeling and comprehensive assessment of the parameters of the intervertebral discs can not only predict and determine the early manifestations of pathological changes, but also help to correct them in advance. The aim of the study was to calculate and evaluate the variability of absolute, calculated and relative metric parameters of intervertebral discs in the norm with the subsequent possibility of modeling standards based on individual linear dimensions of intervertebral discs of the lumbar spine and general anthropometric characteristics (body length and weight) in young men and men of the first period of adulthood (17-28 years), both in separate age groups and in the combined group. The series of MRI scans obtained on a Phillips Achieva 1.5T scanner measured the anterior, middle and posterior vertical dimensions, maximum sagittal and frontal dimensions of the intervertebral discs L1-L2, L2-L3, L3-L4, L4-L5 segments of the spine ($IVD_{L1-L2}$, $IVD_{L2-L3}$, $IVD_{L3-L4}$, $IVD_{L4-L5}$). We calculated the average height of the intervertebral discs, cross-sectional area and volume of intervertebral discs, as well as relative indicators - the ratio of the sum of sagittal and transverse dimensions, the sum of three dimensions, cross-sectional area and volume of intervertebral discs to the average intervertebral disc height. Statistical analysis of the obtained morphometric parameters was performed in the license package "STATISTICA 6.1". The distribution of variation series indicators, their average values and standard errors, coefficients of variation and asymmetry were evaluated. It was determined that the sums of the transverse and sagittal sizes and the sums of the three sizes increase proportionally in the caudal direction, have a distribution of indicators as close as possible to normal, and their coefficients of variation are many times smaller than for cross-sectional areas and volumes. Indicators of the ratio of the sum of the sagittal and transverse size and the sum of the three sizes to the average height of the intervertebral discs have a variability of less than 10% and correspond to the characteristics of the general population. Body weight and length have significantly higher correlation coefficients with the sums of sagittal and transverse dimensions, the sums of three dimensions and cross-sectional areas than with the partial dimensions of the intervertebral discs.*

**Keywords:** *intervertebral disc, lumbar spine, norm, somatometry, young men, men of the first period of adulthood.*

## Introduction

Musculoskeletal pathology, according to the World Health Organization, ranks fourth among the causes of disability and mortality in the world [4, 21]. About 20% of people suffer from temporary or permanent back pain. Diseases of the musculoskeletal system are also one of the most common problems in Ukraine [5, 22], where about 3.5 million people have problems with the musculoskeletal system and their neurological complications [16, 20]. Degenerative changes of the spine are an insidious pathology that carefully hides the symptoms of other diseases, which greatly complicates their diagnosis, especially in the early stages of the disease. Despite the fact that the gradual degeneration of the intervertebral disc is considered a natural process that progresses with age, in recent decades the frequency of

clinical manifestations of these changes in young people is steadily increasing [1, 17].

The leading place in development of a degenerative cascade and disturbance of biomechanics of functional segments is occupied by degenerative changes of intervertebral disks. Chondrosis, osteochondrosis, spondylosis, and in the English literature - degenerative disc disease (DDD) [9, 13, 23, 30] - are the most common terms used to denote diseases of the spine, which, to some extent, reflect the most common morphological basis of this pathology.

The use of only averaged values as indicators of the norm does not take into account individuality and can be a factor in misinterpretations of the results.

Despite the urgency of the problem of pathology of the spine both in the world and in Ukraine, a small number of scientific papers of domestic scientists are devoted to this topic, in particular the detection of pathology at an early stage.

In medical practice, morphometric parameters of intervertebral discs, such as sagittal, transverse and vertical dimensions of intervertebral discs, cross-sectional area, volume are not widely used, but only as single studies are found in the scientific literature [8, 27, 29]. Average and generalized criteria for assessing the norm do not take into account the individual characteristics of each human body. Methods using mathematical modeling and methods of comprehensive assessment of the parameters of the intervertebral discs will identify pathological changes in the early stages, and, consequently, to correct them in advance. The use of more criteria for assessing the condition of the intervertebral disc will allow the application of the principles of evidence-based medicine in determining changes in the intervertebral disc and bring the indicators closer to the individual.

However, it should be noted that the use of a full-scale anthropometric study with the measurement of linear and circumferential dimensions is complex and is not widely used in clinical practice. Therefore, the search for simplified mathematical models and a set of relative indicators that are based on a smaller number of initial parameters and as close as possible in accuracy is a priority.

*The purpose* of the study is to assess the scattering characteristics (variability) of absolute, calculated and relative metric features of intervertebral discs in the norm with the subsequent possibility of modeling standards based on individual linear dimensions $IVD_{L1-L2}$, $IVD_{L2-L3}$, $IVD_{L3-L4}$, $IVD_{L4-L5}$ and general characteristics (length and body weight, weight-growth coefficient and index) in young men and men of the first period of adulthood (17-28 years) both in separate age groups and in the combined group.

## Materials and methods

The study involved 74 young men and men aged 17 to 28 years without clinical signs of spinal diseases. They underwent an anthropometric examination to determine the total parameters (length and body weight), performed MR tomography of the lumbar spine. MRI was performed on a 1.5T scanner (Phillips Achieva 1.5T, Phillips, the Netherlands). MRI scans of the lumbar spine were obtained in the axial, sagittal and frontal planes using T2-weighted turbo-spin-echo sequences.

The obtained MR images were used for further morphometry of intervertebral discs L1-L2, L2-L3, L3-L4, L4-L5 segments of the lumbar spine: measurement of maximum sagittal and frontal dimensions; anterior, middle and posterior vertical sizes of intervertebral discs. Calculated the average height of the intervertebral discs (as the arithmetic mean of the anterior, middle and posterior heights); calculated the cross-sectional areas and volumes of intervertebral discs, as well as relative indicators - the ratio of the sum of sagittal and transverse dimensions, the sum of three dimensions, cross-sectional area and volume of intervertebral discs to the average height of the intervertebral disc.

Statistical analysis was performed in the license package "STATISTICA 6.1". The mean values of the variation series, standard deviations, coefficients of variation and asymmetry, paired t-test, d-test of the Kolmogorov-Smirnov type, Levene's index were evaluated [12, 24, 25].

## Results

The coefficient of variation of the front heights (Table 1) in all age groups had average values of variability in the range from 11.40% to 17.58%. The highest frequency for indicators of anterior height of all groups is in the range of 2 sigma from 65.79% to 78.85% of the total number of observations. When using the paired t-test (Table 2), it was determined that no significant differences in the mean values of the indicators in the groups were determined ($p>0.05$). The difference between the mean values in the samples for $IVD_{L1-L2}$ is 0.327 mm and 0.447 mm, for $IVD_{L2-L3}$ - 0.222 mm and 0.304 mm, for $IVD_{L3-L4}$ - 0.304 mm and 0.087 mm, for $IVD_{L4-L5}$ - 0.009 mm and 0.013 mm.

The highest frequency for the mean height of all groups is in the range of 2 sigma from 57.78% to 78.95% of the total number of observations. The coefficients of variation (see Table 1) have values close to low variability ($\leq$10) - from 8.38% to 12.37%. When using the paired t-test (see Table 2), it was determined that no significant differences in the mean values of the indicators in the groups were determined ($p>0.05$). The difference between the mean values in the samples for $IVD_{L1-L2}$ is 0.327 mm and 0.447 mm, for $IVD_{L2-L3}$ - 0.222 mm and 0.304 mm, for $IVD_{L3-L4}$ - 0.304 mm and 0.087 mm, for $IVD_{L4-L5}$ - 0.009 mm and 0.013 mm.

The coefficients of variation (see Table 1) of the posterior vertical dimensions have average values of variability ($\leq$10) - from 12.46% to 15.74%. The highest frequency for the indicators of the posterior height of all groups is in the range of 2 sigma from 57.89% to 73.68% of the total number of observations. When using a paired t-test (see Table 2), a significant difference between the mean values for $IVD_{L1-L2}$; for $IVD_{L2-L3}$, $IVD_{L3-L4}$, $IVD_{L4-L5}$ ($p>0.05$) significant differences

in the mean values of the indicators were not detected. The difference between the mean values in the samples for $IVD_{L1-L2}$ is 0.432 mm and 0.591 mm, for $IVD_{L2-L3}$ - 0.244 mm and 0.333 mm, for $IVD_{L3-L4}$ - 0.132 mm and 0.181 mm, for $IVD_{L4-L5}$ - 0.004 mm and 0.006 mm.

Transverse dimensions of intervertebral discs $IVD_{L1-L2}$, $IVD_{L2-L3}$, $IVD_{L3-L4}$, $IVD_{L4-L5}$ of the lumbar spine in these age groups have coefficients of variation (see Table 1) less than 10% - from 4.66% to 6.49 %, which corresponds to the weak variability of the trait. The highest frequency for

**Table 1.** Characteristics of intervertebral disks sizes groups $IVD_{L1-L2}$, $IVD_{L2-L3}$, $IVD_{L3-L4}$, $IVD_{L4-L5}$ of lumbar spine.

| Intervertebral discs sizes | IVD | Young men (17-21 years) | | Men (22-28 years) | | Combined group (17-28 years) | |
|---|---|---|---|---|---|---|---|
| | | M±SD (mm) | Cv% | M±SD (mm) | Cv% | M±SD (mm) | Cv% |
| Anterior height | L1-L2 | 7.949±0.920 | 11.57 | 7.370±1.296 | 17.58 | 7.705±1.125 | 14.60 |
| | L2-L3 | 8.667±1.150 | 13.27 | 8.647±1.254 | 14.51 | 8.658±1.188 | 13.73 |
| | L3-L4 | 9.230±1.058 | 11.40 | 9.580±1.537 | 16.05 | 9.407±1.283 | 13.64 |
| | L4-L5 | 9.803±1.364 | 13.92 | 10.38±1.49 | 14.34 | 10.04±1.44 | 14.32 |
| Average height | L1-L2 | 10.04±0.92 | 9.198 | 9.263±1.146 | 12.37 | 9.711±1.087 | 11.20 |
| | L2-L3 | 11.03±0.95 | 8.613 | 10.51±1.22 | 11.66 | 10.81±1.10 | 10.17 |
| | L3-L4 | 11.48±0.96 | 8.378 | 11.33±1.22 | 10.77 | 11.42±1.07 | 9.410 |
| | L4-L5 | 11.74±1.10 | 9.384 | 11.72±1.33 | 11.37 | 11.73±1.20 | 10.21 |
| Posterior height | L1-L2 | 7.182±0.932 | 12.98 | 6.159±0.921 | 14.95 | 6.750±1.053 | 15.60 |
| | L2-L3 | 7.407±0,923 | 12.46 | 6.830±1,037 | 15.18 | 7.163±1.009 | 14.08 |
| | L3-L4 | 7.395±1.059 | 14.33 | 7.082±1.031 | 14.55 | 7.263±1.053 | 14.50 |
| | L4-L5 | 7.270±1.077 | 14.82 | 7.280±1.146 | 15.74 | 7.274±1.100 | 15.13 |
| Transverse size | L1-L2 | 51.64±2.77 | 5.371 | 49.86±3.24 | 6.492 | 50.89±3.09 | 6.071 |
| | L2-L3 | 53.67±2.69 | 5.007 | 52.48±3.33 | 6.341 | 53.16±3.01 | 5.670 |
| | L3-L4 | 55.32±2.58 | 4.659 | 54.71±3.43 | 6.274 | 55.06±2.97 | 5.386 |
| | L4-L5 | 56.90±2.83 | 4.965 | 56.03±3.53 | 6.300 | 56.53±3.15 | 5.577 |
| Sagittal size | L1-L2 | 38.05±2.45 | 6.427 | 37.06±2.62 | 7.078 | 37.63±2.56 | 6.791 |
| | L2-L3 | 39.52±2.18 | 5.510 | 38.43±2.56 | 6.667 | 39.06±2.40 | 6.133 |
| | L3-L4 | 39.75±2.03 | 5.114 | 38.81±3.02 | 7.774 | 39.35±2.52 | 6.413 |
| | L4-L5 | 41.37±2.05 | 4.943 | 40.50±3.31 | 8.145 | 40.99±2.67 | 6.502 |
| The average value of the height | L1-L2 | 8.389±0.740 | 8.818 | 7.598±0.893 | 11.75 | 8.055±0.894 | 11.10 |
| | L2-L3 | 9.035±0.742 | 8.208 | 8.661±0.920 | 10.62 | 8.877±0.838 | 9.435 |
| | L3-L4 | 9.385±0.793 | 8.448 | 9.330±0.995 | 10.66 | 9.362±0.879 | 9.387 |
| | L4-L5 | 9.604±0.910 | 9.479 | 9.791±0.959 | 9.797 | 9.683±0.93 | 9.611 |
| The sum of transverse and sagittal dimensions | L1-L2 | 89.69±4.54 | 5.066 | 86.92±5.20 | 5.978 | 88.52±4.99 | 5.642 |
| | L2-L3 | 93.18±4.02 | 4.317 | 90.91±5.35 | 5.880 | 92.22±4.74 | 5.136 |
| | L3-L4 | 95.07±3.90 | 4.107 | 93.52±5.62 | 6.009 | 94.42±4.74 | 5.019 |
| | L4-L5 | 98.27±4.24 | 4.318 | 96.53±6.35 | 6.582 | 97.53±5.28 | 5.410 |
| The sum of three sizes | L1-L2 | 98.08±4.59 | 4.683 | 94.52±5.84 | 6.177 | 96.57±5.42 | 5.613 |
| | L2-L3 | 102.2±4.13 | 4.037 | 99.57±5.93 | 5.958 | 101.1±5.11 | 5.055 |
| | L3-L4 | 104.5±4.05 | 3.879 | 102.9±6.30 | 6.123 | 103.8±5.15 | 4.963 |
| | L4-L5 | 107.9±4.49 | 4.158 | 106.3±6.80 | 6.396 | 107.2±5.60 | 5.222 |
| Cross-sectional area | L1-L2 | 15.46±1.59 | 10.26 | 14.55±1.76 | 12.07 | 15.08±1.71 | 11.35 |
| | L2-L3 | 16.67±1.44 | 8.653 | 15.88±1.92 | 12.10 | 16.34±1.70 | 10.39 |
| | L3-L4 | 17.29±1.41 | 8.176 | 16.72±2.10 | 12.58 | 17.05±1.75 | 10.27 |
| | L4-L5 | 18.51±1.60 | 8.616 | 17.89±2.43 | 13.61 | 18.25±2.00 | 10.98 |

**Continuation of table 1.**

| Intervertebral discs sizes | IVD | Young men (17-21 years) | | Men (22-28 years) | | Combined group (17-28 years) | |
|---|---|---|---|---|---|---|---|
| | | M±SD (mm) | Cv% | M±SD (mm) | Cv% | M±SD (mm) | Cv% |
| Volume | L1-L2 | 8.644±1.123 | 12.99 | 7.436±1.625 | 21.85 | 8.130±1.476 | 18.15 |
| | L2-L3 | 10.04±1.21 | 12.03 | 9.234±1.878 | 20.34 | 9.700±1.570 | 16.18 |
| | L3-L4 | 10.82±1.33 | 12.28 | 10.48±2.19 | 20.93 | 10.68±1.74 | 16.33 |
| | L4-L5 | 11.87±1.63 | 13.74 | 11.73±2.30 | 19.56 | 11.81±1.93 | 16.33 |
| The ratio of the sum of sagittal and transverse size to height | L1-L2 | 10.77±1.08 | 10.01 | 11.55±1.11 | 9.608 | 11.10±1.15 | 10.38 |
| | L2-L3 | 10.38±0.92 | 8.873 | 10.58±0.94 | 8.861 | 10.46±0.93 | 8.869 |
| | L3-L4 | 10.20±0.94 | 9.168 | 10.10±0.90 | 8.859 | 10.16±0.92 | 9.003 |
| | L4-L5 | 10.32±1.03 | 10.02 | 9.920±0.920 | 9.268 | 10.15±1.00 | 9.863 |
| The ratio of the sum of all sizes to the height | L1-L2 | 11.77±1.08 | 9.160 | 12.55±1.11 | 8.842 | 12.10±1.15 | 9.520 |
| | L2-L3 | 11.38±0.92 | 8.093 | 11.58±0.94 | 8.096 | 11.46±0.93 | 8.096 |
| | L3-L4 | 11.20±0.94 | 8.350 | 11.10±0.90 | 8.061 | 11.16±0.92 | 8.196 |
| | L4-L5 | 11.32±1.03 | 9.134 | 10.92±0.92 | 8.420 | 11.15±1.00 | 8.978 |
| The ratio of cross-sectional area to height | L1-L2 | 1.857±0.248 | 13.350 | 1.925±0.203 | 10.55 | 1.885±0.231 | 12.26 |
| | L2-L3 | 1.857±0.215 | 11.600 | 1.841±0.188 | 10.20 | 1.850±0.203 | 10.99 |
| | L3-L4 | 1.854±0.210 | 11.320 | 1.798±0.186 | 10.35 | 1.831±0.201 | 10.98 |
| | L4-L5 | 1.942±0.234 | 12.040 | 1.835±0.253 | 13.78 | 1.897±0.246 | 13,00 |
| Weight, kg | | 72,15±8,06 | 11.17 | 76.03±2.05 | 15.41 | 73.79±9.90 | 13.41 |
| Body length, m | | 1,787±0,064 | 3.572 | 1.775±0.077 | 4.329 | 1.782±0.069 | 3.897 |
| Mass-growth factor, g/cm | | 403,4±38,6 | 9.568 | 427.4±57.5 | 13.45 | 413.5±48.7 | 11.77 |
| Mass-growth index, kg/m$^2$ | | 22,58±2,05 | 9.068 | 24.07±3.05 | 12.67 | 23.21±2.61 | 11.25 |

indicators of transverse dimensions of all groups is in the range of 2 sigma from 63.46% to 76.32% of the total number of observations; the paired t-test determined (see Table 2) that there were no significant differences in the mean values of the indicators in the groups ($p>0.05$). The difference between the mean values in the samples for $IVD_{L1-L2}$ is 0.751 mm and 1.028 mm, for $IVD_{L2-L3}$ - 0.501 mm and 0.685 mm, for $IVD_{L3-L4}$ - 0.257 mm and 0.351 mm, for $IVD_{L4-L5}$ - 0.367 mm and 0.502 mm.

For sagittal sizes of intervertebral discs $IVD_{L1-L2}$, $IVD_{L2-L3}$, $IVD_{L3-L4}$, $IVD_{L4-L5}$ the distribution asymmetry indices do not differ significantly in young men and in the combined group, according to the observation groups, the asymmetry indices are 0,035, 0,581 and 0,193; the smallest are for $D_{L2-L3}$ - 0.021 in young men and the largest in men for $D_{L4-L5}$ - 0.782. Coefficients of variation (see Table 1) have average values less than 10% from 4.94% to 8.15%, which corresponds to the weak variability of the trait. The highest frequency for sagittal sizes of all groups is in the range of 2 sigma from 65.38% to 78.85% of the total number of observations. Thus, it can be argued that the distribution of traits in the studied groups is as close as possible to normal. When using the paired t-test, it was determined (see Table 2) that no significant differences in the mean values of the indicators in the groups were determined ($p>0.05$). Levene's test confirms the homogeneity of the variance of the indicators ($p>0.05$) in the studied groups. The difference between the mean values of sagittal dimensions in the samples for $IVD_{L1-L2}$ is 0.419 mm and 0.573 mm, for $IVD_{L2-L3}$ - 0.461 mm and 0.630 mm, for $IVD_{L3-L4}$ - 0.396 mm and 0.542 mm, for $IVD_{L4-L5}$ - 0.368 mm and 0.504 mm.

The coefficients of variation of the average height (see Table 1) of all groups have values close to low variability ($\leq$10) - from 8.21% to 11.75%. The paired t-test (see Table 2) revealed significant differences in the mean values of the average height for $IVD_{L1-L2}$, $IVD_{L2-L3}$, $IVD_{L3-L4}$, $IVD_{L4-L5}$ ($p>0.05$) significant differences in mean values are absent. Levene's test confirmed the homogeneity of the variance of the indicators ($p>0.05$) in all study groups for all intervertebral discs. The bilateral d-criterion of the Kolmogorov-Smirnov type did not exceed the critical value (0.05). The difference between the mean values in the samples for $IVD_{L1-L2}$ is 0.334 mm and 0.458 mm, for $IVD_{L2-L3}$ - 0.158 mm and 0.216 mm, for $IVD_{L3-L4}$ - 0.023 mm and 0.032 mm, for $IVD_{L4-L5}$ - 0.079 mm and 0.108 mm.

The following parameters were calculated: the sum of sagittal and transverse dimensions, the sum of three dimensions, the cross-sectional area and the volume of the intervertebral discs.

The coefficients of variation of the sum of transverse and sagittal sizes (see Table 1) have average values corresponding to the weak variability of the trait - from 4.11%

to 6.58%. The highest frequencies for the sum of transverse and sagittal sizes of all groups are in the range of 2 sigma from 65.38% to 76.32% of the total number of observations.

Indicators of the paired t-test (see Table 2) for the sums of transverse and sagittal sizes $IVD_{L1-L2}$, $IVD_{L2-L3}$, $IVD_{L3-L4}$, $IVD_{L4-L5}$ of the lumbar spine in adolescents, men of the first

**Table 2.** Indicators of t-test of intervertebral disks sizes $IVD_{L1-L2}$, $IVD_{L2-L3}$, $IVD_{L3-L4}$, $IVD_{L4-L5}$ of lumbar spine in adolescents, in men of the first period of adulthood and in the combined group.

| Intervertebral discs sizes | Comparison groups | t-value | p |
|---|---|---|---|
| Anterior height | D1 17-21 vs. D1 17-28 | 1.330 | 0.186 |
| | D1 22-28 vs. D1 17-28 | -1.468 | 0.145 |
| | D2 17-21 vs. D2 17-28 | 0.042 | 0.966 |
| | D2 22-28 vs. D2 17-28 | -0.051 | 0.960 |
| | D3 17-21 vs. D3 17-28 | -0.602 | 0.548 |
| | D3 22-28 vs. D3 17-28 | 0.657 | 0.513 |
| | D4 17-21 vs. D4 17-28 | -0.982 | 0.328 |
| | D4 22-28 vs. D4 17-28 | 1.176 | 0.242 |
| Posterior height | D1 17-21 vs. D1 17-28 | 2.453 | 0.015 |
| | D1 22-28 vs. D1 17-28 | -3.006 | 0.003 |
| | D2 17-21 vs. D2 17-28 | 1.429 | 0.155 |
| | D2 22-28 vs. D2 17-28 | -1.694 | 0.093 |
| | D3 17-21 vs. D3 17-28 | 0.719 | 0.473 |
| | D3 22-28 vs. D3 17-28 | -0.894 | 0.373 |
| | D4 17-21 vs. D4 17-28 | -0.023 | 0.982 |
| | D4 22-28 vs. D4 17-28 | 0.028 | 0.978 |
| Transverse size | D1 17-21 vs. D1 17-28 | 1.448 | 0.150 |
| | D1 22-28 vs. D1 17-28 | -1.695 | 0.092 |
| | D2 17-21 vs. D2 17-28 | 0.992 | 0.323 |
| | D2 22-28 vs. D2 17-28 | -1.139 | 0.257 |
| | D3 17-21 vs. D3 17-28 | 0.521 | 0.603 |
| | D3 22-28 vs. D3 17-28 | -0.584 | 0.560 |
| | D4 17-21 vs. D4 17-28 | 0.693 | 0.489 |
| | D4 22-28 vs. D4 17-28 | -0.794 | 0.429 |
| Sagittal size | D1 17-21 vs. D1 17-28 | 0.955 | 0.341 |
| | D1 22-28 vs. D1 17-28 | -1.150 | 0.252 |
| | D2 17-21 vs. D2 17-28 | 1.141 | 0.256 |
| | D2 22-28 vs. D2 17-28 | -1.332 | 0.185 |
| | D3 17-21 vs. D3 17-28 | 0.964 | 0.337 |
| | D3 22-28 vs. D3 17-28 | -1.046 | 0.298 |
| | D4 17-21 vs. D4 17-28 | 0.861 | 0.391 |
| | D4 22-28 vs. D4 17-28 | -0.909 | 0.365 |
| The average value of the height | D1 17-21 vs. D1 17-28 | 2.282 | 0.024 |
| | D1 22-28 vs. D1 17-28 | -2.646 | 0.009 |
| | D2 17-21 vs. D2 17-28 | 1.129 | 0.261 |
| | D2 22-28 vs. D2 17-28 | -1.297 | 0.197 |
| | D3 17-21 vs. D3 17-28 | 0.156 | 0.876 |
| | D3 22-28 vs. D3 17-28 | -0.179 | 0.859 |
| | D4 17-21 vs. D4 17-28 | -0.491 | 0.624 |
| | D4 22-28 vs. D4 17-28 | 0.594 | 0.553 |

| Intervertebral discs sizes | Comparison groups | t-value | p |
|---|---|---|---|
| The sum of transverse and sagittal dimensions | D1 17-21 vs. D1 17-28 | 1.389 | 0.167 |
| | D1 22-28 vs. D1 17-28 | -1.637 | 0.104 |
| | D2 17-21 vs. D2 17-28 | 1.230 | 0.221 |
| | D2 22-28 vs. D2 17-28 | -1.382 | 0.170 |
| | D3 17-21 vs. D3 17-28 | 0.841 | 0.402 |
| | D3 22-28 vs. D3 17-28 | -0.921 | 0.359 |
| | D4 17-21 vs. D4 17-28 | 0.857 | 0.393 |
| | D4 22-28 vs. D4 17-28 | -0.926 | 0.356 |
| The sum of three sizes | D1 17-21 vs. D1 17-28 | 1.681 | 0.095 |
| | D1 22-28 vs. D1 17-28 | -1.918 | 0.057 |
| | D2 17-21 vs. D2 17-28 | 1.346 | 0.181 |
| | D2 22-28 vs. D2 17-28 | -1.476 | 0.142 |
| | D3 17-21 vs. D3 17-28 | 0.812 | 0.418 |
| | D3 22-28 vs. D3 17-28 | -0.867 | 0.388 |
| | D4 17-21 vs. D4 17-28 | 0.722 | 0.472 |
| | D4 22-28 vs. D4 17-28 | -0.777 | 0.439 |
| Cross-sectional area | D1 17-21 vs. D1 17-28 | 1.323 | 0.188 |
| | D1 22-28 vs. D1 17-28 | -1.575 | 0.118 |
| | D2 17-21 vs. D2 17-28 | 1.193 | 0.235 |
| | D2 22-28 vs. D2 17-28 | -1.340 | 0.183 |
| | D3 17-21 vs. D3 17-28 | 0.843 | 0.400 |
| | D3 22-28 vs. D3 17-28 | -0.913 | 0.363 |
| | D4 17-21 vs. D4 17-28 | 0.810 | 0.419 |
| | D4 22-28 vs. D4 17-28 | -0.871 | 0.386 |
| The volume of the intervertebral disc | D1 17-21 vs. D1 17-28 | 2.155 | 0.033 |
| | D1 22-28 vs. D1 17-28 | -2.370 | 0.019 |
| | D2 17-21 vs. D2 17-28 | 1.355 | 0.178 |
| | D2 22-28 vs. D2 17-28 | -1.451 | 0.149 |
| | D3 17-21 vs. D3 17-28 | 0.512 | 0.609 |
| | D3 22-28 vs. D3 17-28 | -0.537 | 0.592 |
| | D4 17-21 vs. D4 17-28 | 0.178 | 0.859 |
| | D4 22-28 vs. D4 17-28 | -0.196 | 0.845 |
| The ratio of the sum of sagittal and transverse size to height | D1 17-21 vs. D1 17-28 | -1.671 | 0.097 |
| | D1 22-28 vs. D1 17-28 | 2.034 | 0.054 |
| | D2 17-21 vs. D2 17-28 | -0.526 | 0.600 |
| | D2 22-28 vs. D2 17-28 | 0.644 | 0.521 |
| | D3 17-21 vs. D3 17-28 | 0.257 | 0.798 |
| | D3 22-28 vs. D3 17-28 | -0.321 | 0.749 |
| | D4 17-21 vs. D4 17-28 | 0.943 | 0.347 |
| | D4 22-28 vs. D4 17-28 | -1.204 | 0.231 |

**Continuation of table 2.**

| Intervertebral discs sizes | Comparison groups | t-value | p |
|---|---|---|---|
| The ratio of the sum of all sizes to the height | D1 17-21 vs. D1 17-28 | -1.671 | 0.097 |
| | D1 22-28 vs. D1 17-28 | 2.034 | 0.044 |
| | D2 17-21 vs. D2 17-28 | -0.526 | 0.600 |
| | D2 22-28 vs. D2 17-28 | 0.644 | 0.521 |
| | D3 17-21 vs. D3 17-28 | 0.257 | 0.798 |
| | D3 22-28 vs. D3 17-28 | -0.321 | 0.749 |
| | D4 17-21 vs. D4 17-28 | 0.943 | 0.347 |
| | D4 22-28 vs. D4 17-28 | -1.204 | 0.231 |
| The ratio of cross-sectional area to height | D1 17-21 vs. D1 17-28 | -0.692 | 0.490 |
| | D1 22-28 vs. D1 17-28 | 0.906 | 0.366 |
| | D2 17-21 vs. D2 17-28 | 0.183 | 0.855 |
| | D2 22-28 vs. D2 17-28 | -0.236 | 0.814 |
| | D3 17-21 vs. D3 17-28 | 0.665 | 0.507 |
| | D3 22-28 vs. D3 17-28 | -0.850 | 0.397 |
| | D4 17-21 vs. D4 17-28 | 1.077 | 0.283 |
| | D4 22-28 vs. D4 17-28 | -1.293 | 0.198 |
| | D1 22-28 vs. D1 17-28 | -1.575 | 0.118 |
| | D2 17-21 vs. D2 17-28 | 1.193 | 0.235 |
| | D2 22-28 vs. D2 17-28 | -1.340 | 0.183 |
| | D3 17-21 vs. D3 17-28 | 0.843 | 0.400 |
| | D3 22-28 vs. D3 17-28 | -0.913 | 0.363 |
| | D4 17-21 vs. D4 17-28 | 0.810 | 0.419 |
| | D4 22-28 vs. D4 17-28 | -0.871 | 0.386 |
| Body weight (kg) | D1 17-21 vs. D1 17-28 | -1.012 | 0.313 |
| | D1 22-28 vs. D1 17-28 | 1.105 | 0.271 |
| Body length, m | D2 17-21 vs. D2 17-28 | 0.412 | 0.681 |
| | D2 22-28 vs. D2 17-28 | -0.478 | 0.634 |
| Mass-growth factor, g/cm | D3 17-21 vs. D3 17-28 | -1.286 | 0.201 |
| | D3 22-28 vs. D3 17-28 | 1.394 | 0.166 |
| Mass-growth index, kg/m$^2$ | D4 17-21 vs. D4 17-28 | -1.492 | 0.138 |
| | D4 22-28 vs. D4 17-28 | 1.620 | 0.108 |

period of adulthood and in the combined the group proved the absence of significant differences in mean values ($p>0.05$).

The coefficients of variation for the sum of the three sizes (see Table 2) have average values from 3.88% to 6.40%, which corresponds to the weak variability of the trait. The indicators of distribution asymmetry are small, on average do not differ significantly (according to the observation groups - -0.199, 0.498 and 0.054), the lowest for $D_{L4-L5}$ - 0.004 in young men and the highest for $IVD_{L2-L3}$ in men - 0.832. T-test and Levene's test scores for the sum of all sizes $IVD_{L1-L2}$, $IVD_{L2-L3}$, $IVD_{L3-L4}$, $IVD_{L4-L5}$ did not show significant differences in mean values in the groups ($p>0.05$).

The coefficients of variation of cross-sectional areas for intervertebral discs $IVD_{L1-L2}$, $IVD_{L2-L3}$, $IVD_{L3-L4}$, $IVD_{L4-L5}$ had average values close to low variability ($\leq 10$) - from 8.18% to 13.61%. When using the paired t-test, it was determined that no significant differences in the mean values of the indicators in the groups were determined ($p>0.05$).

Coefficients of variation of intervertebral disc volumes have average values within the average variability - from 12.03% to 21.85%. When using the paired t-test, it was

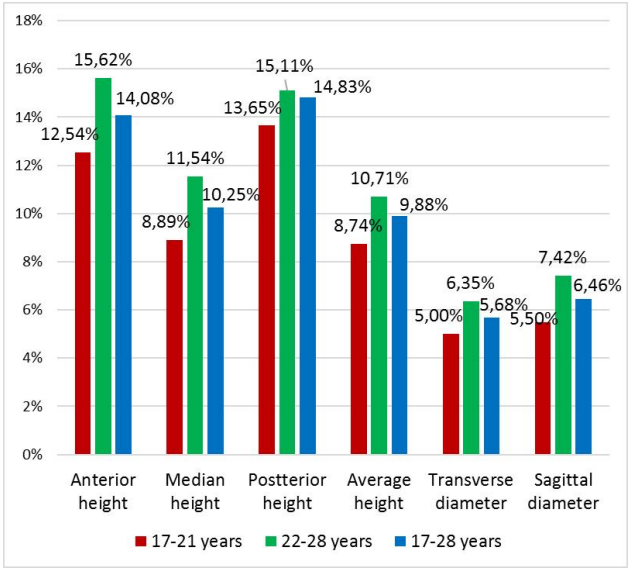


**Fig. 1.** Coefficients of variation of anterior, middle, average heights, transverse and sagittal sizes of intervertebral discs $IVD_{L1-L2}$, $IVD_{L2-L3}$, $IVD_{L3-L4}$, $IVD_{L4-L5}$ in young men (17-21 years), in men of the first period of adulthood (22-28 years) and in the combined group (17-28 years).

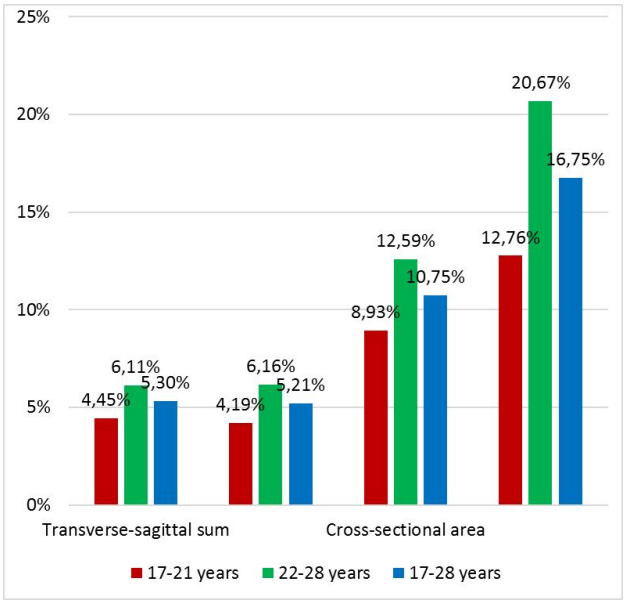


**Fig. 2.** Coefficients of variation of indicators of the sum of cross-sectional and sagittal sizes, the sum of all sizes, cross-sectional areas and volumes of intervertebral disks $IVD_{L1-L2}$, $IVD_{L2-L3}$, $IVD_{L3-L4}$, $IVD_{L4-L5}$ in young men (17-21 years), in men of the first period of adulthood (22-28 years) and in the combined group (17-28 years).

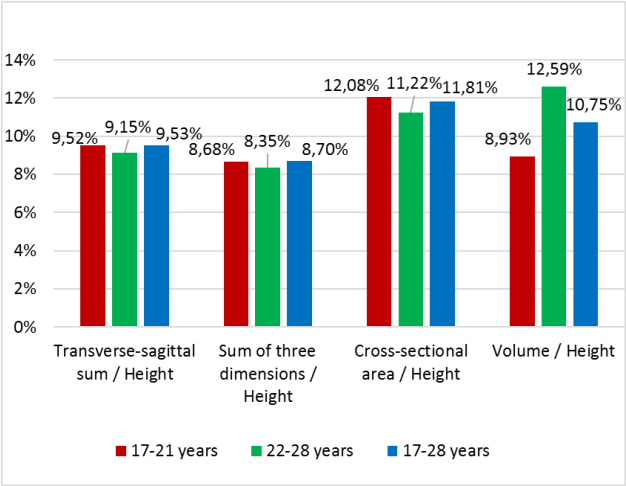


**Fig. 3.** Coefficients of variation of relative indicators of the sum of transverse and sagittal sizes, the sum of all sizes, cross-sectional areas and volumes of intervertebral disks $IVD_{L1-L2}$, $IVD_{L2-L3}$, $IVD_{L3-L4}$, $IVD_{L4-L5}$ to the average height in young men (17-21 years), in men of the first period of adulthood (22-28 years) and in the combined group (17-28 years).

determined that significant differences in the mean values of the indicators in the groups were not determined for $IVD_{L1-L2}$, $IVD_{L2-L3}$, $IVD_{L3-L4}$, $IVD_{L4-L5}$ ($p>0.05$).

The increase in the coefficients of variation of the areas of transverse dimensions and their volumes attracts attention (Fig. 2). The average values of the coefficients of variation for the sums of transverse and sagittal sizes - 5.29%, for the sum of the three sizes of intervertebral discs and 5.19%, for cross-sectional areas - 10.75%, for the volumes of intervertebral discs - 16.73%. Thus, the coefficients of variation of the cross-sectional areas of the intervertebral discs are on average more than 2 times (2.033 and 2.073) and the volumes more than 3 times (3.162 and 3.223) higher than the coefficients of variation of the sums of the transverse and sagittal sizes and the sum of three sizes.

Coefficients of variation of the ratio of the sum of sagittal and transverse size to height (see Table 1) of all groups have average values close to low variability ($\leq$10) - from 8.86% to 10.38%, for the ratio of cross-sectional areas to height disks coefficients of variation from 10.20% to 13.78%, for the ratio of disk volumes to height - from 8.18% to 13.61%.

T-test indicators (see Table 2) for the ratios of the sums of sagittal and transverse dimensions, the ratios of cross-sectional areas, the ratios of disk volumes to the height $IVD_{L1-L2}$, $IVD_{L2-L3}$, $IVD_{L3-L4}$, $IVD_{L4-L5}$ of the lumbar spine in young men, men of the first period of adulthood and in the combined group show no significant differences in the average values of these indicators in the groups ($p>0.05$).

The coefficients of variation of the ratio of the sum of the three dimensions to the height (see Table 1) are characterized by low variability, their values range from 8.06% to 9.52%. The highest frequency for the ratio of the sum of all sizes to the height of the studied groups are in the range of 2 sigma from 65.38% to 86.84% of the total number of observations. When using the paired t-test (see Table 2), significant differences in the mean values of the indicators in the groups were not determined ($p>0.05$).

Body weight had significant moderate correlations with transverse dimensions of intervertebral discs (IVDs) ($r=0.45$), with the sum of transverse and sagittal dimensions of IVDs ($r=0.43$), with the sum of three sizes of IVDs ($r=0.43$) , with a cross-sectional area of IVDs ($r=0.41$), with a volume of IVDs ($r=0.37$).

Body length was characterized by the presence of significant moderate correlations with sagittal sizes of IVDs ($r=0.48$), with the volume of IVDs ($r=0.49$); noticeable correlations were observed with the transverse dimensions of IVDs ($r=0.51$), with the sum of the transverse and sagittal dimensions of IVDs ($r=0.56$), with the sum of the three dimensions of IVDs ($r=0.56$), with the cross-sectional area of IVDs ($r=0.56$).

The mass-growth factor had a weak correlation with the transverse dimensions of IVDs ($r=0.35$), with the sum of the transverse and sagittal dimensions of IVDs ($r=0.30$), with the sum of the three dimensions of IVDs ($r=0.31$).

The mass-growth index had no significant correlations with anterior, posterior, and average height and sagittal size of IVDs ($r<0.10$) and had only significant weak correlations with mean height ($r=0.12$) and transverse dimensions of IVDs ($r=0.19$).

## Discussion

The variability of quantitative traits is a biological feature of the organism and is due to the genotype and environmental conditions. The problem of variability of symptoms has been relevant for centuries and not only in medicine. As early as the mid-nineteenth century, one of the founders of experimental medicine, the French scientist Claude Bernard, argued that if we could prove that deviation from the norm is a simple quantitative deviation, then we would have the key to treating any particular person, regardless, how its individual indicators differ from those of other people [3]. Nowadays, an important area of improvement in medicine is to identify the parameters of individual variability of the norm, which is the basis for early preclinical detection of abnormalities. The use of averages as indicators of the norm does not take into account individuality and can be a factor in misinterpretations of the results.

Determination of the linear dimensions of the vertebral bodies and intervertebral discs has diagnostic value [2, 7, 11, 14, 18], which is due to the relevance of this topic, due to the high prevalence of spinal pathology [6, 28].

Our results show no significant differences in the studied groups in terms of anterior and middle height in the groups of young men, men and in the combined group. Regarding the posterior height of the intervertebral discs when using the paired t-test, there was a significant

difference between the mean values in the groups for IVDL1-L2 6,159±0,921 mm, 7,182±0,932 mm for young men and men, the difference between the mean values was 1,023 mm. This indicator has significant variability due to the variability (individuality) of lumbar lordosis, which largely depends on conscious posture control [31] and has a fairly wide range of norm (20°- 45°) [19].

The coefficient of variation serves as a characteristic of variability (scattering) and is a criterion for the homogeneity of the population. Comparison of the average coefficients of variation (see Fig. 1) of medium and average heights with the indicators of the anterior and posterior vertical dimensions shows much less variability of the former. The values of the coefficients of variation of the anterior and posterior heights from 12.54% to 15.62% refer to the average variability, and the coefficients of variation for the middle height (8.74%, 10.71%, 9.88%) and for the average height (8 , 89%, 11.54%, 10.25%) are as close as possible to low variability. The variability for the average heights in the studied groups is insignificant, but less than for the middle heights. Thus, the use of variable front and rear heights in the integrated indicator (average height) not only does not increase the variability of the latter, but also slightly reduces it, proving their interdependence. These results indicate the advantages of using the average height of the intervertebral disc for further mathematical analysis.

Degenerative changes of intervertebral discs are accompanied by changes in the MR signal from the nucleus pulposus and fibrous ring (Pfirrmann degeneration scores) due to dehydration of varying degrees, structural changes in fibrous, cartilaginous elements, and changes in the closing plates of adjacent vertebrae [10] and protrusion of the nucleus pulposus in the form of protrusions, extrusions and sequesters.

Reduction of the height of the unaltered disc due to uniform stretching of the fibers of the fibrous ring, followed by its uniform thinning without local damage to the fibrous ring and without pathological changes in the closing plates of adjacent vertebrae also occurs. With this variant of deformation of the intervertebral disc there is a change in shape without changing its volume due to redistribution, while there is an increase in the area of the intervertebral disc with decreasing height. The described scenario of changes does not fit into the traditional model and is not taken into account by clinicians. The increase in area is usually accompanied by an increase in sagittal and transverse dimensions with a simultaneous decrease in the height of the intervertebral disc and an increase in pressure on the fibrous ring.

The high variability of indicators of cross-sectional areas and volumes of intervertebral discs determines the lower suitability of these indicators for further processing, reduces the reliability of the conclusions obtained on their basis.

Significant differences in the coefficients of variation of the sums of transverse and sagittal sizes and the sum of three sizes are not defined, which is also confirmed by the absence of a significant difference in the ratios of their average values and their standard errors [15].

The homogeneity of the sample and belonging to one general population is evidenced by the weak variability of the trait with a coefficient of variation not exceeding 10% [26]. Given the results obtained, it can be argued that the relative ratio of the sum of the three dimensions to the height has the most homogeneous sampling rates.

Total somatometric features and indices have their own characteristics in variability. The least variable is the length of the body - from 3.57% in young men to 4.33% in men without significant differences between groups of studies. Body weight variability increased in the male group to 15.41% compared to 11.17% of young men. The mass-growth coefficient and the mass-growth index, respectively, also show a tendency to higher values for these age groups, as body weight plays a dominant role in these calculated indicators.

Correlation analysis showed that the arithmetic mean values of the correlation coefficients of the linear dimensions of IVDs were the smallest for the mass-growth index and the largest for body length. The mass-growth index had the lowest correlation coefficients with the measured parameters of the intervertebral discs, with the maximum value for the transverse dimensions of the intervertebral discs (r=0.19), which calls into question the further use of the indicator in the simulation.

Given the observed variability in posterior and anterior intervertebral disc heights and the relatively smaller difference between the mean values in the IVD1 average height groups in subsequent studies, more vertical vertebral disc measurements are likely to be made to determine the average height. Increasing the number of vertical measurements of the intervertebral disc will, among other things, increase the accuracy of calculating the area of the upper and lower surfaces of the intervertebral disc, its volume and reduce the influence of posture on the average height.

## Conclusions

1. The gradual increase of linear indicators of the anterior, middle and posterior vertical dimensions, sagittal and transverse dimensions of the intervertebral discs from L1-L2 to L4-L5 segment is determined. There are no significant differences in the linear dimensions of the intervertebral discs (except for L1-L2) in the studied groups.

2. The sums of transverse and sagittal sizes, the sums of three sizes and the average height of the intervertebral discs, also increase proportionally in the caudal direction, have a distribution as close as possible to normal and is more acceptable for further mathematical regression analysis, as their coefficients of variation are 2 times smaller than in cross-sectional areas and 3 times smaller than in volumes.

3. The determined ratios of the sum of sagittal and transverse size and the sum of three sizes to the average

height of intervertebral discs are homogeneous, have low variability (coefficients of variation from 8.09% to 9.52%), correspond to the characteristics of the general population and can serve as auxiliary quantitative indicators assessment of the norm for intervertebral discs.

4. Body weight and length have relatively higher correlation coefficients with the sums of sagittal and transverse dimensions, the sums of three dimensions and cross-sectional areas than with other parameters of the intervertebral discs. With almost equal correlation coefficients, lower variability in the sum of the transverse and sagittal dimensions and the sums of the three dimensions make them more acceptable for further mathematical modeling than the calculated values of cross-sectional areas and volumes.

## References


[1] Adams, M.A. (2004). Biomechanics of back pain. *Acupunct. Med.,* 22(4), 178-188. doi: 10.1136/aim.22.4.178

[2] Alam, M.M., Waqas, M., Shallwani, H., & Javed, G. (2014). Lumbar morphometry: a study of lumbar vertebrae from a pakistani population using computed tomography scans. *Asian Spine Journal,* 8(4), 421-426. https://doi.org/10.4184/asj.2014.8.4.421

[3] Bernard, K. (2010). *Введение к изучению опытной медицины [An introduction to the study of experienced medicine]*. М.: Красанд - M.: Krasand.

[4] Bezsmertnyi, Yu.O., & Bezsmertna, H.V. (2018). Аналіз рекомендацій з медичної реабілітації осіб з інвалідністю [Analysis of recommendations for medical rehabilitation of persons with disabilities]. *Медицина болю - Pain Medicine*, 3(2/1), 11-12. doi.org/10.31636/pmjua.t1.34530

[5] Bozhenko, N.L. (2015). Біль у спині: деякі аспекти діагностики та лікування [Back pain: some aspects of diagnosis and treatment]. *Ліки України - Medicines of Ukraine*, 190(4), 58-65.

[6] Cai, X.Y., Sun, M.S., Huang, Y.P., Liu, Z.X., Liu, C.J., Du, C.F., & Yang, Q. (2020). Biomechanical Effect of L4-L5 Intervertebral Disc Degeneration on the Lower Lumbar Spine: A Finite Element Study. *Orthopaedic Surgery,* 12(3), 917-930. https://doi.org/10.1111/os.12703

[7] Campbell-Kyureghyan, N., Jorgensen, M., Burr, D., & Marras, W. (2005). The prediction of lumbar spine geometry: method development and validation. *Clinical Biomechanics* (Bristol, Avon), 20(5), 455-464. https://doi.org/10.1016/j.clinbiomech.2005.01.006

[8] Feng, H., Li, H., Ba, Z., Chen, Z., Li, X., & Wu, D. (2019). Morphometry evaluations of cervical osseous endplates based on three dimensional reconstructions. *International Orthopaedics,* 43(6), 1521-1528. https://doi.org/10.1007/s00264-018-4053-1

[9] Gertzbein, S.D., Seligman, J., & Holtby, R. (1985). Centrode patterns and segmental instability in degenerative disc disease. *Spine* (Phila Pa 1976), 10(3), 257-261. doi: 10.1097/00007632-198504000-00014

[10] Griffith, J.F., Wang, Y.X., Antonio, G.E., Choi, K.C., Yu, A., Ahuja, A.T., & Leung, P.C. (2007). Modified Pfirrmann grading system for lumbar intervertebral disc degeneration. *Spine,* 32(24), E708-E712. https://doi.org/10.1097/BRS.0b013e31815a59a0

[11] Grivas, T.B., Savvidou, O., Binos, S., Vynichakis, G., Lykouris, D., Skaliotis, M. …Velissarios, K. (2019). Morphometric characteristics of the thorac-lumbar and lumbar vertebrae in the Greek population: a computed tomography-based study on 900 vertebrae-"Hellenic Spine Society (HSS) 2017 Award Winner". *Scoliosis and Spinal Disorders*, 14, 2. https://doi.org/10.1186/s13013-019-0176-4

[12] Hayes, A.F., & Cai, L. (2007). Further evaluating the conditional decision rule for comparing two independent means. *The British Journal of Mathematical and Statistical Psychology*, 60(2), 217-244. https://doi.org/10.1348/000711005X62576

[13] Huang, R.C., Lim, M.R., Girardi, F.P. & Cammisa Jr, F.P. (2004) The prevalence of contraindications to total disc replacement in a cohort of lumbar surgical patients. *Spine* (Phila Pa 1976) 29(22), 2538-2541. doi: 10.1097/01.brs.0000144829.57885.20

[14] Iliescu, D.M., Bordei, P., Ionescu, E.V., Albina, S., Oprea, C., Obada, B. … Iliescu, M.G. (2017). Anatomic-Imaging Correlations of Lumbar Disk-Vertebral Morphometric Indices. *Int. J. Morphol.,* 35(4), 1553-1559. http://dx.doi.org/10.4067/S0717-95022017000401553

[15] Kokorina, N.V., & Tatarintsev, P.B. (2010). Методические вопросы выбора тест-объектов биоиндикации с использованием алгоритма сравнения коэффициентов вариации [Methodological issues of choosing test objects for bioindication using the algorithm for comparing the coefficients of variation]. *Вестник Томского государственного университета. Биология - Bulletin of Tomsk State University. Biology,* 11(3), 141-151.

[16] Kornus, O.H., Kornus, A.O., Shyshchuk, V.D., & Nurein, N.M. (2018). Regional morbidity profile of the Sumy region population by diseases of the musculoskeletal system and connective tissue. *Journal of Geology, Geography and Geoecology,* 27(3), 431-443. doi.org/10.15421/11188201

[17] Leckie, S., & Kang, J. (2009). Recent advances in nucleus pulposus replacement technology. *Current Orthopaedic Practice,* 20(3), 222-226 doi: 10.1097/BCO.0b013e31819d5bdd

[18] Lee, K., Shin, J.S., Lee, J., Lee, Y.J., Kim, M.R., Seong, I., ... Ha, I. (2017). Lumbar intervertebral disc space height in disc herniation and degeneration patients aged 20 to 25. *Int. J. Clin. Exp. Med.,* 10(4), 6828-6836.

[19] Lin, R.M., Jou, I.M., & Yu, C.Y. (1992). Lumbar lordosis: normal adults. *Journal of the Formosan Medical Association = Taiwan yi zhi,* 91(3), 329-333.

[20] Linhardt, O., Grifka, J., & Benditz, A. (2016). Are There Correlations Between Disc Degeneration and the Appearance of Lumbar Disc Herniations? *Zh. Orthop. Unfall.,* 154(6), 595-600. doi: 10.1055/s-0042-109568

[21] Maher, C., Underwood, M., & Buchbinder, R. (2017). Non-specific low back pain. *Lancet,* 389, 736-747. doi.org/10.1016/S0140-6736(16)30970-9

[22] Niankovskyi, S.L., & Plastunova, O.B. (2016). Особливості стану здоров'я, рухової активності та харчування школярів-спортсменів (огляд літератури) [Features of the state of health, motor activity and nutrition of athletes (review of literature)]. *Буковинський медичний вісник - Bukovynian Medical Bulletin,* 20(1), 77, 206-214.

[23] Ninel, V.G., Norkin, N.A., & Ostrovsky, V.V. (2008). *Лечение хронических дискогенных болевых и радикуломиелопатических синдромов у больных с поясничным остеохондрозом [Treatment of chronic discogenic pain and*

*radiculomyelopathic syndromes in patients with lumbar osteochondrosis].* Саратов: Новый ветер - Saratov: Novyy veter.

[24] Nordstokke, D.W. & Zumbo, B.D. (2007). A Cautionary Tale about Levene's Tests for Equal Variances. *Journal of Educational Research & Policy Studies,* 7(1), 1-14.

[25] Orlov, A.I. (2014). Непараметрические критерии согласия Колмогорова, Смирнова, омега-квадрат и ошибки при их применении [Nonparametric goodness-of-fit kolmogorov, smirnov, omega-square tests and the errors in their application]. *Научный журнал КубГАУ - Scientific journal of the Kuban State Agrarian University*, 97(03), 1-29.

[26] Popov, G.I. (2007). *Высшая математика и математическая статистика [Higher mathematics and mathematical statistics].* М.: Физическая культура - M.: Physical culture.

[27] Schmidt, H., & Reitmaier, S. (2013). Is the ovine intervertebral disc a small human one? A finite element model study. *Journal of the Mechanical Behavior of Biomedical Materials,* 17, 229-241. https://doi.org/10.1016/j.jmbbm.2012.09.010

[28] Shmagel, A., Foley, R., & Ibrahim, H. (2016). Epidemiology of Chronic Low Back Pain in US Adults: Data From the 2009-2010 National Health and Nutrition Examination Survey. *Arthritis Care & Research*, 68(11), 1688-1694. https://doi.org/10.1002/acr.22890

[29] Tang, R., Gungor, C., Sesek, R.F., Foreman, K.B., Gallagher, S., & Davis, G.A. (2016). Morphometry of the lower lumbar intervertebral discs and endplates: comparative analyses of new MRI data with previous findings. *European Spine Journal,* 25(12), 4116-4131. doi: 10.1007/s00586-016-4405-8

[30] Volkov, A.V., Goldshtein D.V., Shevelev, I.N., Konovalov, N.A., Bol'shakova, G.B., Fathudinov, T.Kh. … Zelenkov, P.V. (2007). Compression asymmetric static experimental model of degenerative disk diseases. *Bull. Exp. Biol. Med.*, 144(1), 123-125. doi: 10.1007/s10517-007-0270-0

[31]Żurawski, A.Ł., Kiebzak, W.P., Kowalski, I.M., Śliwiński, G., & Śliwiński, Z. (2020). Evaluation of the association between postural control and sagittal curvature of the spine. *PloS One*, 15(10), e0241228. https://doi.org/10.1371/journal.pone.0241228)

**МІЖХРЕБЦЕВІ ДИСКИ ПОПЕРЕКОВОГО ВІДДІЛУ ХРЕБТА: МОРФОМЕТРИЧНІ ПАРАМЕТРИ ТА КОЕФІЦІЄНТИ**

***Данилевич В.П., Гумінський Ю.Й., Григор'єва О.А., Данилевич С.Г.***

*Важливим елементом доказової медицини є врахування індивідуальної варіативності показників норми міжхребцевих дисків, що беззаперечно є основою раннього доклінічного виявлення їх патології. Математичне моделювання та комплексна оцінка параметрів міжхребцевих дисків можуть не лише передбачити та визначати ранні прояви патологічних змін, а й допомогти завчасно їх коригувати. Метою дослідження було розрахувати та оцінити мінливість абсолютних, розрахункових та відносних метричних параметрів міжхребцевих дисків в нормі з подальшою можливістю моделювання нормативів на основі індивідуальних лінійних розмірів міжхребцевих дисків поперекового відділу хребта та загальних антропометричних характеристик (довжина та маса тіла, масо-ростовий коефіцієнт та індекс) у юнаків та чоловіків першого періоду зрілого віку (17-28 років), як у окремих вікових групах, так і у об'єднаній групі. На серії МРТ-томограм, отриманих на сканері Phillips Achieva 1,5T, вимірювали передній, середній та задній вертикальні розміри, максимальний сагітальний та фронтальний розміри міжхребцевих дисків L1-L2, L2-L3, L3-L4, L4-L5 сегментів хребтового стовпа ($IVD_{L1-L2}$, $IVD_{L2-L3}$, $IVD_{L3-L4}$, $IVD_{L4-L5}$). Вираховували усереднену висоту міжхребцевих дисків, площі поперечного перерізу та об'єми міжхребцевих дисків, а також відносні показники - відношення суми сагітального і поперечного розмірів, суми трьох розмірів, площі поперечного перерізу та об'єму міжхребцевих дисків до усередненої висоти міжхребцевого диску. Статистичний аналіз отриманих морфометричних показників виконували у ліцензійному пакеті "STATISTICA 6.1". Оцінювали розподіл показників варіаційного ряду, їх середні значення та стандартні помилки, коефіцієнти варіації та асиметрії. Визначили, що суми поперечного і сагітального розмірів та суми трьох розмірів пропорційно зростають у каудальному напрямку, мають розподіл показників максимально наближений до нормального, а їх коефіцієнти варіації у рази менші, ніж для показників площ поперечного перерізу та об'ємів. Показники співвідношень суми сагітального та поперечного розміру і суми трьох розмірів до усередненої висоти міжхребцевих дисків мають варіабельність менше 10% та відповідають характеристикам генеральної сукупності. Маса та довжина тіла мають значимо вищі коефіцієнти кореляції з сумами сагітального та поперечного розмірів, сумами трьох розмірів та площами поперечних перерізів, аніж з парціальними розмірами міжхребцевих дисків.*

**Keywords:** *міжхребцевий диск, поперековий відділ хребта, норма, соматометрія, юнаки, чоловіки першого періоду зрілого віку.*

**DOI: 10.31393/morphology-journal-2021-27(2)-09** **Reports of Morphology, Vol. 27, №2, Pages 63-69**

**ISSN 1818-1295 eISSN 2616-6194**

**REPORTS OF MORPHOLOGY**

***Official Journal of the Scientific Society of Anatomists, Histologists, Embryologists and Topographic Anatomists of Ukraine***

journal homepage: https://morphology-journal.com

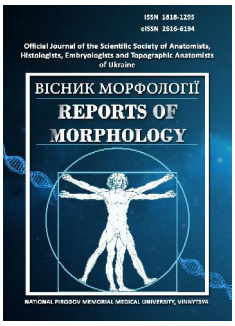


# Morphometric characteristics of skull and face parameters in fetuses and newborns

***Slobodian O.M., Kostyuk V.O., Dundiuk-Berezyna S.I.***
Bukovinian State Medical University, Chernivtsi, Ukraine

**ARTICLE INFO**
Received: 25 February 2021
Accepted: 14 April 2021

**UDC:** 611.714.06-053.15-053.31

**CORRESPONDING AUTHOR**
e-mail: slobodyanaleksandr@ukr.net
Slobodian O.M.

*Modern science has a significant number of diagnostic methods: craniological, anatomical, ultrasound, radiological. The development of new research methods, such as ultrasound and X-ray methods (magnetic resonance imaging), forms the concept of ultrasound and X-ray norms at different stages of human development. Now it is important to study the anatomical variability of people, morphometric characteristics, relationships of organs, anatomical structures, their parts at all stages of human development. The purpose of the work is to establish normative morphometric parameters of the skull and face in fetuses and newborns, followed by construction of mathematical models. The study was performed on 57 preparations of human fetuses 4-10 months and 7 newborns using adequate anatomical methods: macropreparation, topographic anatomical sections, computed tomography, craniometry. The main parameters of the facial and cerebral skull were measured with the help of a centimeter tape, a thick, sliding compass and a caliper. Statistical analysis of the obtained data was performed using a licensed program RStudio. It is established that according to the graphs of the average values of the parameters of the skull and face, there are two periods of accelerated and two periods of slow development. For transverse skull length, face width and skull height, two periods of accelerated development from the 6th to the 8th month of fetal development and from the 9th month of fetal development to the neonatal period and two periods of delayed development from the 5th to the 6th months and from the 8th to the 9th month of fetal development were revealed. For the total height of the face - periods of accelerated development - from the 4th to the 6th month of fetal development and from the 7th to the 9th month of fetal development, periods of delayed development - from the 6th to the 7th month of fetal development and from the 9th month of fetal development to the neonatal period. On the basis of arithmetic mean data of transverse skull length, face width, skull height, total face height, models for predicting normative morphometric parameters in fetuses and newborns are constructed. The constructed models will serve as a norm for the subsequent determination of certain morphometric deviations to establish variants of the structure and malformations of the skull and face. Thus, our systematized data on the features of spatio-temporal transformations of morphometric parameters of transverse skull length, face width, skull height, total face height with subsequent construction of mathematical models will contribute to the individualization of the norm, improvement of early diagnosis methods and development of new methods for surgical correction of congenital defects of the skull and face.*

**Keywords:** *skull, morphometry, fetus, newborn, human.*

## Introduction

Congenital malformations of the maxillofacial area rank third among other congenital anomalies. 70% of them are congenital nonunion of the upper lip and palate, and 30% - craniofacial dysostosis [15, 18]. The most diverse are congenital malformations of the upper and lower jaws, which are expressed in deviations from the norm of their size, shape, position of the jaws and changes in syntopia (agnathia, micro- and macrognathia, prognathia, nonunion of the upper jaw and palate) [4, 10, 13, 20].

The severity of malformations of the face is manifested not only by external ugliness and the severity of functional disorders, but also negatively affects the mental

development of the child [6, 12, 16].

Modern science has a significant number of diagnostic methods: craniological, anatomical, ultrasound, radiological. The development of new research methods, such as ultrasound and X-ray methods (magnetic resonance imaging), forms the concept of ultrasound and X-ray norms at different stages of human development [2, 7]. Nowadays it is important to study the anatomical variability of man, morphometric characteristics, relationships of organs, anatomical structures, their parts at all stages of human development, the study of bone formations of the skull: foramens, fissures, channels [3, 9, 5, 17]. It is also important to predict the state of the structures located in these formations, their possible causes and consequences, for example, compression lesions [9, 11].

*The purpose* of the work is to establish normative morphometric parameters of the skull and face in fetuses and newborns, followed by construction of mathematical models.

## Materials and methods

The study was performed on 57 preparations of human fetuses 4-10 months and 7 newborns (including 5 isolated organ complexes) of both sexes, without external signs of anatomical abnormalities or anomalies and without obvious macroscopic deviations from the normal structure of the skull using adequate anatomical methods: macropreparation, topography sections, computed tomography, craniometry. The craniometric study was performed in the horizontal ear-eye plane, in the so-called "Frankfurt horizontal". Prior to that, each object was fixed in a craniostat. Using a centimeter tape, a thick, sliding compass and a caliper, the main parameters of the facial and cerebral skull were measured: skull height, transverse skull length, total face height, face width.

The work was performed in compliance with the main provisions of the Helsinki Declaration of the World Medical Association on ethical principles of scientific medical research with human participation (1964-2000) and the order of the Ministry of Health of Ukraine №690 from 23.09.2009 and is a fragment of comprehensive planned initiative research work of departments human anatomy named after M.G. Turkevich, anatomy, clinical anatomy and operative surgery of Bukovynian State Medical University of the Ministry of Health of Ukraine: "Regularities of sex-age structure and topographic-anatomical transformations of organs and structures of the organism at pre- and postnatal stages of ontogenesis. Peculiarities of perinatal anatomy and embryotopography", state registration number 0120U101571.

Statistical analysis of the obtained data was performed using a licensed program RStudio. We tested the null hypothesis that the samples were taken from one distribution, or from distributions with the same medians:

$H_0$: {each group has the same distribution}

$H_1$: {each group does not have the same distribution}

We used the Student's test, the non-parametric Kruskal-Wallis test (answers the question of whether there is a difference between group distributions, but does not specify which groups differ), the Conover-Iman test to compare stochastic dominance and obtain results between different pairwise comparisons after the Kruskal-Wallis test for stochastic dominance among groups. The values at $p<0.05$ were considered statistically significant.

Evaluated the nature of the distributions for each of the obtained variation series, averages for each trait studied, the standard deviation, the percentile range of indicators.

## Results

Analyzing the morphometric parameters of the transverse length of the skull in fetuses and newborns by constructing a box diagram (Fig. 1), we can state that the difference between the medians of the samples (horizontal line in the box) is significantly statistically significant. The Kruskal-Wallis test gave the following results: since $p<0.05$, the difference between the medians of the groups is statistically significant. Using the Conover-Iman test, comparing the morphometric parameters of the transverse length of the skull by age groups found that for all possible pairs the median difference is statistically significant, except for pairs "5 months - 6 months", "8 months - 9 months", "9 months - 10 months" and "10 months - Newborns".

The described statistical parameters of the transverse length of the skull in fetuses and newborns (Table 1), prove that there is a significant (statistically significant) difference between the averages for all groups, except for pairs "5 months - 6 months", "7 months - 8 months", "8 months - 9 months", "9 months - 10 months" and "10 months - Newborns".

The graph of the average values of the transverse length of the skull in fetuses and newborns (Fig. 2) indicates the intensity of transformations of these parameters.

After analyzing the morphometric parameters of facial width in fetuses and newborns, a box diagram was constructed (Fig. 3), on which we observe the difference between the medians of the samples (horizontal line in the box), which is statistically significant.

The Kruskal-Wallis test gave the following results: since

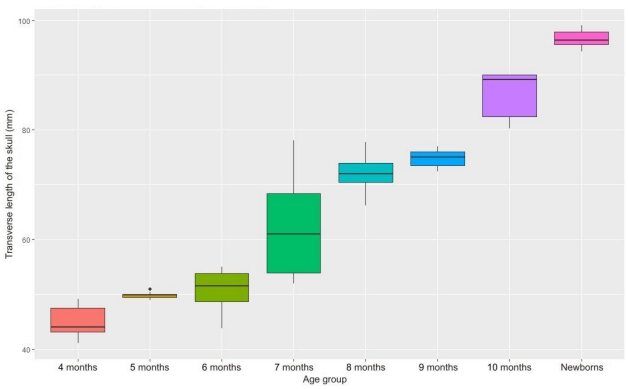


**Fig. 1.** Box diagram of the transverse length of the skull in fetuses and newborns (mm).

**Table 1.** Statistical indicators of transverse skull length in fetuses and newborns (mm).

| Age group | Average | Standard error for average | Confidence interval for the average |
|---|---|---|---|
| 4 months | 45.13 | 1.17 | (42.28; 47.98) |
| 5 months | 49.86 | 0.17 | (49.47; 50.25) |
| 6 months | 50.98 | 1.01 | (48.75; 53.21) |
| 7 months | 62.01 | 2.78 | (55.82; 68.20) |
| 8 months | 72.10 | 1.60 | (67.98; 76.22) |
| 9 months | 74.78 | 0.83 | (72.48; 77.08) |
| 10 months | 86.42 | 2.10 | (80.58; 92.26) |
| Newborns | 96.69 | 0.64 | (95.12; 98.26) |

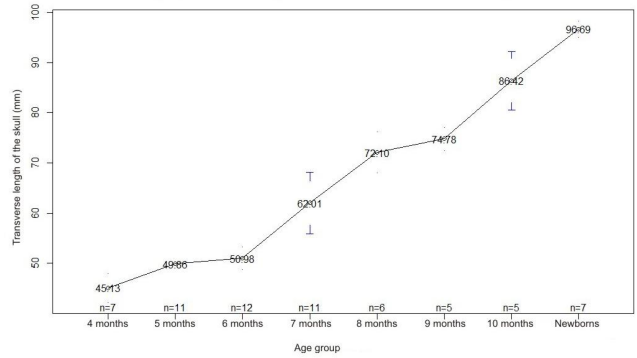


**Fig. 2.** Graph of mean values of transverse skull length in fetuses and newborns (mm).

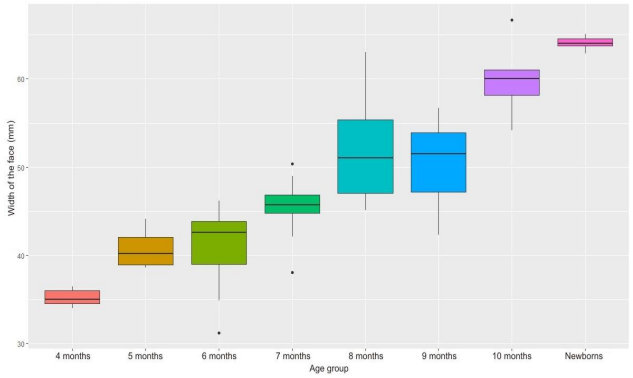


**Fig. 3.** Box diagram of the width of the face in fetuses and newborns (mm).

**Table 2.** Statistical indicators of facial width in fetuses and newborns (mm).

| Age group | Average | Standard error for average | Confidence interval for the average |
|---|---|---|---|
| 4 months | 35.23 | 0.37 | (34.34; 36.12) |
| 5 months | 40.80 | 0.62 | (39.43; 42.17) |
| 6 months | 41.04 | 1.28 | (38.23; 43.85) |
| 7 months | 45.46 | 0.99 | (43.25; 47.67) |
| 8 months | 52.12 | 2.75 | (45.04; 59.20) |
| 9 months | 50.32 | 2.54 | (43.27; 57.37) |
| 10 months | 60.02 | 2.03 | (54.37; 65.67) |
| Newborns | 64.09 | 0.29 | (63.37; 64.81) |

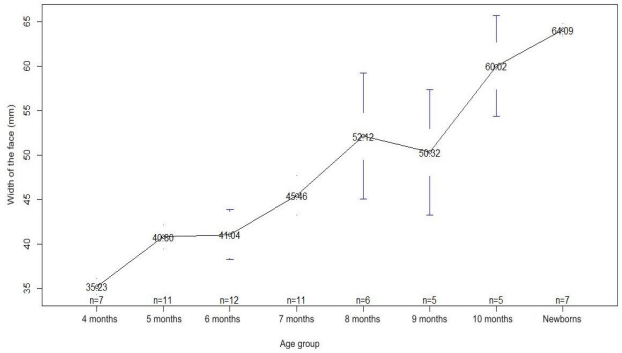


**Fig. 4.** Graph of average values of facial width in fetuses and newborns (mm).

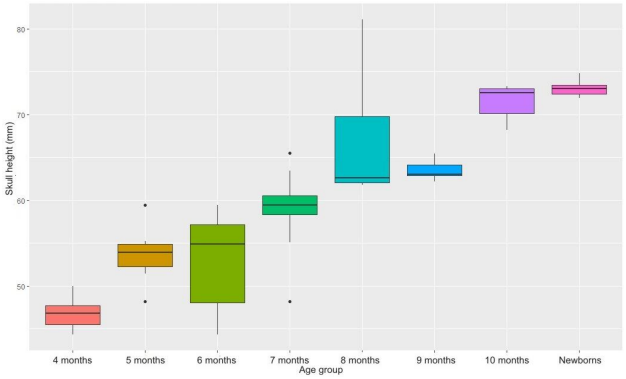


**Fig. 5.** Box diagram of skull height in fetuses and newborns (mm).

p<0.05, the difference between the medians of the groups is statistically significant. Using the Conover-Iman test, comparing the morphometric parameters of facial width by age groups, he found that for all possible pairs the median difference is statistically significant, except for the pairs "5 months - 6 months", "7 months - 9 months", "8 months - 9 months" and "10 months - Newborns".

The described statistical parameters of facial width in fetuses and newborns (Table 2) prove that there is a significant (statistically significant) difference between the averages for all groups, except for pairs "5 months - 6 months", "6 months - 7 months", "6 months - 9 months", "7 months - 8 months", "7 months - 9 months", "9 months - 10 months" and "10 months - Newborns".

The graph of the average values of facial width in fetuses and newborns (Fig. 4) indicates the intensity of transformations of these parameters.

Analyzing the morphometric parameters of skull height in fetuses and newborns by constructing a box diagram (Fig. 5), we can observe the difference between the medians of the samples (horizontal line in the box), which is significantly statistically significant. The Kruskal-Wallis test gave the following results: since p<0.05, the difference between the medians of the groups is statistically significant. Using the Conover-Iman test, comparing the morphometric parameters of skull height by age groups found that for all

**Table 3.** Statistical indicators of skull height in fetuses and newborns (mm).

| Age group | Average | Standard error for average | Confidence interval for the average |
|---|---|---|---|
| 4 months | 46.79 | 0.74 | (44.98; 48.60) |
| 5 months | 53.66 | 0.85 | (51.77; 55.55) |
| 6 months | 53.15 | 1.55 | (49.74; 56.56) |
| 7 months | 58.95 | 1.35 | (55.94; 61.96) |
| 8 months | 67.02 | 3.24 | (58.69; 75.35) |
| 9 months | 63.52 | 0.56 | (61.97; 65.07) |
| 10 months | 71.42 | 0.98 | (68.69; 74.15) |
| Newborns | 73.04 | 0.38 | (72.11; 73.97) |

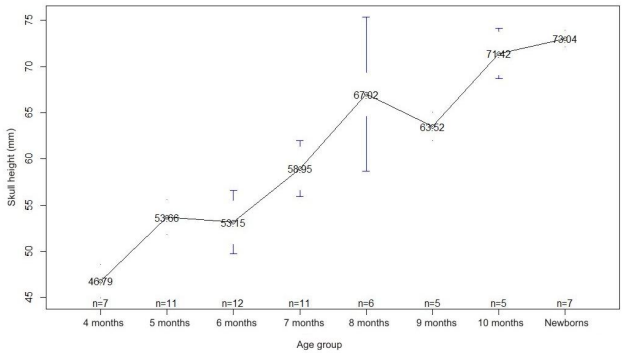


**Fig. 6.** Graph of mean values of skull height in fetuses and newborns (mm).

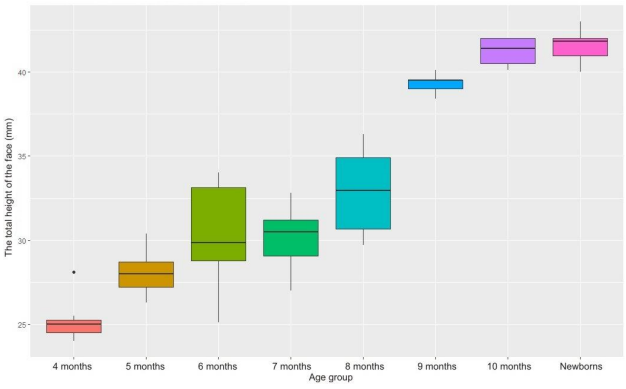


**Fig. 7.** Box diagram of the total height of the face in fetuses and newborns (mm).

possible pairs the median difference is statistically significant, except for pairs "5 months - 6 months", "8 months - 9 months", "9 months - 10 months", "8 months - 10 months" and "10 months - Newborns".

The determined statistical parameters of skull height in fetuses and newborns (Table 3) prove that there is a significant (statistically significant) difference between the averages for all groups, except for pairs "5 months - 6 months", "6 months - 7 months", "7 months - 8 months", "8 months - 9 months", "8 months - 10 months" and "10 months - Newborns".

The graph of average values of skull height in fetuses and newborns (Fig. 6) indicates the intensity of transformations of these parameters.

The analysis of morphometric parameters of the total face height in fetuses and newborns by constructing a box diagram (Fig. 7) shows that the difference between the medians of the samples (horizontal line in the box) is statistically significant. The Kruskal-Wallis test gave the following results: since $p<0.05$, the difference between the medians of the groups is statistically significant. Using the Conover-Iman test, comparing the morphometric parameters of the total height of the face by age groups found that for all possible pairs the median difference is statistically significant, except for pairs "5 months - 6 months", "9 months - 10 months", "9 months - Newborns" and "10 months - Newborns".

The described statistical parameters of the total face height in fetuses and newborns (Table 4), prove that there is a significant (statistically significant) difference between the averages for all groups, except for pairs "5 months - 6 months", "5 months - 7 months", "6 months - 7 months", "6 months - 8 months", "7 months - 8 months", and "10 months - Newborns".

The graph of the average values of the total height of the face in fetuses and newborns (Fig. 8) indicates the intensity of transformations of these parameters.

After correlating all morphometric parameters of the skull and face of fetuses and newborns using Pearson's correlation coefficient, it was found that between the values

**Table 4.** Statistical indicators of the total height of the face in fetuses and newborns (mm).

| Age group | Average | Standard error for average | Confidence interval for the average |
|---|---|---|---|
| 4 months | 25.23 | 0.52 | (23.96; 26.50) |
| 5 months | 28.03 | 0.38 | (27.17; 28.89) |
| 6 months | 30.39 | 0.81 | (28.60; 32.18) |
| 7 months | 30.03 | 0.55 | (28.80; 31.26) |
| 8 months | 32.90 | 1.11 | (30.04; 35.76) |
| 9 months | 39.30 | 0.28 | (38.51; 40.09) |
| 10 months | 41.20 | 0.39 | (40.12; 42.28) |
| Newborns | 41.53 | 0.39 | (40.58; 42.48) |

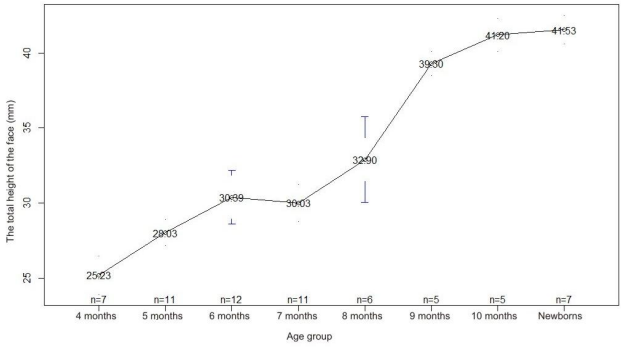


**Fig. 8.** Graph of average values of total face height in fetuses and newborns (mm).

of all paired correlation coefficients are positive and quite close to 1 (>0.90), which indicates a close strong positive correlation relationship between all morphometric parameters.

Comparing the mean values of all morphometric parameters of transverse skull length, face width, skull height, total face height in all age groups using the Wilcoxon test, it can be stated that all p-values are greater than the significance level α=0.05, which means no significant difference. Thus, based on the arithmetic mean of transverse skull length, face width, skull height, total face height, models for predicting normative morphometric parameters in fetuses and newborns were constructed using fetal age and crown-heel length.

The model of the transverse length of the skull in fetuses and newborns has the form:

Transverse length of the skull = $\beta_0$+0.224 x crown-heel length of the fetus,

where $\beta_0$: 3.412, if age period = 4 months; 1.399 = 5 months; 11.11 = 6 months; 10.92 = 7 months; 13.49 = 8 months; 21.44 = 9 months; 19.87 = 10 months; 15.20 = Newborns.

The coefficient of determination of the model is 96.34%.

The model of the width of the face in fetuses and newborns has the form:

Face width = $\beta_0$+0.071 x crown-heel length of the fetus,

where $\beta_0$: 22.00, if age period = 4 months; 24.54 = 5 months; 21.35 = 6 months; 22.34 = 7 months; 24.98 = 8 months; 19.81 = 9 months; 26.32 = 10 months; 28.61 = Newborns.

The coefficient of determination of the model is 86.84%.

The model of skull height in fetuses and newborns has the form:

Skull height = $\beta_0$+0.030 x crown-heel length of the fetus,

where $\beta_0$: 41.27, if age period = 4 months; 46.88 = 5 months; 44.94 = 6 months; 49.30 = 7 months; 55.69 = 8 months; 50.79 = 9 months; 57.36 = 10 months; 58.24 = Newborns.

The coefficient of determination of the model is 82.19%.

The model of the total height of the face in fetuses and newborns has the form:

Total face height = $\beta_0$+0.021 x crown-heel length of the fetus,

where $\beta_0$: 21.28, if age period = 4 months; 23.18 = 5 months; 24.52 = 6 months; 23.13 = 7 months; 24.80 = 8 months; 30.19 = 9 months; 31.14 = 10 months; 30.94 = Newborns.

The coefficient of determination of the model is 90,85%.

## Discussion

Comparing the graphs of the average values of transverse skull length, facial width, skull height, facial height in fetuses and newborns, it should be noted that these parameters are characterized by non-synchronicity of their changes, they are characterized by periods of accelerated and slow increase. According to the graphs of the average values of these parameters, we can say that there are two periods of accelerated and slow development. For transverse skull length, face width and skull height, two periods of accelerated development from the 6th to the 8th month of fetal development and from the 9th month of development to the neonatal period and two periods of delayed development from the 5th to the 6th months and from the 8th to the 9th month of fetal development were revealed. Regarding the total height of the face, periods of accelerated development - from the 4th to the 6th month of development and from the 7th to the 9th month of fetal development, periods of delayed development - from the 6th to the 7th month of development and from the 9th of fetal development to the neonatal period. Analyzing the data of the Conover-Iman test on statistically significant medians of the studied parameters of the skull and face, we can conclude that the pair "10 months - Newborns" is unlikely for transverse skull length, face width, skull height, total face height. In our opinion, this is justified by the fact that each person has an individual anatomical variability [16].

The constructed models will serve as a norm for the subsequent determination of certain morphometric deviations for the establishment of variants of the structure and defects of the development of the skull and face [1, 8, 14].

## Conclusions

1. During the fetal period of ontogenesis and in the neonatal period, the transverse length of the skull increases from 45.13±1.17 mm in fetuses of the 4th month to 96.69±0.64 mm in newborns, the width of the face - from 35.23±0.37 mm to 64.09±0.29 mm, skull height - from 46.79±0.74 mm to 73.04±0.38 mm, total face height - from 25.23±0.52 mm to 41.53±0.39 mm, respectively.

2. According to the graphs of the average values of the parameters of the skull and face, there are two periods of accelerated and two periods of slow development. For the transverse length of the skull, the width of the face and the height of the skull, two periods of accelerated development were revealed: from the 6th to the 8th month of fetal development and from the 9th month of fetal development to the neonatal period and two periods of delayed development: from the 5th to the 6th month and from the 8th to the 9th month of fetal development. Regarding the total height of the face, periods of accelerated development - from the 4th to the 6th month of development and from the 7th to the 9th month of fetal development, periods of delayed development - from the 6th to the 7th month of development and from the 9th to the of fetal development to the neonatal period.

3. On the basis of arithmetic mean data of transverse skull length, face width, skull height, total face height, models for predicting normative morphometric parameters in fetuses and newborns are constructed. Systematized data on the features of spatio-temporal transformations of morphometric parameters of transverse skull length, facial width, skull height, total facial height with their subsequent construction of mathematical models will contribute to the

individualization of the norm, improvement of early diagnosis methods and development of new methods of surgical correction of congenital malformations.

## References


[1] Bahsi, I., Orhan, M., Kervancioglu, P., & Yalcin, E.D. (2019). Morphometric evaluation and surgical implications of the infraorbital groove, canal and foramen on cone-beam computed tomography and a review of literature. *Folia Morphologica,* 78(2), 331-343. doi: 10.5603/FM.a2018.0084

[2] Bertoglio, B., Corradin, S., Cappella, A., Mazzarelli, D., Biehler-Gomez, L., Messina, C., ... Cattaneo, C. (2020). Pitfalls of Computed Tomography 3D Reconstruction Models in Cranial Nonmetric Analysis. *Journal of Forensic Sciences*, 65(6), 2098-2107. doi: 10.1111/1556-4029.14535

[3] Borghei-Razavi, H., Raghavan, A., Eguiluz-Melendez, A., Joshi, K., Fernandez-Miranda, J.C., Kshettry, V.R., & Recinos, P.F. (2020). Anatomical variations in the location of veins draining into the anterior superior sagittal sinus: implications for the transbasal approach. *Operative Neurosurgery,* 18(6), 668-675. doi: 10.1093/ons/opz339

[4] Constantine, S., Kiermeier, A., & Anderson, P. (2020). The Normal fetal cephalic Index in the second and third trimesters of pregnancy. *Ultrasound Quarterly*, 36(3), 255-262. doi: 10.1097/RUQ.0000000000000444

[5] Dmytrenko, R.R., Tsyhykalo, O.V., & Honcharenko, V.A. (2020). Особливості морфогенезу кісток основи черепа у ранньому періоді онтогенезу людини [Features of morphogenesis of skull base bones in the early period of human ontogenesis]. *Буковинський медичний вісник - Bukovynian Medical Bulletin,* 24(3 (95)), 22-27. doi: 10.24061/2413-0737. XXIV.3.95.2020.67

[6] Dursun, A., Ozturk, K., & Albay, S. (2018). Development of hard and soft palate during the fetal period and hard palate asymmetry. *Journal of Craniofacial Surgery*, 29(8), 2358-2362. doi: 10.1097/SCS.0000000000005016

[7] Grill, F.D., Behr, A.V., Rau, A., Ritschl, L.M., Roth, M., Bauer, F.X. ... Loeffelbein, D.J. (2019). Prenatal intrauterine maxillary development - An evaluation with three-dimensional ultrasound. *Journal of Cranio-Maxillofacial Surgery,* 47(7), 1077-1082. doi: 10.1016/j.jcms.2019.01.029

[8] Grzonkowska, M., Baumgart, M., Badura, M., Wisniewski, M., & Szpinda, M. (2020). Morphometric study of the primary ossification center of the frontal squama in the human fetus. *Surgical and Radiologic Anatomy,* 42(7), 733-740. doi: 10.1007/s00276-020-02425-7

[9] Hizay, A., & Sindel, M. (2019). Metoptic Canal and Warwick's Foramen: Incidence and Morphometric Analysis by Several Reference Points in the Human Orbit. *The Eurasian Journal of Medicine*, 51(1), 1-4. doi: 10.5152/eurasianjmed.2018.17353

[10] Horbatiuk, O.M., Makedonskyi, I.O., & Kurylo, H.V. (2019). Сучасні стратегії діагностики, хірургічної корекції та профілактики вроджених вад розвитку у новонароджених [Modern strategies for diagnosis, surgical correction and prevention of congenital malformations in newborns]. *Неонатологія, хірургія та перинатальна медицина - Neonatology, Surgery and Perinatal Medicine,* 9(4), 88-97. doi: 10.24061/2413-4260.IX.4.34.2019.10

[11] Katsube, M., Rolfe, S.M., Bortolussi, S.R., Yamaguchi, Y., Richman, J.M., Yamada, S., & Vora, S.R. (2019). Analysis of facial skeletal asymmetry during foetal development using μCT imaging. *Orthodontics & Craniofacial Research*, 22(1), 199-206. doi: 10.1111/ocr.12304

[12] Khmara, T.V., Ryznychuk, M.O., Kuzniak, N.B., Melnychuk, S.P., Batranovska, S.O., & Zamorskyi, I.I. (2021). Онтологія варіантів будови та вад розвитку черепа. Частина II. Спадкові синдроми [Ontology of variants of structure and defects of skull development. Part II. Hereditary syndromes]. *Український журнал медицини, біології та спорту - Ukrainian Journal of Medicine, Biology and Sports,* 6(3), 71-77. doi: 10.26693/jmbs06.03.071

[13] Korchynska, N.S., Slobodian, O.M., & Kostyuk, V.O. (2019). Fetal anatomy of the maxillary cellular process. *Клінічна анатомія та оперативна хірургія - Clinical Anatomy and Operative Surgery,* 18(1), 62-66. doi: 10.24061/1727-0847.18.1.2019.10

[14] Marchenko, A.V., Petrushanko, T.O., & Gunas, I.V. (2017). Моделювання за допомогою регресійного аналізу трансверзальних розмірів верхньої й нижньої щелепи та сагітальних характеристик зубної дуги в юнаків в залежності від особливостей донтометричних і кефалометричних показників [Simulation using regression analysis transversal sizes of upper and lower jaw and sagittal performance of dental arch in young depending on the characteristics of odontometric and cephalometric indicators]. *Вісник морфології - Reports of Morphology*, 23(1), 107- 111.

[15] Ng, A.F., Quintero, R.B., Lahirish, I.A.M., Holanda, V., Neto, M.R., & De Oliveira, E. (2020). Microsurgical Anatomy Review of Bifrontal Limited Transbasal Approach-Quantitative and Anatomy Study. *World Neurosurgery,* 141, e1-e8. doi: 10.1016/j.wneu.2020.02.114

[16] Rawhani, R., Abdellatif, A., Abushama, M., & Ahmed, B. (2018). Antenatal diagnosis of fetal skeletal malformation. *Donald School Journal of Ultrasound in Obstetrics and Gynecology,* 12(2), 116-123. doi: 10.5005/jp-journals-10009-1561

[17] Slobodian, O.M., Kuzniak, N.B., & Lavriv, L.P. (2016). Закономірності перинатальних органометричних параметрів ділянок і структур голови [Regularities of perinatal organometric parameters of areas and structures of the head]. *Вісник проблем біології і медицини - Bulletin of Problems of Biology and Medicine*, (2 (2)), 314-317.

[18] Slobodian, O.M., Proniaiev, D.V., & Tovkach, Yu.V. (2020). *Анатомо-функціональні особливості окремих структур та органів голови [Anatomical and functional features of individual structures and organs of the head]*. Чернівці. БДМУ - Chernivtsi. BSMU.

[19] Vovk, Yu.M., Vovk, O.Yu. (2019). *Індивідуальні анатомічна мінливість та їх клініко-морфологічне значення [Individual anatomical variability and their clinical and morphological significance]*. Харків: ФОП Бронін О.В. - Kharkiv: FOP Bronin O.V.

[20] Zhang, Y., Ji, D., Li, L., Yang, S., Zhang, H., & Duan, X. (2019). ClC-7 Regulates the pattern and early development of craniofacial bone and tooth. *Theranostics*, 9(5), 1387-1400. doi: 10.7150/thno.29761


**МОРФОМЕТРИЧНА ХАРАКТЕРИСТИКА ПАРАМЕТРІВ ЧЕРЕПА ТА ЛИЦЯ ПЛОДІВ І НОВОНАРОДЖЕНИХ**

***Слободян О.М., Костюк В.О., Дундюк-Березина С.І.***

*Сучасна наука володіє значною кількістю діагностичних методів: краніологічних, анатомічних, ультразвукових, рентгенологічних. Розвиток нових методів дослідження, таких як ультразвукові та рентгенологічні методи (магнітно-*

*резонансної томографії), формує поняття ультразвукової та рентгенологічної норми на різних етапах розвитку людини. Нині є актуальним вивчення анатомічної мінливості людини, морфометричних характеристик, взаємовідношень органів, анатомічних структур, їх частин на всіх етапах розвитку людини. Мета роботи - встановити нормативні морфометричні параметри черепа і лиця в плодів та новонароджених з наступною побудовою математичних моделей. Дослідження виконано на 57 препаратах плодів людини 4-10 місяців та 7 новонароджених за допомогою адекватних анатомічних методів: макропрепарування, виготовлення топографоанатомічних зрізів, комп'ютерної томографії, краніометрії. За допомогою сантиметрової стрічки, товстотного, ковзаючого циркулів та штангель-циркуля вимірювали основні параметри лицевого та мозкового черепа. Статистичний аналіз отриманих даних проводили за допомогою ліцензованої програми RStudio. За даними графіків середніх значень параметрів черепа та лиця встановлено два періода прискореного та два періода уповільненого розвитку. Для поперечної довжини черепа, ширини лиця та висоти черепа виявлено два періоди прискореного розвитку з 6-го по 8-й місяці внутрішньоутробного розвитку та з 9-го місяця розвитку до періоду новонародженості і два періода сповільненого розвитку - з 5-го до 6-го місяця та з 8-го до 9-го місяці внутрішньоутробного розвитку. Для загальної висоти лиця - періоди прискореного розвитку - з 4-го по 6-й місяці розвитку та з 7-го до 9-й місяця внутрішньоутробного розвитку, періоди сповільненого розвитку - з 6-го до 7-го місяця розвитку та з 9-го місяця внутрішньоутробного розвитку до періоду новонародженості. На основі середніх арифметичних даних поперечної довжини черепа, ширини лиця, висоти черепа, загальної висоти лиця, побудовані моделі прогнозування нормативних морфометричних їх параметрів у плодів та новонароджених. Побудовані моделі слугуватимуть нормою для наступного визначення певних морфометричних відхилень для встановлення варіантів будови та вад розвитку черепа і лиця. Таким чином, систематизовані нами дані про особливості просторово-часових перетворень морфометричних параметрів поперечної довжини черепа, ширини лиця, висоти черепа, загальної висоти лиця з наступною їх побудовою математичних моделей сприятимуть індивідуалізації норми, удосконаленню методів ранньої діагностики та розробці нових способів хірургічної корекції природжених вад черепа і лиця.*

**Ключові слова:** *череп, морфометрія, плід, новонароджений, людина.*

DOI: 10.31393/morphology-journal-2021-27(2)-10 Reports of Morphology, Vol. 27, №2, Pages 70-75

ISSN 1818-1295 eISSN 2616-6194

REPORTS OF MORPHOLOGY

*Official Journal of the Scientific Society of Anatomists, Histologists, Embryologists and Topographic Anatomists of Ukraine*

journal homepage: https://morphology-journal.com

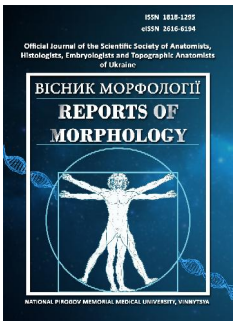


# Quantitative changes in the microstructure of the pancreas under the influence of sublethal dehydration, subsequent readaptation and correction

***Kovchun V.Yu.***
Medical Institute of Sumy State University, Sumy, Ukraine

**ARTICLE INFO**
Received: 3 March 2021
Accepted: 21 April 2021

**UDC:** 616.37:616.395-092.9

**CORRESPONDING AUTHOR**
e-mail: vu.kovchun@ukr.net
Kovchun V.Yu.

*Dehydration is a pathological condition caused by insufficient water intake and is accompanied by metabolic disorders that have significant consequences for human health and performance. The endocrine system takes part in a number of functions of the water exchange system, optimizing body fluid volume. In the literature, there is no systematic data on changes in the pancreas under conditions of various types of dehydration. This article is devoted to the study of structural changes in the pancreas in conditions of sublethal degrees of various types of dehydration, followed by readaptation and correction with a drug that has anti-ischemic, membrane-stabilizing, antioxidant, hepatoprotective and immunomodulatory properties that allow to normalize protein, carbohydrate and lipid metabolism. The purpose of the study was to research the features of changes in the endocrine and exocrine parenchyma of the pancreas by the method of morphometry of histological preparations under conditions of sublethal dehydration with subsequent readaptation and correction with thiazotic acid morpholinium salt. The study group consisted of 60 mature male rats, which were simulated sublethal degree of general, cellular and extracellular dehydration by the method of A.D.Soboleva, V.Z.Sikora, J.Ya.Bodnar. After reaching a severe degree of dehydration, part of the rats were transferred to a regular drinking diet, the second part received a corrector drug for 14 days. The animals were withdrawn from the experiment by decapitation under anesthesia on 24th, 44th and 104th days in accordance with the type of dehydration. After analyzing the results obtained, it was found that there were no significant differences in most morphometric parameters under conditions of exposure to sublethal dehydration in comparison with subsequent readaptation. Significant changes in the area of the islets of Langerhans and the area of nuclei of exocrinocytes were revealed under conditions of exposure to various types of sublethal dehydration in comparison with readaptation and correction; in all experimental groups. Other morphometric parameters of the pancreatic parenchyma had changes of varying statistical significance, which depended on the type of dehydration. It has been established that the use of the thiazotic acid morpholinium salt leads to partial restoration of the structural components of the pancreatic parenchyma in comparison with the period of readaptation.*

**Keywords:** *pancreas, islets of Langerhans, acini, sublethal dehydration, thiazotic acid morpholinium salt.*

## Introduction

Water is necessary for the development of life and survival [1, 8, 10, 13, 24], this is its participation in metabolism, facilitation of cellular metabolism [3, 22], modulation of normal osmotic pressure, maintenance of electrolyte balance, regulation of body temperature and many others physiological processes [9, 19, 23]. It has been proven that both excessive and insufficient water consumption has a negative effect on the health of our body [2, 11, 14, 26, 28]. Dehydration reduces a person's ability to engage in physical activity and increases the risk of diseases of the cardiovascular, genitourinary and digestive systems. The endocrine system is involved in a number of water metabolism processes, optimizing the flow and excretion of fluid in the body. The pancreas, as an

organ of the digestive and endocrine systems, undergoes pronounced structural changes under conditions of dehydration [4, 5, 7], as well as during the use of alcohol, opioids and smoking [15, 18, 20, 21, 27]. Therefore, an important issue today is the understanding of risk factors, physiological and pathogenetic links of pancreas diseases, systematization and expansion of data in the world literature on this issue [6, 16, 20, 25].

*The aim* of the study was to study in the experiment the morphometric features of structural transformations of changes in the parenchyma of the pancreas under the influence of sublethal degree of general, cellular and extracellular dehydration of the organism with the subsequent period of readaptation and correction.

## Materials and methods

To achieve the goal of the experiment, 70 laboratory male adult rats weighing from 160 to 200 g were used, which were in the vivarium of the Medical Institute of Sumy State University. The experiment was conducted in compliance with the main provisions of the Council of Europe Convention on the Protection of Vertebrate Animals Used for Experimental and Other Scientific Purposes (March 18, 1986), EEC Directive 9609 (November 24, 1986), Resolution of the First National Congress on Bioethics "General ethical principles of animal experiments" (2001), and orders of the Ministry of Health of Ukraine №690 from 23.09.2009, №944 from 14.12.2009, №616 from 03.08.2012 and the laws of Ukraine.

60 rats were divided into 3 experimental groups, each of which included 20 rats with a simulated sublethal degree of different types of dehydration according to the methods of A.D.Soboleva, V.Z.Sikora, J.Ya.Bodnar, proposed in 1975. Subsequently, the animals of each group were divided into subgroups of 10 rats, which were transferred to the usual drinking diet for 14 days, and those that in addition to the usual drinking diet for the same period received thiazotic acid morpholinium salt in a dose of 0.1 ml as a preparation corrector of morphological changes that occurred during the experiment. The calculation of the dose of the preparation for animals was performed taking into account the recommendations of Y.R. Rybolovlev and R.S. Rybolovlev [17]. The control group included 10 rats.

Pancreas material collection, fixation, and sample fabrication were performed according to traditional methods [11]. To determine the structural components of the gland, paraffin sections 5-7 ?m thick were stained with hematoxylin-eosin and Van Gieson. Micropreparations were investigated using a digital image output system "SEO Scan Lab 2.0" (Ukraine).

Morphometric analysis included Langerhans islet area (AIL), pancreatic acinus area (PA), pancreatocyte area (PAC), pancreatocyte nuclei area (PCN), pancreatocyte cytoplasm area (PCAC), and nuclear-cytoplasmic ratio (NCR) determination.

The results of morphometric measurements were processed using the statistical program IBM SPSS Statistic 21. In order to verify the normality of the distribution used Kolmogorov-Smirnov test, the average values are presented as M±m. The Mann-Whitney test was used to compare the performance in the experimental groups. Statistically significant indicators were considered under the condition $p<0.05$.

## Results

In rats of the control group, the average size of AIL (area of islets of Langerhans) was 13934.1±636.92 $\mu m^2$, PA (pancreatic acinus area) - 983.4±67.1 $\mu m^2$; PAC (pancreatocyte area) - 149.5±3.16 $\mu m^2$; PCN (pancreatocyte nuclei area) - 10.70±0.41 $\mu m^2$; PCAC (pancreatocyte cytoplasm area) - 138.7±4.72 $\mu m^2$; NCR (nuclear-cytoplasmic ratio) - 8.200±0.980 (Fig. 1).

Under the influence of sublethal degree of different types of dehydration, pronounced structural changes were observed in all experimental groups (Fig. 2).

Under the influence of sublethal degree of general dehydration and the period of further readaptation, there was a decrease in the area of AIL - by 3.5% (p=0.880), PA - by 1.4% (p=1.0), PAC - by 1.96% (p=0.571), PCAC - by 1.42% (p=0.650), PCN - by 6.7% (p=0.151), NCR - by 5,93% (p=0.364). Under the conditions of using the thiazotic acid morpholinium salt, we observed a decrease in AIL - by 32.27% (p<0.001), PA - by 15,91% (p=0.041), PAC - by 7.42% (p=0.096), PCAC - by 6,21% (p=0.290), PCN - by 17.82% (p=0.038), NCR - by 12.71% (p=0.406). Comparing the periods of readaptation and correction, a decrease in Langerhans islet area by 29.8% (p<0.001), acinus area - by 14,67% (p=0.019), pancreatocyte area - by 5.57% (p=0.051), pancreatocyte cytoplasm area - by 4.85% (p=0.406), pancreatocyte nuclei area - by 11.97% (p=0.290), nuclear-cytoplasmic ratio - by 7.2% (p=0.597). Detailed morphometric changes in the parenchyma of the pancreas conditions of the sublethal degree of general dehydration, the period of subsequent readaptation and correction are shown in Table 1.

Under the influence of sublethal degree of cellular

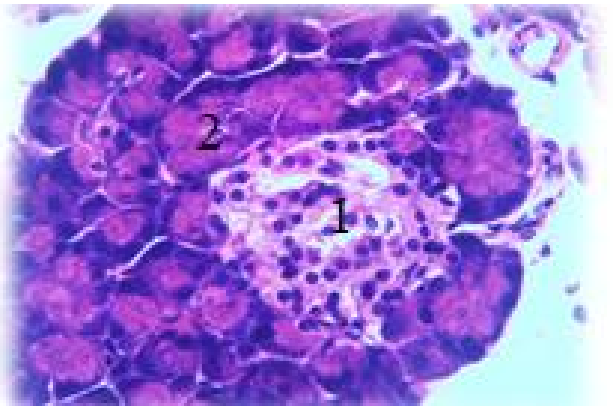


**Fig. 1.** Pancreas of the rat from control group: 1 - islet of Langerhans, 2 - acini. Hematoxylin-eosin. x400.

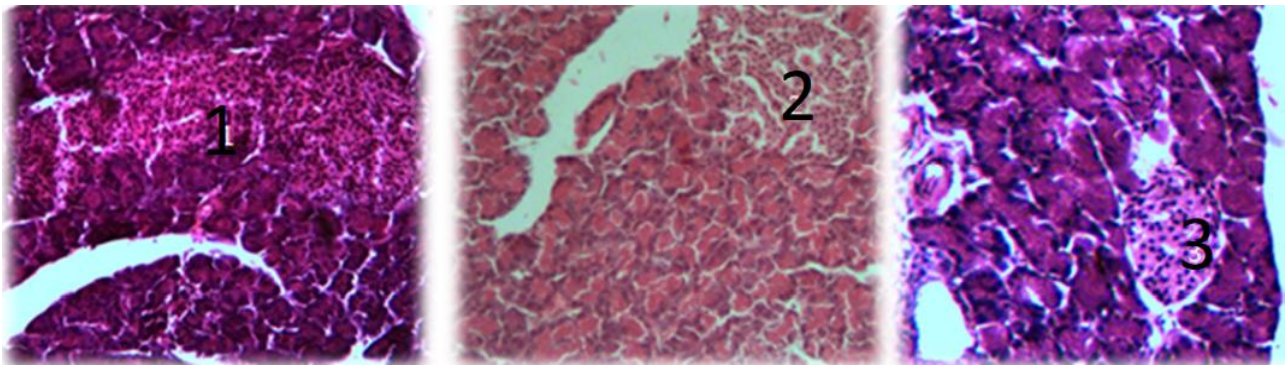


**Fig. 2.** The islet of Langerhans of the rat pancreas: 1 - under conditions of general dehydration, 2 - cellular dehydration, 3 - extracellular dehydration. Hematoxylin-eosin. x200.

**Table 1.** Morphometric changes of islets, acini and pancreatocytes under conditions of sublethal degree of general dehydration, period of readaptation and correction.

| Indicator | Control | Severe dehydration | Readaptation | Correction |
|---|---|---|---|---|
| AIL, μm² | 13934.1±636.92 | 31280.9±1992.7 | 30176.7±1144.1 | 21184.01±1992.1 |
| | $p_1$=0.880; $p_2$<0.001; $p_3$<0.001 | | | |
| PA, μm² | 983.4±67.1 | 1326.2±69.7 | 1307.4±64.1 | 1115.5±34.9 |
| | $p_1$=1.0; $p_2$=0.041; $p_3$=0.019 | | | |
| PAC, μm² | 149.5±3.16 | 172.4±5.8 | 169.0±5.0 | 159.6±5.1 |
| | $p_1$=0.571; $p_2$=0.096; $p_3$=0.151 | | | |
| PCAC, μm² | 138.7±4.7 | 154.5±5.9 | 152.3±5.2 | 144.9±5.4 |
| | $p_1$=0.650; $p_2$=0.290; $p_3$=0.406 | | | |
| PCN, μm² | 10.76±0.41 | 17.91±0.52 | 16.69±1.14 | 14.65±0.94 |
| | $p_1$=0.151; $p_2$=0.038; $p_3$=0.290 | | | |
| NCR, % | 8.270±0.984 | 11.80±0.83 | 11.11±0.92 | 10.31±0.93 |
| | $p_1$=0.364; $p_2$=0.406; $p_3$=0.597 | | | |

**Notes:** $p_1$ - the probability of differences in the indicators of severe general dehydration and the period of readaptation; $p_2$ - probability of differences in indicators of severe general dehydration and correction period; $p_3$ - the probability of differences in readaptation and correction. AIL - Langerhans islet area; PA - pancreatic acinus area; PAC - pancreatocyte area; PCAC - pancreatocyte cytoplasm area; PCN - pancreatocyte nuclei area; NCR - nuclear-cytoplasmic ratio.

dehydration and the period of readaptation, there was a decrease in AIL - by 2.86% (p=0.762), pancreatocyte nuclei area - by 10.55% (p=0.199), nuclear-cytoplasmic ratio - by 16.22% (p=0.112), and increase of acinus area by 2.49% (p=0.705), pancreatocyte area - by 2.82% (p=0.364), pancreatocyte cytoplasm area - by 6.47% (p=0.041). Under the conditions of simultaneous use of the thiazotic acid morpholinium salt, we observed a decrease in AIL - by 24.85% (p<0.001), PCN - by 25.62% (p=0.019), NCR - by 42.26% (p<0.001), and increase of PA - by 6.69% (p=0.762), PAC - by 17.45%, PCAC - by 28.79% (p<0.001). Comparing the periods of readaptation and correction revealed a decrease in AIL (Langerhans islet area) - by 22,63% (p=0,01), PCN (pancreatocyte nuclei area) - by 16.85% (p=0.130), NCR (nuclear-cytoplasmic ratio) - by 31.08% (p=0.04), and increase of PA (acinus area ) - by 4.35% (p=0.406), PAC (pancreatocyte area ) - by 14.22% (p=0.004), PCAC (pancreatocyte cytoplasm area) - by 20.96% (p<0.001). Detailed morphometric changes in the parenchyma of the pancreas conditions of sublethal degree of cellular dehydration, the period of subsequent readaptation and correction are shown in Table 2.

Under the influence of sublethal degree of extracellular dehydration and the period of subsequent readaptation, there was an increase in AIL - by 7.04% (p=0.131), PA - by 3.16% (p=0.406), PAC - by 10.9% (p=0.07), PCAC - by 19.57% (p=0.023), and reducing of PCN - by 16.42% (p=0.005), NCR - by 31.61% (p=0.003). Under the conditions of simultaneous use of the thiazotic acid morpholinium salt, we observed an increase in AIL - by 17.04% (p=0.013), PA - by 9.84% (p=0.082), PAC - by 18.93% (p=0.007), PCAC - by 34.71% (p<0,001), and reducing of PCN - by 30.43% (p<0.001), NCR - by 49.24% (p<0.001). Comparing the periods of readaptation and correction revealed an increase in AIL - by 9.33% (p=0.059), PA - by 6.48% (p=0.226), PAC - by 7.23% (p=0.096), PCAC - by 12.65% (p=0.038), PCN - by 16.76% (p=0.010) and only nuclear-cytoplasmic ratio and reduced by 25.77%

**Table 2.** Morphometric changes of islets, acini and pancreatocytes under conditions of sublethal degree of cellular dehydration, period of readaptation and correction.

| Indicator | Control | Severe dehydration | Readaptation | Correction |
|---|---|---|---|---|
| AIL, μm² | 13934.1±636.9 | 25774.2±1316.3 | 25035.6±979.6 | 19368.6±701.3 |
| | $p_1$=0.762; $p_2$<0.001; $p_3$<0.001 | | | |
| PA, μm² | 983.4±67.1 | 800.8±57,2 | 820.8±33.1 | 856.6±29.1 |
| | $p_1$=0.705; $p_2$=0.762; $p_3$=0.406 | | | |
| PAC, μm² | 149.5±3.1 | 95.72±1.25 | 98.42±1.79 | 112.4±2.8 |
| | $p_1$=0.364; $p_2$<0.001; $p_3$=0.004 | | | |
| PCAC, μm² | 138.7±4.7 | 75.75±1.29 | 80.61±1.59 | 97.52±2.53 |
| | $p_1$=0.041; $p_2$<0.001; $p_3$<0.001 | | | |
| PCN, μm² | 10.76±0.41 | 19.94±1.23 | 17.81±1.31 | 14.81±1.18 |
| | $p_1$=0.199; $p_2$=0.019; $p_3$=0.130 | | | |
| NCR, % | 8.241±0.99 | 26.54±1.93 | 22.22±1.79 | 15.29±1.22 |
| | $p_1$=0.112; $p_2$<0.001; $p_3$=0.04 | | | |

**Notes:** $p_1$ - the probability of differences in the indicators of severe cellular dehydration and the period of readaptation; $p_2$ - the probability of differences in the indicators of severe cellular dehydration and the correction period; $p_3$ - the probability of differences in readaptation and correction. AIL - Langerhans islet area; PA - pancreatic acinus area; PAC - pancreatocyte area; PCAC - pancreatocyte cytoplasm area; PCN - pancreatocyte nuclei area; NCR - nuclear-cytoplasmic ratio.

**Table 3.** Morphometric changes of islets, acini and pancreatocytes under conditions of sublethal degree of extracellular dehydration, period of readaptation and correction.

| Indicator | Control | Severe dehydration | Readaptation | Correction |
|---|---|---|---|---|
| AIL, μm² | 13934.1±636.92 | 10925.41±655.25 | 11695.4±385.01 | 12787.4±246.1 |
| | $p_1$=0.131; $p_2$=0.013; $p_3$=0.059 | | | |
| PA, μm² | 983.4±67.1 | 784.3±29.2 | 809.1±31.1 | 861.5±27.00 |
| | $p_1$=0.406; $p_2$=0.082; $p_3$=0.226 | | | |
| PAC, μm² | 149.5±3.16 | 86.14±3.59 | 95.49±2.51 | 102.4±2.9 |
| | $p_1$=0.070; $p_2$=0.007; $p_3$=0.096 | | | |
| PCAC, μm² | 138.7±4.72 | 65.41±3.76 | 78.21±2.82 | 88.12±3.31 |
| | $p_1$=0.023; $p_2$<0.001; $p_3$=0.038 | | | |
| PCN, μm² | 10.74±0.41 | 20.74±0.85 | 17.30±0.62 | 14.40±0.65 |
| | $p_1$=0.005; $p_2$<0.001; $p_3$=0.010 | | | |
| NCR, % | 8.27±0.98 | 32.87±2.61 | 22.51±1.34 | 16.69±1.22 |
| | $p_1$=0.003; $p_2$<0.001; $p_3$=0.005 | | | |

**Notes:** $p_1$ - the probability of differences in the indicators of severe extracellular dehydration and the period of readaptation; $p_2$ - the probability of differences in the indicators of severe extracellular dehydration and the correction period; $p_3$ - the probability of differences in readaptation and correction. AIL - Langerhans islet area; PA - pancreatic acinus area; PAC - pancreatocyte area; PCAC - pancreatocyte cytoplasm area; PCN - pancreatocyte nuclei area; NCR - nuclear-cytoplasmic ratio.

(p=0.005). Detailed morphometric changes in the parenchyma of the pancreas conditions of sublethal degree of extracellular dehydration, the period of subsequent readaptation and correction are shown in Table 3.

## Discussion

Water is one of the main components of the human body, which is vital for the performance of physiological processes, thermoregulation, and transport of nutrients [1, 6, 7, 8]. Water consumption is influenced by numerous factors, including temperature, humidity, as well as the level of physical activity and lifestyle [15, 18, 21, 27]. The most vulnerable groups to dehydration are children and adolescents, who are prone to excessive water loss, especially during physical activity and may not be aware of the need to restore lost fluid [26, 28].

Numerous literature data confirm that disability and mortality from cardiovascular diseases and diseases of the gastrointestinal tract are inversely proportional to water intake [10, 14, 19, 25].

Analyzing the results, it was found that the histostructure of the pancreas, endocrine system and gastrointestinal

tract, undergoes pronounced structural changes under the influence of sublethal degree of various types of dehydration, which coincides with the data of L.M.Davydova with co-authors (2017), who noted similar morphological changes in the structural components of the tongue in violation of water-electrolyte balance [4]. The absence of significant differences in indicators in the experimental groups under the influence of sublethal dehydration and the period of readaptation was established.

However, under conditions of sublethal degree of general dehydration and the subsequent period of correction with the thiazotic acid morpholinium salt, statistically significant changes were detected in the form of a decrease in the areas of the islets of Langerhans, acini and exocrinocyte nuclei. Comparative analysis of the size of the results of the periods of readaptation and correction showed significant changes in the area of the islets of Langerhans and the area of the acini.

Analysis of the sublethal degree of cellular dehydration and the subsequent period of correction with the thiazotic acid morpholinium salt revealed a significant increase in the areas of exocrinocytes and cytoplasm of exocrinocytes, with a simultaneous decrease in the areas of islets of Langerhans, nuclei of exocrinocytes and nuclear cytoplasms. The obtained results of the periods of readaptation and correction show statistically significant changes in the indicators of the areas of the islets of Langerhans, exocrinocytes, cytoplasm of exocrinocytes and nuclear-cytoplasmic ratio.

However, under conditions of sublethal degree of extracellular dehydration and the subsequent period of correction, significant changes in the areas of islets of Langerhans, exocrinocytes and cytoplasm of exocrinocytes in the form of their increase, with a probable decrease in the area of exocrinocyte nuclei and nuclear cytoplasmic ratio. Comparison of readaptation and correction indicators shows statistically significant changes in the indicators of cytoplasm areas of exocrinocytes, exocrinocyte nuclei and nuclear-cytoplasmic ratio.

Prospects for further research are to study the ultramorphometric characteristics of the parenchyma of the pancreas under different types of dehydration.

## Conclusions

1. The use of thiazotic acid morpholinium salt as a corrective drug for changes that have occurred under conditions of various types of dehydration of the body, leads to a reliable leveling of changes in the structural components of the pancreatic parenchyma, compared with readaptation.

2. The most reversible changes that are easier to correct are observed in conditions of general dehydration, while the deepest changes that are most difficult to correct are found in conditions of extracellular dehydration.

## References


[1] Ali, H., Al Dhaheri, A., Elmi, F., Ng, S., Zaghloul, S., Ohuma, E., & Qazaq, H. (2019). Water and Beverage Consumption among a Nationally Representative Sample of Children and Adolescents in the United Arab Emirates. *Nutrients,* 11(9), 2110. doi: 10.3390/nu11092110

[2] Barley, O., Chapman, D., & Abbiss, C. (2020). Reviewing the current methods of assessing hydration in athletes. *Journal of the International Society of Sports Nutrition,* 17(1). doi: 10.1186/s12970-020-00381-6

[3] Bruni, A., Bornstein, S., Linkermann, A., & Shapiro, A. (2018). Regulated Cell Death Seen through the Lens of Islet Transplantation. *Cell Transplantation*, 27(6), 890-901. doi: 10.1177/0963689718766323

[4] Davydova, L., Tkach, G., German, S., Bushtruk, A., & Maksymova, O. (2017). Особливості морфогенезу язика щурів при порушенні водно-електролітного балансу організму [Features of morphogenesis of rat tongue in violation of water-electrolyte balance of the organism]. *Здобутки клінічної і експериментальної медицини - Achievements of Clinical and Experimental Medicine,* 1(3). doi: 10.11603/1811-2471.2017.v1.i3.7956

[5] Davydova, L., Tkach, G., Tymoshenko, A., Moskalenko, A., Sikora, V., Kyptenko, L., Lyndin, M. … Suchonos, O. (2017). Anatomical and morphological aspects of papillae, epithelium, muscles, and glands of rats' tongue: Light, scanning, and transmission electron microscopic study. *Interventional Medicine and Applied Science,* 9(3), 168-177. doi: 10.1556/1646.9.2017.21

[6] Cheuvront, S., Kenefick, R., Charkoudian, N., & Sawka, M. (2013). Physiologic basis for understanding quantitative dehydration assessment. *The American Journal of Clinical Nutrition,* 97(3), 455-462. doi: 10.3945/ajcn.112.044172

[7] Gamble, J., & McIver, M. (1928). Body fluid changes due to continued loss of the external secretion of the pancreas. *Journal of Experimental Medicine,* 48(6), 859-869. doi: 10.1084/jem.48.6.859

[8] James, L., Funnell, M., James, R., & Mears, S. (2019). Does Hypohydration Really Impair Endurance Performance? Methodological Considerations for Interpreting Hydration Research. *Sports Medicine,* 49(S2), 103-114. doi: 10.1007/s40279-019-01188-5

[9] Johnson, R., Lichtenstein, A., Anderson, C., Carson, J., Despres, J., Hu, F. … Wylie-Rosett, J. (2018). Low-Calorie Sweetened Beverages and Cardiometabolic Health: A Science Advisory From the American Heart Association. *Circulation*, 138(9). doi: 10.1161/cir.0000000000000569

[10] Malisova, O., Athanasatou, A., Pepa, A., Husemann, M., Domnik, K., Braun, H. … Kapsokefalou, M. (2016). Water Intake and Hydration Indices in Healthy European Adults: The European Hydration Research Study (EHRS). *Nutrients,* 8(4), 204. doi: 10.3390/nu8040204

[11] Merkulov, G.A. (1969). *Курс патологической техники [Pathological Technique Course]*. М.: Медицина - M.: Medicine.

[12] Monaghan, T., Kavoussi, A., Agudelo, C., Rahman, S., Michelson, K., & Bliwise, D. et al. (2020). Nocturnal Urine Production in Women With Global Polyuria. *International Neurourology Journal,* 24(3), 270-277. doi: 10.5213/inj.2040166.083.

[13] Munoz, C., Johnson, E., McKenzie, A., Guelinckx, I., Graverholt, G., & Casa, D. et al. (2015). Habitual total water intake and dimensions of mood in healthy young women. *Appetite*, 92, 81-86. doi: 10.1016/j.appet.2015.05.002

[14] Özen, A., Bibiloni, M., Bouzas, C., Pons, A., & Tur, J. (2018).

Beverage Consumption among Adults in the Balearic Islands: Association with Total Water and Energy Intake. *Nutrients,* 10(9), 1149. doi: 10.3390/nu10091149

[15] Lugea, A., Gerloff, A., Su, H., Xu, Z., Go, A., & Hu, C. et al. (2017). The Combination of Alcohol and Cigarette Smoke Induces Endoplasmic Reticulum Stress and Cell Death in Pancreatic Acinar Cells. *Gastroenterology,* 153(6), 1674-1686. doi: 10.1053/j.gastro.2017.08.036

[16] Reid, I. (1994). Role of Nitric Oxide in the Regulation of Renin and Vasopressin Secretion. *Frontiers in Neuroendocrinology,* 15(4), 351-383. doi: 10.1006/frne.1994.1014

[17] Rybolovlev, Yu.R., & Rybolovlev, R.S. (1979). Дозирование веществ для млекопитающих по константе биологической активности [Dosing of substances for mammals according to the constant of biological activity]. *Доклады АН СССР - Reports of the USSR Academy of Sciences*.

[18] Sahin-Toth, M., & Hegyi, P. (2017). Smoking and Drinking Synergize in Pancreatitis: Multiple Hits on Multiple Targets. *Gastroenterology,* 153(6), 1479-1481. doi: 10.1053/j.gastro.2017.10.031

[19] Savoie, F., Kenefick, R., Ely, B., Cheuvront, S., & Goulet, E. (2015). Effect of Hypohydration on Muscle Endurance, Strength, Anaerobic Power and Capacity and Vertical Jumping Ability: A Meta-Analysis. *Sports Medicine*, 45(8), 1207-1227. doi: 10.1007/s40279-015-0349-0

[20] Sharon, N., Chawla, R., Mueller, J., Vanderhooft, J., Whitehorn, L., Rosenthal, B. … Melton, D. (2019). A Peninsular Structure Coordinates Asynchronous Differentiation with Morphogenesis to Generate Pancreatic Islets. *Cell*, 176(4), 790-804.e13. doi: 10.1016/j.cell.2018.12.003

[21] Srinivasan, M.P., Bhopale, K.K., Caracheo, A.A., Amer, S.M., Khan, S., Kaphalia, L. … Kaphalia, B.S. (2020). Activation of AMP-activated protein kinase attenuates ethanol-induced ER/oxidative stress and lipid phenotype in human pancreatic acinar cells. *Biochemical Pharmacology,* 180, 114174. doi: 10.1016/j.bcp.2020.114174

[22] Scratcherd, T., Hutson, D., & Case, R.M. (1981). Ionic transport mechanisms underlying fluid secretion by the pancreas. *Philosophical Transactions of the Royal Society B.*, 296(1080), 167-178. doi: 10.1098/rstb.1981.0180

[23] Tan, B., Philipp, M., Hill, S., Che Muhamed, A., & Mündel, T. (2020). Pain Across the Menstrual Cycle: Considerations of Hydration. *Frontiers in Physiology*, 11. doi: 10.3389/fphys.2020.585667

[24] Vieux, F., Maillot, M., Constant, F., & Drewnowski, A. (2017). Water and beverage consumption patterns among 4 to 13-year-old children in the United Kingdom. *BMC Public Health*, 17(1). doi: 10.1186/s12889-017-4400-y

[25] Villiger, M., Stoop, R., Vetsch, T., Hohenauer, E., Pini, M., Clarys, P. … Clijsen, R. (2017). Evaluation and review of body fluids saliva, sweat and tear compared to biochemical hydration assessment markers within blood and urine. *European Journal of Clinical Nutrition*, 72(1), 69-76. doi: 10.1038/ejcn.2017.136

[26] Zhang, J., Zhang, N., Liu, S., Du, S., He, H., & Ma, G. (2021). The comparison of water intake patterns and hydration biomarkers among young adults with different hydration statuses in Hebei, China. *Nutrition & Metabolism*, 18. doi: 10.1186/s12986-020-00531-2

[27] Zhang, J., Zhang, N., Wang, Y., Liang, S., Liu, S., Du, S. … Ma, G. (2020). Drinking patterns and hydration biomarkers among young adults with different levels of habitual total drinking fluids intake in Baoding, Hebei Province, China: a cross-sectional study. *BMC Public Health*, 20(1). doi: 10.1186/s12889-020-08558-z

[28] Zhang, J., Zhang, N., He, H.R., Cai, H., Yan, X.Y., Guo, X.H. … Ma, G. (2019). The total fluids intake, volume of urine and hydration status among young adults from Hebei Province in spring. *Zhonghua Yu Fang Yi Xue Za Zhi*, 53(4), 6. doi: 10.3760/cma.j.issn.0253-9624.2019.04.005

**КІЛЬКІСНІ ЗМІНИ МІКРОСТРУКТУРИ ПІДШЛУНКОВОЇ ЗАЛОЗИ ЗА УМОВ ВПЛИВУ СУБЛЕТАЛЬНОГО ЗНЕВОДНЕННЯ, ПОДАЛЬШОЇ РЕАДАПТАЦІЇ ТА КОРЕКЦІЇ**

***Ковчун В.Ю.***

*Зневоднення - це патологічний стан, що викликаний недостатнім надходженням води та супроводжується метаболічними порушеннями, які мають значні наслідки для здоров'я та працездатності людини. Ендокринна система приймає участь у низці функцій системи обміну води, оптимізуючи об'єм рідини організму. У літературі немає систематизованих даних щодо змін підшлункової залози за умов різних видів зневоднення. Актуальним є вивчення структурних порушень підшлункової залози за умов сублетальних ступенів різних видів зневоднення з подальшою реадаптацією та корекцією препаратом, котрий має протишемічну, мембраностабілізуючу, антиоксидантну, гепатопротекторну та імуномодулюючу властивості, що дозволяє нормалізувати білковий, вуглеводний та ліпідний обмін. Метою дослідження було вивчення особливостей змін ендокринної та екзокринної паренхіми підшлункової залози методом морфометрії гістологічних препаратів за умов сублетального зневоднення з подальшою реадаптацією та корекцією морфолінієвою сіллю тіазотної кислоти. Досліджувану групу становили 60 зрілих щурів-самців, котрим моделювали сублетальний ступінь загального, клітинного та позаклітинного зневоднення за А.Д.Соболєвою, В.З.Сікорою, Я.Я.Боднаром. Після досягнення тяжкого ступеня зневоднення частину щурів переводили на звичайний питний раціон, друга частина отримувала препарат-коректор впродовж 14 діб. Тварин було виведено з експерименту шляхом декапітації під наркозом на 24, 44 та 104 добу відповідно до виду зневоднення. Проаналізувавши отримані результати, встановлено відсутність статистично значущих відмінностей більшості морфометричних показників за умов впливу сублетального зневоднення порівняно з подальшою реадаптацією всіх експериментальних груп тварин. Виявлено достовірні зміни площі острівців Лангерганса та площі ядер екзокриноцитів за умов впливу різних видів сублетального зневоднення у порівнянні з групою реадаптації та групою корекції в усіх експериментальних групах. Інші морфометричні показники паренхіми підшлункової залози мали зміни різної статистичної значущості, котрі залежали від виду зневоднення. З'ясовано, що застосування морфолінієвої солі тіазотної кислоти призводить до часткового відновлення структурних компонентів паренхіми підшлункової залози, порівняно з періодом реадаптації.*

**Ключові слова:** *підшлункова залоза, острівці Лангерганса, ацинуси, сублетальне зневоднення, морфолінієва сіль тіазотної кислоти.*

**REQUIREMENTS FOR ARTICLES**

For publication, scientific articles are accepted only in English only with translation on Ukrainian, which contain the following necessary elements: UDC code; title of the article (in English and Ukrainian); surname, name and patronymic of the authors (in English and Ukrainian); the official name of the organization (institution) (in English and Ukrainian); city, country (in English and Ukrainian); structured annotations (in English and Ukrainian); keywords (in English and Ukrainian); introduction; purpose; materials and methods of research; research results; discussion; conclusions; bibliographic references.

**The title of the article** briefly reflects its contents and contains no more than 15 words.

**Abstract.** The volume of the annotation is 1800-2500 characters without spaces. The text of an annotation in one paragraph should not contain general phrases, display the main content of the article and be structured. The abstract should contain an introductory sentence reflecting the relevance of the study, the purpose of the study, a brief description of the methods of conducting research (2-3 sentences with the mandatory provision of the applied statistical methods), a description of the main results (50-70% of the volume of the abstract) and a concise conclusion (1 sentence). The abstract should be clear without familiarizing the main content of the article. Use the following expressions: "Detected ...", "Installed ...", "Fixed ...", "Impact assessed ...", "Characterized by regularities ...", etc. In an annotation, use an active rather than passive state.

**Keywords:** 4-6 words (or phrases).

**"Introduction"**

The introduction reflects the state of research and the relevance of the problem according to the world scientific literature (at least 15 references to English articles in international journals over the past 5 years). At the end of the entry, the purpose of the article is formulated (contains no more than 2-3 sentences, in which the problem or hypothesis is addressed, which is solved by the author).

**"Materials and methods"**

The section should allow other researchers to perform similar studies and check the results obtained by the author. If necessary, this section may be divided into subdivisions. Depending on the research objects, the ethical principles of the European Convention for the protection of vertebrate animals must be observed; Helsinki Declaration; informed consent of the surveyed, etc. (for more details, see "Public Ethics and its Conflict"). At the end of this section, a "statistical processing of results" section is required, which specifies the program and methods for processing the results obtained by the automobile.

**"Results"**

Requirements for writing this section are general, as well as for all international scientific publications. The data is presented clearly, in the form of short descriptions, and must be illustrated by color graphics (no more than 4) or drawings (no more than 8) and tables (no more than 4), the information is not duplicated.

**"Discussion"**

In the discussion, it is necessary to summarize and analyze the results, as possible, compare them with the data of other researchers. It is necessary to highlight the novelty and possible theoretical or practical significance of the results of the research. You should not repeat the information already listed in the "Introduction" section. At the end of the discussion, a separate paragraph should reflect the prospects for using the results obtained by the author.

**"Conclusion"**

5-10 sentences that summarize the work done (in the form of paragraphs or solid text).

**"Acknowlegements"**

Submitted after conclusion before bibliographic references.

**"References"**

References in the text are indicated by Arabic numerals in square brackets according to the numerology in the list of references. The list of references (made without abbreviations) sorted by alphabet, in accordance with the requirements of APA Style (American Psychological Association Style): with the obligatory referencing of all authors, work titles, journal names, or books (with obligatory publication by the publishing house, and editors when they are available), therefore, numbers or releases and pages. In the Cyrillic alphabets references, give the author's surnames and initials in English (Cyrillic alphabet in brackets), the title of the article or book, and the name of the magazine or the publisher first to be submitted in the original language of the article, and then in square brackets in English. If available, doi indexes must be provided on www.crossref.org (at least 80% of the bibliographic references must have their own doi indexes). Links to online publications, abstracts and dissertations are not welcome.

After the list of references, it is necessary to provide information about all authors (in English, Ukrainian and Russian): last name, first name and patronymic of the author, degree, place of work and position, **ORCID number** (each of the authors of the ORCID personal number if absence - free creation on the official website http://www.orcid.org) to facilitate the readers of this article to refer to your publications in other scientific publications.

**The last page of the text** should include the surname, name and patronymic of the author, degree, postal address, telephone number and e-mail of the author, with which the editors will maintain contact.

**Concluding remarks**

The manuscript should be executed in such a way that the number of refinements and revisions during the editorial of the article was minimal.

When submitting the article, please observe the following requirements. The volume of the article - not less than 15 and not more than 25 pages, Times New Roman, 14 pt, line spacing - one and a half, fields - 2 cm, sheet A4. Text materials should be prepared in the MS Word editor (* .docx), without indentations. Math formulas and equations to prepare in the embedded editor; graphics - in MS Excel. Use the units of the International Measurement System. Tables and drawings must contain the name, be numbered, and references to them in the text should be presented as follows: (fig. 1), or (table 1). The drawings should be in the format "jpg" or "tif"; when scanned, the resolution should be at least 800 dpi; when scanning half-tone and color images, the resolution should be at least 300 dpi. All figures must be represented in the CMYK palette. The statistical and other details are given below the table in the notes. Table materials and drawings place at the end of the text of the manuscript. All elements of the text in images (charts, diagrams, diagrams) must have the Times New Roman headset.

Articles are sent to the editorial board only in electronic form (one file) at the e-mail address nila@vnmu.edu.ua

Responsible editor - Gunas Igor Valeryovich (phone number: + 38-067-121-00-05; e-mail: igor.v.gunas@gmail.com).

Signed for print 25.06.2021
Format 60x84/8. Printing offset. Order № 1012. Circulation 100.
Vinnytsia. Printing house “TVORY”, Nemyrivske shose St., 62a,
Vinnytsya, 21034
Phone: 0 (800) 33-00-90, (096) 97-30-934, (093) 89-13-852,
(098) 46-98-043
e-mail: tvory2009@gmail.com
http://www.tvoru.com.ua